AUTOREGULATORY AND STRUCTURAL CONTROL OF CAMKII SUBSTRATE SPECIFICITY

Derrick E. Johnson

Submitted to the faculty of the University Graduate School

in partial fulfillment of the requirements

for the degree

Doctor of Philosophy

in the Department of Biochemistry and Molecular Biology,

Indiana University

September 2016

Accepted by the Graduate Faculty, Indiana University, in partial fulfillment of the requirements for the degree of Doctor of Philosophy.

_____

Andy Hudmon, Ph.D. - Chair

_____

Thomas D. Hurley, Ph.D.

Doctoral Committee

_____

Quyen Q. Hoang, Ph.D.

July 6, 2016

_____

Patricia J. Gallagher, Ph.D.

DEDICATION

This dissertation is dedicated to my family, especially my wife, Melissa Johnson, my parents, Doug and Caroline Johnson, and to my children, Dylan and Addison. Their dedication to my education, encouragement, prayers and love, supported me in the completion of this work.

ACKNOWLEDGEMENTS

I would like to thank my advisor, Dr. Andy Hudmon for being an extraordinary mentor and for his continual support and motivation during my dissertation work. Thank you to my dissertation committee members Dr. Thomas Hurley, Dr. Quyen Hoang, and Dr. Patricia Gallagher, for their advice and guidance. Additionally, I thank both present and past Hudmon lab members who have played an important role in shaping my research and training me as a scientist. Dr. Nicole Ashpole, Dr. Aarthi Chawla, and Dr. Swarna Ramaswamy: you've each been wonderful colleagues and I greatly appreciate your help and friendship over the years. Other lab members I'd like to thank: Idamarie Collazo, Derek Kaiser, Dr. Jingwei Meng, Dr. Weihua Song, Jason Meno, Benjamin Leeds, Ross Nelson, Jay Patel, Melissa Peden, Agnieszka Zybura and Thatcher Ladd. Thank you Dr. Ted Cummins lab members your time in lab meetings that pushed me think about my research in new ways.

Special thanks to the Department of Biochemistry and Molecular Biology front office, as well as to the Stark Neuroscience Research Institute front office, especially Nastassia and Diana for their assistance and support.

I would like to thank my parents Doug and Caroline, my sister Erica and brother-in-law Blake Hansen, my grandparents, and my wife's family. Your support, love, and encouragement have tremendously helped me through this long journey. I also want to thank my children, Dylan and Addison, for brightening up my night after long days in the lab. Finally, I want to thank my wife Melissa who has taken on far too many roles so that I could pursue this degree. You've worked full-time while taking on the majority of tasks in the home including caring for our two children. Thank you for patience, love, and care.

Derrick E. Johnson

AUTOREGULATORY AND STRUCTURAL CONTROL OF CAMKII

SUBSTRATE SPECIFICITY

Calcium/calmodulin (CaM)-dependent protein kinase II (CaMKII) is a multimeric holoenzyme composed of 8–14 subunits from four closely related isoforms (α, β, γ, δ). CaMKII plays a strategic, multifunctional role in coupling the universal second messenger calcium with diverse cellular processes including metabolism, cell cycle control, and synaptic plasticity. CaMKII exhibits broad substrate specificity, targeting numerous substrates with diverse phosphorylation motifs. Binding of the calcium sensor CaM to the autoregulatory domain (ARD) of CaMKII functions to couple kinase activation with calcium signaling. Important sites of autophosphorylation, namely T^{287} and $T^{306/7}$ (δ-isoform numbering), reside within the ARD and control either CaM dependence or ability to bind to CaMKII respectively, thus determining various activation states of the kinase. Because autophosphorylation is critical to the function of CaMKII in vivo, we sought to determine the relationship between the activation state of the kinase and substrate selectivity. We show that the ARD of activated CaMKII tunes substrate selectivity by competing for substrate binding to the catalytic domain, thus functioning as a selectivity filter. Specifically, in the absence of T^{287} autophosphorylation, substrate phosphorylation is limited to high-affinity, consensus substrates. T^{287} autophosphorylation restores maximal kinase activation and broad substrate selectivity by disengaging ARD filtering. The unique multimeric architecture of CaMKII is an ideal sensor which encodes calcium-spike frequency into graded levels of subunit activation/autophosphorylation within the holoenzyme. We find that differential activation states of the holoenzyme produce distinct

substrate phosphorylation profiles. Maximal holoenzyme activation/autophosphorylation leads to further broadening of substrate specificity beyond the effect of autophosphorylation alone, which is consistent with multivalent avidity. Thus, the ability of calcium-spike frequency to regulate T^{287} autophosphorylation and holoenzyme activation permits cellular activity to dictate switch-like behavior in substrate selectivity that is required for diverse cellular responses by CaMKII.

Andy Hudmon, Ph.D. - Chair

TABLE OF CONTENTS

LIST OF TABLES

LIST OF FIGURES

LIST OF ABBREVIATIONS

AC-2	Autocamtide-2
ADP	Adenosine diphosphate
AMPA-R	α-amino-3-hydroxy-5-methyl-4-isoxazolepropionic acid receptor
ANOVA	Analysis of Variance
ARD	Autoregulatory domain
ATP	Adenosine triphosphate
BSA	Bovine serum albumin
Ca^{2+}	Calcium
CaM	Calmodulin
CaMKII	Calcium/calmodulin-dependent protein kinase II
$CaMKII_{cf}$	CaMKII catalytic fragment
$CaMKII_{holo}$	CaMKII holoenzyme
$CaMKII_{holo}^{+P}$	CaM bound, T^{287} autophosphorylated $CaMKII_{holo}$
$CaMKII_{m}$	Monomeric $CaMKII_{1-317}$
$CaMKII_{m}^{-P}$	CaM activated, non-T^{287} autophosphorylated $CaMKII_{m}$
$CaMKII_{m}^{+P}$	CaM bound, T^{287} autophosphorylated $CaMKII_{m}$
EDTA	Ethylenediaminetetraacetic acid
EGTA	Ethylene glycol tetraacetic acid
GluA1	Glutamate ionotropic receptor AMPA type subunit 1
GluN2B	N-methyl D-aspartate receptor subtype 2B
GST	Glutathione *S*-transferases
GTP	Guanosine-5'-triphosphate

HEPES	4-(2-hydroxyethyl)-1-piperazineethanesulfonic acid
KN-92	2-[N-(4-Methoxybenzenesulfonyl)]amino-N-(4-chlorocinnamyl)-N-methylbenzylamine, monohydrochloride
KN-93	N-[2-[[[3-(4-Chlorophenyl)-2-propenyl]methylamino]methyl]phenyl]-N-(2-hydroxyethyl)-4-methoxybenzenesulphonamide
LTD	Long-term depression
LTP	Long-term potentiation
PBS	Phosphate buffered saline
PSD	Post-synaptic density
PTM	Post-translational modification
SD	Standard deviation
SDS-PAGE	sodium dodecyl sulfate polyacrylamide gel electrophoresis
SEM	Standard error of the mean

CHAPTER 1. Introduction

1.1 Overview

One of the fundamental roles of the brain is to encode information within the vast neuronal circuitry in response to external stimuli for recollection in the future. We often take learning and memory for granted, not giving a second thought to the incredible gift we have been given. Nevertheless, a growing population of people experience various forms of memory disorders. These may be the result of neurodegenerative diseases such as Alzheimer's, or the result of traumatic brain injury (TBI), vascular disease, etc. The World Health Organization estimates that 47.5 million people worldwide suffer from dementia, with another 7.7 million new cases each year (WHO Fact sheet N°362, March 2015). The overall cost on society in 2010 alone was an estimated 1% of the worldwide gross domestic product (GDP), or US$ 604 billion.

At the cellular level, the processes of learning and memory are manifested by the strengthening and weakening of neuronal connections; known as long-term potentiation (LTP) and long-term depression (LTD), respectively. The generation of LTP and LTD occur within the post-synaptic neuron (though presynaptic modes of generation have also been described) as the signals from the presynaptic neuron are integrated in the macromolecular signaling complex known as the post-synaptic density (PSD). This structure contains key transmembrane receptors and ion channels that convert the extracellular signals into intracellular signaling cascades that modulate synaptic plasticity. Alteration of protein function within the cell is crucial for the proper regulation of cellular processes. One way in which this is achieved is through enzymes which modify other proteins/substrates. Kinases are an important class of enzymes which phosphorylate proteins, DNA, or other enzymes; that is they transfer a phosphate group from ATP (or

GTP) to a substrate. It is one of the most studied types of modifying enzymes (termed post-translational modification or PTM when associated with proteins) as this small modification can lead to essential changes in the substrate/protein function including activation/deactivation, binding/unbinding to downstream targets, folding/unfolding, etc. The pathways or cascades that these types of enzymes are generally a part of can be switched on by second messengers such as calcium upon release from intracellular stores or through various ion channels.

1.2 Calcium Signaling

Calcium signaling, with calcium acting as a nearly universal second messenger, has long been known to be a major regulatory pathway in many cellular processes including neuronal excitability, cell motility, exocytosis, muscle contraction, and gene transcription (Berridge, Lipp et al. 2000). Intracellular calcium is buffered and sequestered to rather low levels (~100 nM) and typical only varies from ~100 hundred nM up to one μM (Sabatini, Oertner et al. 2002). Cells, including neurons, tightly regulate calcium homeostasis, as aberrant calcium signaling events lead to various detrimental outcomes. Dysregulation of calcium signaling is a prevalent characteristic of many forms of neurodegenerative diseases (Berridge 2012). Increases in intracellular calcium associated with normal synaptic activity stimulate calcium-sensitive proteins, such as the ubiquitous calmodulin (CaM), which subsequently activates a variety of other downstream signaling effectors. However, it is not merely the amplitude of the calcium signal, but also the localization and the frequency of the stimulus (and the changes in the frequency) that lead to differing cellular actions and physiological outcomes (Boulware and Marchant 2008). One key class of signaling

molecules that is modulated by neuronal activity and subsequent calcium/calmodulin activation is the calcium/calmodulin-dependent protein kinases (CaMK); a group of multifunctional serine/threonine kinases comprised of CaMKI, CaMKII, and CaMKIV.

1.3 CaMKII: A Historical Perspective

Among the CaMK class, CaMKII has been in the spotlight of research related to regulatory mechanisms of learning and memory. CaMKII is highly enriched in the brain where it contributes up to around 1-2% of the total protein (Lisman, Schulman et al. 2002); a level of expression more like a cytoskeletal protein than an enzyme. While found ubiquitously expressed throughout the cell (or neuron), CaMKII was found to be enriched in the PSDs of excitatory synapses. Early reports identified a kinase similar to CaMKII that was integral to the PSD and was hence known as the major PSD protein (mPSDp) (Grab, Carlin et al. 1981, Kelly and Montgomery 1982). Subsequent studies found that this kinase was in fact CaMKII (Kelly, McGuinness et al. 1984). The close association of CaMKII to the PSD makes sense in light of CaMKII knock-out studies in mice that were the first to show alteration in learning and memory (Silva, Paylor et al. 1992). The localization of CaMKII in the PSD places it in an ideal position to regulate synaptic plasticity. It is known that CaMKII targets, phosphorylates, and regulates a large number of substrates within the PSD (Figure 1.1) (Yoshimura, Aoi et al. 2000, Yoshimura, Shinkawa et al. 2002). Additionally, CaMKII phosphorylates proteins involved in the release of neurotransmitter in the presynaptic terminal (Hinds, Goussakov et al. 2003, Liu, Chen et al. 2007). Many studies over the course of the past 25 years have established that CaMKII plays important structural and signaling roles in synaptic plasticity, the cellular correlates of learning and

memory, by regulating the generation of long-term potentiation (LTP) (Silva, Stevens et al. 1992, Lisman, Yasuda et al. 2012) and more recently long-term depression (LTD). In addition to its role in synaptic plasticity, this multifunctional kinase plays a role in many cellular processes, regulating processes as diverse as carbohydrate, amino acid and lipid metabolism, neurotransmitter synthesis and release, ion channels, receptors, transcription and translation, cytoskeletal organization, cell cycle control and calcium homoeostasis (Hudmon and Schulman 2002). CaMKII targets diverse phosphorylation motifs within a host of different substrates. Thus, this kinase has been known to have broad substrate specificity.

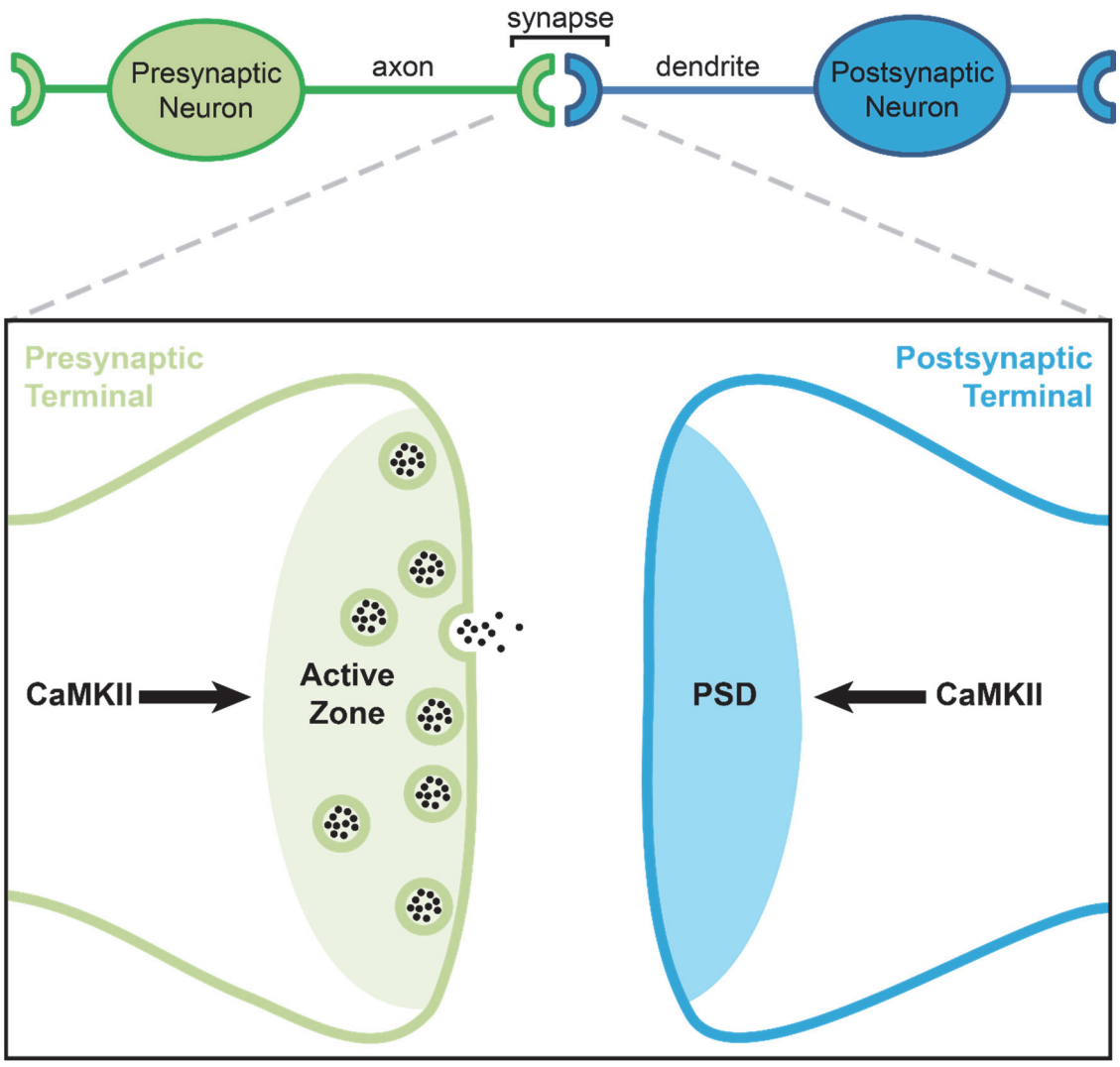

Figure 1.1 CaMKII action at the neuronal junction.
Illustration of a simplified neuronal connection (i.e. the synapse). The axon from a presynaptic neuron interfaces with a dendrite from a postsynaptic neuron to form the synapse or synaptic junction. The region below the cell surface facing the synaptic cleft of either the pre- and post-synaptic termini (inset) contain two structural important environments in which CaMKII functions (i.e. the active zone and the post-synaptic density (PSD), respectively). While the active zone has vesicles containing neurotransmitter waiting to be released, the PSD is made of the necessary receptors, channels, etc. required for responding to neurotransmitters.

The importance of CaMKII was further tied to the enzyme's ability to escape the required binding of Ca^{2+}/CaM for enzymatic activity, through an autophosphorylation event in the regulatory domain that occurs in response to the amplitude of frequency of Ca^{2+} stimulation (De Koninck and Schulman 1998). By extending the activity beyond the stimulating action of the Ca^{2+} transient, this kinase has the ability to behave in a way that has been described as a form of a "molecular memory switch" (Hanson, Meyer et al. 1994, Lisman, Schulman et al. 2002) and to do so as a Ca^{2+} frequency decoder. In order to fully appreciate these features of the kinase, it is important to consider the architecture of the holoenzyme as well as the structural components of each of the subunits.

1.4 CaMKII Isoforms, Cellular Distribution, and Holoenzyme Structure

CaMKII is a family of kinases with four isoforms (α, β, γ, δ) encoded by separate genes in mammals with high sequence conservation between species. The four isoforms are expressed variably in different tissues in cell-, developmental-, and subcellular-specific manners. CaMKIIγ and CaMKIIδ are expressed in many cell-types and tissues. For example, CaMKIIδ is the predominantly expressed isoform in cardiomyocytes and has been well-studied for its role in normal cardiac physiology as well as pathophysiological issues such as arrhythmias, contractile dysfunction, and heart failure (Hund and Mohler 2015). CaMKIIα and CaMKIIβ can be found in various tissues types, but they are predominantly expressed in the neurons. While CaMKIIγ and CaMKIIδ are also found in lower levels in neurons, they are expressed in other cell types in the brain such as astrocytes (Vallano, Beaman-Hall et al. 2000). In addition, CaMKII in other organisms such as *Drosophila melanogaster* and *Caenorhabditis elegans*, which are both highly conserved,

have been shown to regulate a variety of important functions such as those related to learning and memory (Griffith, Verselis et al. 1993), synaptic plasticity (Wang, Renger et al. 1994), heart rate and arrhythmias (Santalla, Valverde et al. 2014), photoreceptor function (Lu, Leung et al. 2009), and neuronal mitochondrial maintenance (Jiang, Hsu et al. 2015).

All four mammalian CaMKII isoforms have similar domain organization (Chao, Stratton et al. 2011); each subunit containing a catalytic, autoregulatory, and association (hub or oligomerization) domain (Figure 1.2A) (Hudmon and Schulman 2002). In addition, the sequences possess a high degree of conservation (Figure 1.3). Alternative splicing for each isoform generates multiple variants of each isoform totaling ~40 mammalian variants (Tombes, Faison et al. 2003). These variations generally occur in the variable insert linker region located between the autoregulatory and hub domains, and can confer multiple functions such as F-actin binding or nuclear localization (reviewed in (Gray and Heller Brown 2014)) as well as alter the kinases frequency response to calcium transients (Bayer, De Koninck et al. 2002). The holoenzyme (consisting of varying ratios of multiple isoforms (Bennett, Erondu et al. 1983, Yamauchi, Ohsako et al. 1989, Kolb, Hudmon et al. 1998, Brocke, Chiang et al. 1999)) is formed by the assembly of 12-14 hub domains into a hexameric or heptadecameric doublet configuration with catalytic domains projecting out from the central hub core (Kolodziej, Hudmon et al. 2000, Chao, Stratton et al. 2011). However, there is some discrepancy between positioning of the catalytic domain; early studies involving cryo-EM reconstructions (Kolodziej, Hudmon et al. 2000) show the catalytic domain extended in an axial orientation whereas in the recent crystal structure of the dodecameric holoenzyme they are tightly nestled to the hub domain in a more

equatorial arrangement (Chao, Stratton et al. 2011). While the construct used to generate the first crystal structure of a CaMKII holoenzyme utilized a short linker region between the autoregulatory and hub domains, reconstructions from small-angle x-ray scattering (SAXS) analysis with either the short or a longer linker suggested an equatorial orientation in solution (Kolodziej, Hudmon et al. 2000). Though the catalytic and hub domains are intrinsically ordered structures, the autoregulatory domain, linker, and variable inserts are much less structurally ordered. In fact, based on various experimental data including electron paramagnetic resonance (EPR) (Hoffman, Stein et al. 2011), the autoregulatory domain appears to undergo transitions between order and disorder in response to Ca^{2+}/CaM binding and various activation states. The autoregulatory domain itself can be divided into several segments, designated R1 to R3 (Figure 1.2A) (Chao, Pellicena et al. 2010). Sequence analysis of the various linkers and alternatively spliced inserts from the different isoforms all exhibit high levels of predicted intrinsic disorder (PONDR-Fit) (Figure 1.2B). Hence, the holoenzyme construct used to generate the first full-length crystal structure benefited from a lack of the flexible linker region.

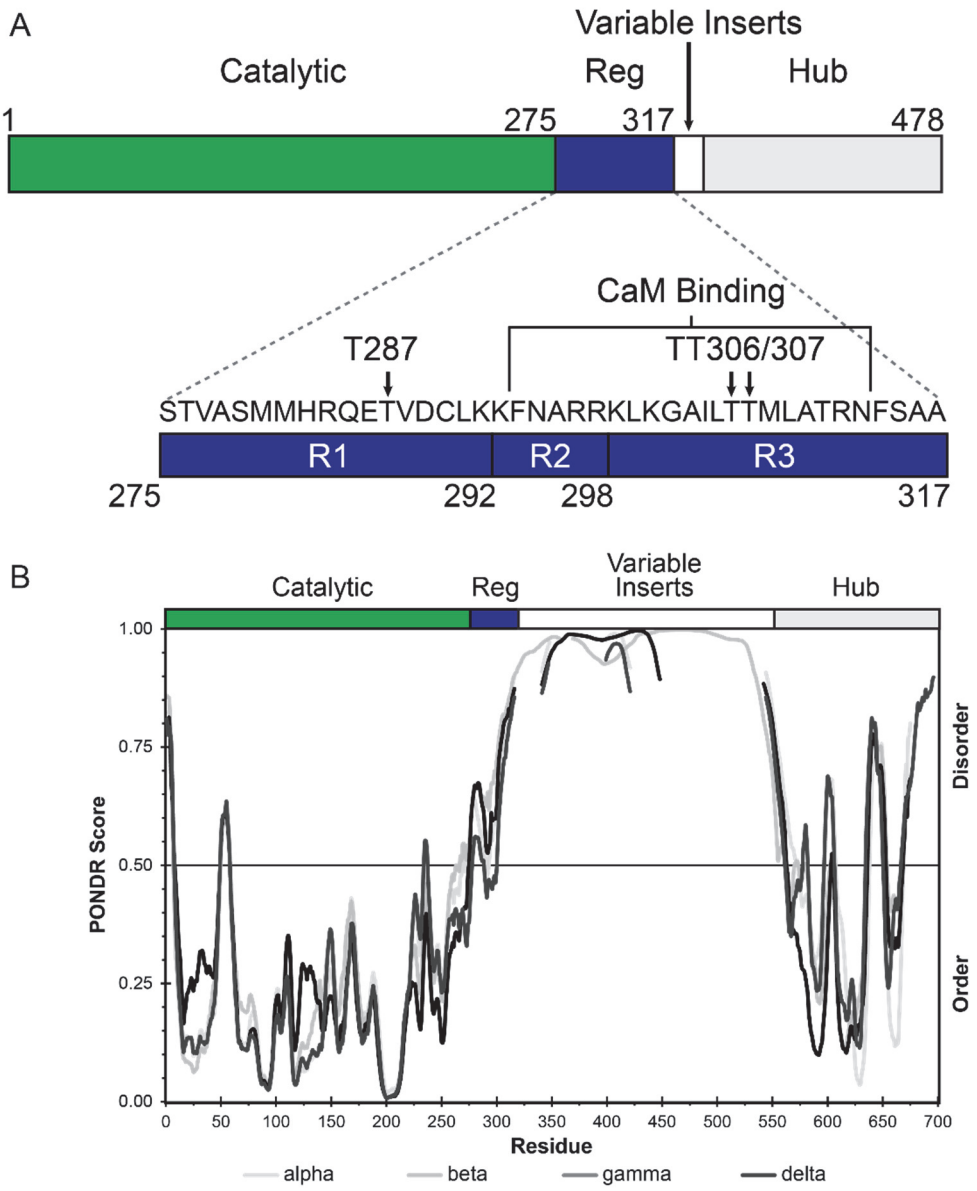

Figure 1.2 CaMKII domains and intrinsic order/disorder predictions.
(**A**) Linear schematic of a single subunit within the CaMKII holoenzyme (delta isoform) representing the catalytic domain (green), autoregulatory domain (ARD) (blue), and hub domain (gray). Expanded view shows the ARD (blue) with subdivisions R1 (T^{287} containing region) and R2/R3 (CaM binding and $T^{306/7}$ region) (Chao, Pellicena et al. 2010). (**B**) Sequence analysis for the four CaMKII isoforms show the predicted intrinsically disordered/ordered regions with the protein using PONDR (VSL2 variant) (Obradovic, Peng et al. 2005, Peng, Radivojac et al. 2006).

Figure 1.3 Sequence alignment of CaMKII isoforms.
Multiple sequence alignment performed using CLUSTAL Omega (v1.2.1) for the canonical sequence obtained from UniProt.

CaMKII is similar to other monomeric multifunctional Ca^{2+}/CaM activated protein kinases (CaMKI and CaMKIV) in that it has an autoregulatory domain that is disinhibited by Ca^{2+}/CaM binding (Figure 1.4); however, it is structurally quite different in that CaMKII has a multimeric architecture and does not require phosphorylation by an upstream CaMK kinase (CaMKK) in an activation loop for maximal activity (Lee and Edelman 1995, Tokumitsu, Enslen et al. 1995). CaMKII does undergo autophosphorylation in its autoregulatory domain by a special intermolecular-intraholoenzyme autophosphorylation reaction (Hanson, Meyer et al. 1994, Rich and Schulman 1998). The catalytic domain resembles a prototypical Ser/Thr kinase domain with a characteristic kinase fold in which the N-terminal portion consists mainly of anti-parallel beta sheets while the C-terminal portion is comprised mostly of alpha-helical segments. All the isoforms of CaMKII are nearly identical within the catalytic surface and substrate binding region of catalytic domain, (Figure 1.5).

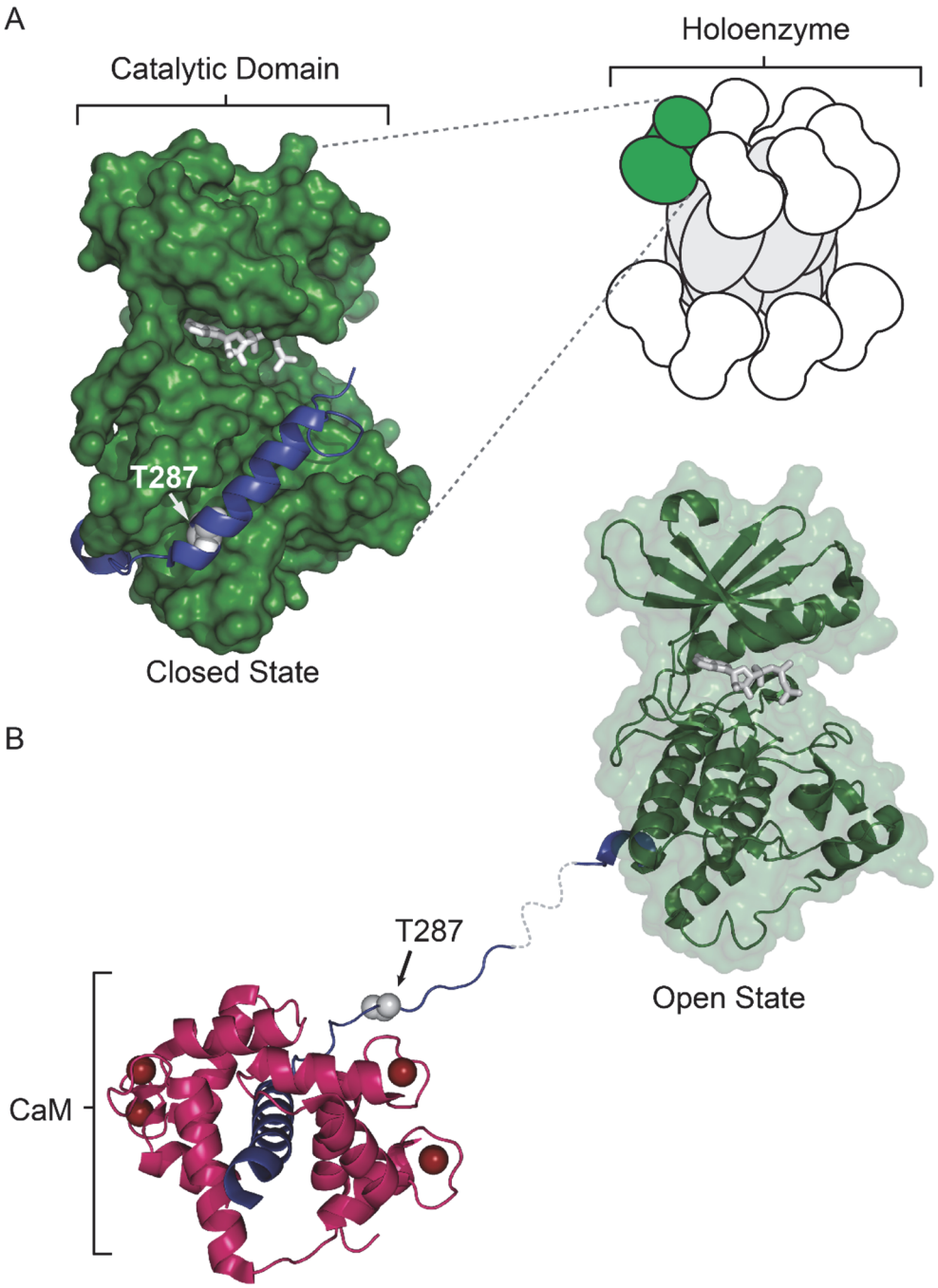

Figure 1.4 Structure of autoinhibited versus activated CaMKII.
(**A**) Illustration of the CaMKII holoenzyme with detailed view of the catalytic domain. X-ray crystal structure shows monomeric human CaMKII$\delta_{11\text{-}309}$ (PDB ID: 2VN9) in the autoinhibited state with the ARD (blue) and modified to include ATP in the active site (PDB ID: 1ATP). (**B**) hCaMKII$\delta_{11\text{-}335}$ activated (PDB ID: 2WEL) by calcium (red spheres) and calmodulin (CaM) (magenta) and exposing T^{287} (white) for autophosphorylation.

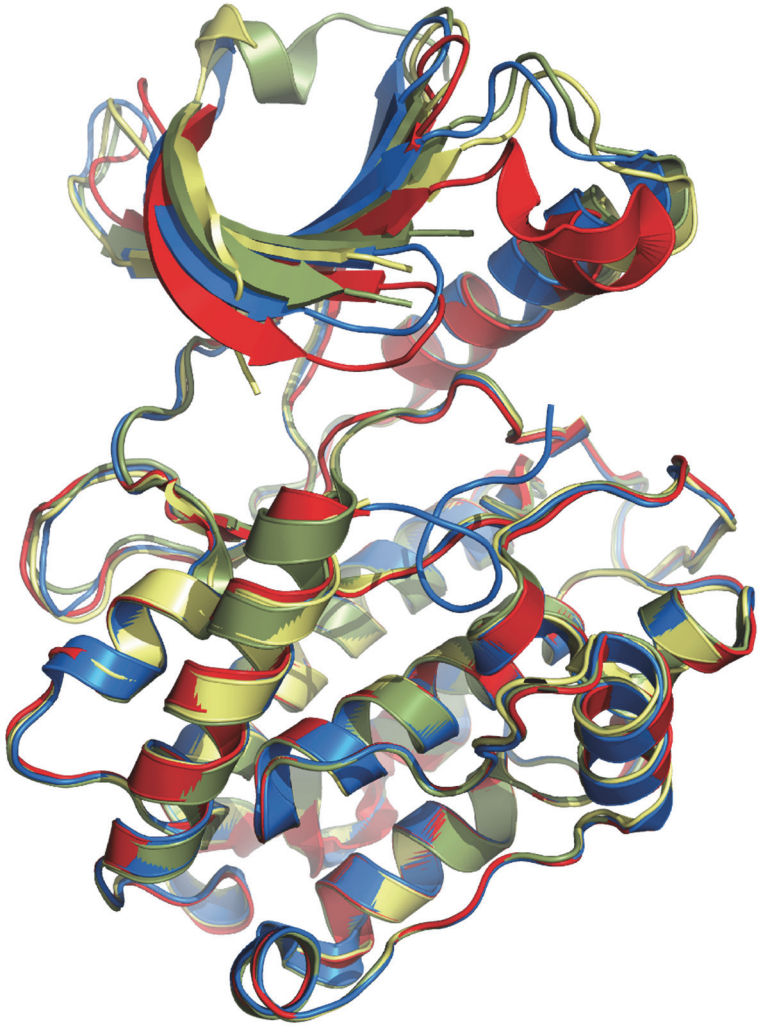

Figure 1.5 Structural alignment of CaMKII catalytic domains.
Structural alignment of CaMKII's catalytic domain and autoregulatory domain (ARD) from X-ray crystal structures of the autoinhibited state; hCaMKIIα_{13-302} (PDB ID: 2VZ6; COLOR), hCaMKIIβ_{11-303} (PDB ID: 3BHH; COLOR), hCaMKIIγ_{5-317} (PDB ID: 2V7O; COLOR), and hCaMKIIδ_{11-309} (PDB ID: 2VN9; blue).

1.5 Activation States of CaMKII

Under basal conditions, CaMKII exists in an autoinhibited state in which the autoregulatory domain occludes the catalytic surface; blocking substrate access to the active site and preventing substrate phosphorylation. Removal of the regulatory domain via proteolytic digestion or mutational truncation yields a fully active catalytic fragment devoid of the required activation by calmodulin (CaM) (Levine and Sahyoun 1987, Kwiatkowski and King 1989, Yamagata, Czernik et al. 1991, Cruzalegui, Kapiloff et al. 1992). CaM is a highly conserved, ubiquitous, eukaryotic protein that functions as the major calcium transducer in the cell. Made up of four Ca^{2+}-binding sites (EF-hands) with two in each lobe (N-terminal and C-terminal) connected by a flexible linker, CaM binding to Ca^{2+} leads to structural changes that increase CaM's affinity for its targets, one of which is CaMKII. Thus, CaMKII activation occurs following increased intracellular Ca^{2+} concentrations through the binding of Ca^{2+}/CaM to the CaM-binding domain of the autoregulatory domain which allows for the disengagement of the active site by the autoregulatory domain. Activation of each catalytic subunit within the holoenzyme requires the stoichiometric binding of Ca^{2+}/CaM for maximal activity; the degree of bound Ca^{2+}/CaM correlating with the level of substrate phosphorylation (Katoh and Fujisawa 1991, Meyer, Hanson et al. 1992). Prolonged activation through the binding of Ca^{2+}/CaM, can lead to autophosphorylation of T^{287} (β, γ , δ numbering used throughout this dissertation; CaMKIIα numbering is T^{286}), producing an autonomous form of the kinase (i.e. retained catalytic activity after CaM dissociation) (Lai, Nairn et al. 1986, Lou, Lloyd et al. 1986, Miller and Kennedy 1986, Lai, Nairn et al. 1987, Miller, Patton et al. 1988, Schworer, Colbran et al. 1988, Lou and Schulman 1989, Waxham, Aronowski et al. 1990).

The ability of CaMKII to retain enzymatic activity following the loss of its activator (Ca^{2+}/CaM) has led to the idea of CaMKII being a "memory switch" (Hanson, Meyer et al. 1994). T^{287} autophosphorylation is thought to disengage the autoregulatory domain from interacting with the autoinhibitory groove of the catalytic surface (Figure 1.3B). Autonomous (Ca^{2+}-independent) activity can reach 100% of the Ca^{2+}-dependent activity in *in vitro* assays with saturating levels of its activator Ca^{2+}/CaM. However, though the basal level of autonomous activity is dependent on the method and handling of tissue preparations and measurements of CaMKII activity (Lengyel, Cammarota et al. 2001), the level of autonomous activity generated in neurons by various stimulation protocols appears to reach 15-50% of the total CaMKII activity (Gorelick, Wang et al. 1988, MacNicol, Jefferson et al. 1990, Molloy and Kennedy 1991, Lengyel, Cammarota et al. 2001). These observations of submaximal CaMKII autophosphorylation are consistent with the studies by Persechini and colleagues that suggest free CaM is limiting in cells (Estep, Alexander et al. 1989, Persechini and Stemmer 2002). For this reason, it is likely that substrate phosphorylation by CaMKII operates under conditions of autophosphorylated and non-autophosphorylated subunits when Ca^{2+} is elevated in cells.

CaMKII is known to exhibit autophosphorylation at multiple sites and to varying degrees *in vivo*. Like T^{287}, $T^{306/307}$ (β, γ, δ numbering used throughout this dissertation; CaMKIIα numbering is $T^{305/306}$) reside within the autoregulatory domain of CaMKII; however, unlike T^{287} these residues lie within CaM binding domain (Figure 1.2A). The state of autophosphorylation for these sites has been shown to be important for synaptic plasticity and learning and memory. A consequence of their location in the CaM binding domain is that autophosphorylation at $T^{306/307}$ prevents subsequent CaM binding (Colbran

1993). Therefore, if this autophosphorylation event occurs prior to Ca^{2+}/CaM activation, the corresponding CaMKII subunit cannot be activated in the future unless the site is dephosphorylated or the autoregulatory domain is cleaved. However, if T^{287} autophosphorylation occurs first, a rapid phosphorylation of $T^{306/307}$ ensues if Ca^{2+}/CaM is removed (e.g. with the addition of EGTA). It is this state of the kinase that contributes to the enzymatic activity described as "autonomous" activity or when Ca^{2+}-independent activity is reported following T^{287} autophosphorylation.

1.6 Frequency Decoding/Tuning via Alternative Splicing and Isoform Differences

In the mid-1990's, Mayford and colleagues used transgenic mice containing CaMKII with a T^{287} phosphomimetic substitution to show that T^{287} autophosphorylation played an important role in regulating the frequency-dependent synaptic plasticity outputs of LTP and LTD (Mayford, Wang et al. 1995). Specifically, CaMKII was shown to modulate the frequency-response of CaMKII in hippocampal synapses; mice overexpressing CaMKII $T^{286}D$ exhibited normal LTP with high frequency stimulation. However, a shift in the threshold for LTD generation toward higher frequencies (10 Hz) was observed for mutant mice than typically required for wild-type mice (1 Hz). How this kinase is able to perform these important regulatory functions became a major focus in the field, as minor changes in the frequency of Ca^{2+} transients can lead to diverse cellular outputs (Boulware and Marchant 2008). The CaMKII holoenzyme was subsequently found to encode calcium-spike frequency into T^{287} autophosphorylation; a switch-like property influenced by calcium-spike duration and amplitude both *in vitro* (De Koninck and Schulman 1998) and *in vivo* (Eshete and Fields 2001). Furthermore, studies comparing different CaMKII

isoform variants showed that alternative splicing modulates the frequency-dependent response (T^{287} autophosphorylation and autonomous activity) (Bayer, De Koninck et al. 2002). Alternative splicing in CaMKII is predominantly associated with changes in the length of the linker region between the ARD and the hub domain (Figure 1.2A). Thus, even though the catalytic surface and substrate binding region of catalytic domains for all CaMKII isoforms are nearly identical, sensitivities for activation and autophosphorylation can be regulated by genetic encoding of linker length. A more recent study characterizing the first crystal structure of the holoenzyme also explored the mechanism of this tunable model of activation (Chao, Stratton et al. 2011). Their work suggests that the holoenzyme exists in an equilibrium between a compact and extended state in its autoinhibited form. In particular, the catalytic domain was either nestled close to the hub domain or projected away from the hub domain while being tethered by the ARD and linker region. SAXS analysis revealed that with a longer linker region, the kinase adopts a more extended conformation. Consistent with their model in which a more extended equilibrium state exposes the ARD (and CaM binding domain) for longer periods of time, reduced concentrations of Ca^{2+}/CaM were required to activate and autophosphorylate CaMKII. However, it must be noted that the compact state used to generate the crystal structure used a kinase lacking a typical linker region (though it was from a splice variant of beta) in addition to having a mutation in the ARD presumably to stabilize hydrophobic contacts.

1.7 Role of T^{287} Autophosphorylation in Synaptic Plasticity

Autophosphorylation of Thr^{287} is required for the function of CaMKII in synaptic plasticity and learning and memory as mouse models expressing non-autophosphorylatable

(A^{287}) or phosphomimetic (D^{287}) mutants alter both the generation of LTP and spatial learning in animals (Silva, Paylor et al. 1992, Silva, Stevens et al. 1992, Cho, Giese et al. 1998). Although the role of autonomous activity in regulating synaptic plasticity and learning is unknown, early studies speculated that autonomous activity generation served as a "molecular switch" of previous neuronal activation states to lead to a form of molecular memory (Lisman 1985, Miller and Kennedy 1986, Lisman 1994). Autophosphorylation was also found to regulate CaM binding affinity by creating further access to the autoregulatory domain; resulting in maximized CaM contacts with the CaM target domain and leading to >1000-fold increase in affinity (Meyer, Hanson et al. 1992, Putkey and Waxham 1996, Singla, Hudmon et al. 2001). Autophosphorylation also regulates CaMKII translocation and interaction with its substrates. Neuronal activation induces GFP-CaMKII to translocate from the cytoplasm to the presynaptic active zone (Tao-Cheng, Dosemeci et al. 2006) and the post-synaptic density (PSD) (Strack, Choi et al. 1997, Shen and Meyer 1999, Dosemeci, Tao-Cheng et al. 2001). The active zone is a macromolecular complex essential for docking and release of neurotransmitter vesicles (Figure 1.1) into the synaptic cleft. The PSD is a tightly-packed macromolecular structure of cytoskeletal, scaffolding, effectors, and receptors/ion channels required for responding to the presynaptic release of neurotransmitters from the receiving dendritic spine of the post-synaptic neuron (Sheng and Hoogenraad 2007, Swulius, Kubota et al. 2010). The mechanism of active zone recruitment of CaMKII is unknown; however, the GluN2B (formally referred to as NR2B) subunit of the NMDA receptor channel has been shown to be important for CaMKII binding to the PSD (Strack and Colbran 1998, Leonard, Bayer et al. 2002). Studies have found that autophosphorylation enhances CaMKII association with GluN2B, suggesting

that GluN2B could function to target autophosphorylated CaMKII to the PSD (Strack and Colbran 1998, Leonard, Bayer et al. 2002). Indeed, while autophosphorylation is not required for CaMKII translocation to the PSD, it is required for a delayed dissociation from this subcellular compartment as evidenced by the reduced retention times observed with autophosphorylation deficient CaMKII ($T^{287}A$) (Shen and Meyer 1999, Bayer, LeBel et al. 2006). In fact, a recent knock-in study using a mutant form of GluN2B deficient in CaMKII binding has shown that although CaMKII translocation is normal, CaMKII retention, LTP, and behavior are disrupted (Halt, Dallapiazza et al. 2012). The phosphorylation site of GluN2B (Ser^{1303}), which is important for CaMKII translocation to the PSD (Omkumar, Kiely et al. 1996, Strack, McNeill et al. 2000, Halt, Dallapiazza et al. 2012), conforms to a classical consensus phosphorylation motif for CaMKII. Classical CaMKII substrates have been found by oriented peptide libraries to follow a consensus motif (KRQQSFDLF) (Songyang, Blechner et al. 1994, Songyang, Lu et al. 1996); a sequence which also happens to mimic the autoregulatory domain of CaMKII. The role of GluN2B regulation by CaMKII in LTP and learning is unknown, as CaMKII phosphorylation produced small changes in this receptor's function directly. Which CaMKII substrates in the PSD are important for LTP and learning is hotly debated; however, the AMPA glutamate receptor subtype phosphorylation by CaMKII has been shown to be one substrate in particular that is critical for LTP. LTP requires enhanced AMPA receptor function and increased trafficking of GluA1 receptors to the PSD (Benke, Luthi et al. 1998, Malinow and Malenka 2002, Holmes and Grover 2006, Shepherd and Huganir 2007); two processes that CaMKII phosphorylation has been shown to regulate (Lu, Isozaki et al. 2010, Kristensen, Jenkins et al. 2011).

1.8 Structural Changes upon Activation

In addition to the holoenzyme structure (3SOA) (Chao, Stratton et al. 2011), several x-ray crystal structures of a monomeric catalytic domain along with the autoregulatory domain have been produced in various activation states. Knapp's lab (Rellos, Pike et al. 2010) produced structures of the autoinhibited catalytic domains from human CaMKII; CaMKIIα_{13-302} (2VZ6), CaMKIIβ_{11-303} (3BHH), CaMKIIγ_{5-317} (2V7O), and CaMKIIδ_{11-309} (2VN9). Overall, these structures exhibited very little structural differences (2° and 3°) (Figure 1.5) as expected by their high sequence similarity (Figure 1.3). They also generated CaMKIIδ_{11-335} (2WEL) in the Ca^{2+}/CaM activated state as well as the oligomerized hub domains of CaMKII$\delta_{333-475}$ (2W2C) and CaMKII$\gamma_{387-527}$ (2UX0). Though the crystal structures of the autoinhibited versus activated state only provide two snapshots and not a whole dynamic scene depicting activation, they suggest the types of structural rearrangements associated with the process. In the autoinhibited state, the autoregulatory domain region around T^{287} adopts an alpha-helical structure and interacts with a hydrophobic, autoinhibitory groove that starts at the base of the catalytic surface and extends up near the active site positioned at the intersection of the N- and C-terminal lobes. Activation via Ca^{2+}/CaM binding displaces the autoregulatory domain, leading to a subsequent collapse of the autoinhibitory groove by the shifting of the αD-helix.

1.9 CaM Trapping

In addition the establishment of Ca^{2+}/CaM-independent activity, T^{287} autophosphorylation also leads to an enormous increase in the binding affinity of CaM,

termed “CaM trapping” (Meyer, Hanson et al. 1992, Putkey and Waxham 1996, Waxham, Tsai et al. 1998, Singla, Hudmon et al. 2001). Using fluorescence emission anisotropy coupled with stop-flow device to measure a fluorescently tagged (dansylated) CaM, Meyer and colleagues (Meyer, Hanson et al. 1992) were able to show an increase of >3 orders of magnitude for the binding of CaM upon T^{287} autophosphorylation. However, for a mutant CaMKIIα lacking the ability to be autophosphorylated ($T^{287}A$), no trapping phenomena was observed (Meyer, Hanson et al. 1992). Of potential importance to the physiological role of autophosphorylation is that the autoregulatory domain of CaMKII transitions from one of the weakest targets of CaM to one of the strongest CaM-binding interactions observed. This trapping seems to ensure the association of CaMKII’s activator and may function to sequester CaM which already has limited availability in regions like the PSD; possibly prioritizing CaMKII signaling within this cellular compartment. Structurally, CaM trapping is not due to the holoenzyme architecture, as it was shown to occur in monomeric CaMKII (Meyer, Hanson et al. 1992). The changes in the affinity of the CaM were found to be the result of a drastic change in the off-rate (Meyer, Hanson et al. 1992) that was modeled using two peptides generated from the autoregulatory domain ($CaMKII_{296-312}$ and $CaMKII_{290-314}$) coupled with fluorescently labeled CaM ($CaM_{IAEDANS}$) (Putkey and Waxham 1996). Additional analysis using the peptide model (with more peptides of varying lengths) revealed that F^{294} and N^{295} contribute the most significantly to the changes in the dissociation rate mediated specifically through alterations in the off-rate. Furthermore, isothermal titration calorimetry (ITC) experiments revealed that differences in binding between long ($CaMKII_{291-312}$) and intermediate ($CaMKII_{296-312}$) peptides of autoregulatory domain (which differentially included $FN^{294/5}$) was due to enthalpy and not

entropy, suggesting that CaM trapping involves the formation of new hydrogen bonds instead of the burying of hydrophobic surface area (Tse, Giannetti et al. 2007). Mutational analysis also revealed that $F^{294}A$ and $N^{295}A$ led to an increase in the binding of CaM to non-T^{287} autophosphorylated CaMKII (16- or 13-fold decrease is in the dissociation rate constant (k_{off}), respectively (Singla, Hudmon et al. 2001), which is thought to be the result of decreased autoinhibitory interactions that these residues contribute to prior to autophosphorylation. However, these same mutations in the T^{287} autophosphorylated state resulted in 160- and 330-fold decreases in the k_{off}.

In light of the crystal structures of the apoCaMKII versus Ca^{2+}/CaM-activated form of human CaMKIIδ (Figure 1.3) (Rellos, Pike et al. 2010) which display autoinhibition (i.e., closed state) versus complete disinhibition of the ARD (i.e., open state) including F^{294} and N^{295}, it remained unclear how CaM trapping is prevented prior to T^{287} autophosphorylation with F^{294} and N^{295} contributing significantly to this process. A structural explanation of the prior biochemical studies was recently provided via electron paramagnetic resonance studies of dynamic conformational changes and CaMKII activation states in solution. This work showed that the R2 region (which includes F^{294} and N^{295}) of the ARD retains contacts with the catalytic domain in the Ca^{2+}/CaM-stimulated, yet non-T^{287} autophosphorylated state ($CaMKII_m^{-P}$) (Hoffman, Stein et al. 2011). Full displacement of the ARD occurs with autophosphorylation or phosphomimetic substitution at T^{287}. The tethering of the ARD could provide several mechanisms: 1) preventing CaM-trapping, 2) limiting intrasubunit autophosphorylation, and 3) limiting substrate access and phosphorylation.

1.10 Non-Canonical Activation/Autonomy

Disruption of the autoregulatory domain interaction with the catalytic surface via Ca^{2+}/CaM binding represents the canonical mechanism for direct activation of CaMKII, while the canonical mechanism for autonomous activation is through T^{287} autophosphorylation which further exposes the catalytic surface and serves to extend the activity after CaM dissociation. Yet several other mechanisms have recently been reported to fulfill the role of either Ca^{2+}/CaM binding or T^{287} autophosphorylation. Through interactions with the CaM-binding region of the autoregulatory domain, it was shown that alpha-actinin-2 could partially activate CaMKII (Jalan-Sakrikar, Bartlett et al. 2012). While sequence analysis revealed that the C-terminal domain of alpha-actinin-2 is homologous to the C-lobe of CaM, the activation was both Ca^{2+}-independent and substrate-selective. Similar to Ca^{2+}/CaM binding to CaMKII, phosphorylation of T^{307} blocked this interaction. While the interaction of alpha-actinin-2 appears to partially mimic the activation by Ca^{2+}/CaM, another type of non-canonical activation mimics phosphorylation of the autoregulatory domain and the autonomous activity thus generated; specifically oxidation (Erickson, Joiner et al. 2008, Erickson, He et al. 2011), nitrosylation (Coultrap and Bayer 2014), and glycosylation (Erickson, Pereira et al. 2013). The autoregulatory domain of CaMKII (Figure 1.2) contains several sites available for post-translation modification near T^{287}. Thus multiple signaling pathways funnel into a common mediator and are capable of generating a functionally important activation state of CaMKII.

1.11 Substrate-Kinase Interactions

While conserved in lower organisms such as prokaryotes, protein phosphorylation, the post-translational modification (PTM) involving the reversible addition of phosphate to amino acid side chains within proteins, is the most utilized form of PTM in signal transduction and plays a key role in the regulation of almost every type of cellular function in eukaryotes (Cohen 2002). Imbalances in the regulation of kinase activity can lead to a number of disorders (Roskoski 2015). Therefore protein kinases, the enzymes responsible for this reaction, have become one of the most studied classes of therapeutic targets by the pharmaceutical industry (Johnson 2009, Zhang, Yang et al. 2009, Dar and Shokat 2011). The human kinome is made up of 518 protein kinases, making it the second largest enzyme class and third largest protein family representing 1.7% of the human genome (Manning, Whyte et al. 2002). Of the 478 which are members of the sequence related superfamily of typical eukaryotic protein kinase (ePK) catalytic domains (the other 40 are labeled atypical protein kinases (aPKs)), 388 are classified as Ser/Thr kinases, while the others phosphorylate Tyr residues (Manning, Whyte et al. 2002). The ePKs all possess structurally similar catalytic domains (~290 amino acids) comprised of an N-terminal lobe of mainly β-sheets and a larger C-terminal lobe; the active site situated between the two domains. Kinases are responsible for maintaining the vast and complex phosphoproteome network; considered to include at a minimum ~33% of all cellular proteins (Cohen 2001) and more likely in the 40-45% range (Junger and Aebersold 2014); yet the full scope of the complete phosphoproteome for any species remains to be experimentally mapped. The many benefits to this type of modification, namely that it is catalytically fast, reversible, single/binary addition, are only appreciated by the specificity with which these kinases can modify their

targets. These can range from one substrate to hundreds of substrates, all while distinguishing between the estimated ~500,000-700,000 phosphorylatable sites in a typical eukaryotic cell (Ubersax and Ferrell 2007, Lemeer and Heck 2009). For this reason, mechanisms regulating substrate selection and specificity are important for understanding both the normal physiological actions of a given kinase as well as ways to target the kinase for intervention in pathophysiological states.

Substrate selection among kinases is a complex, multifaceted process with multiple different determinants which allow kinases to phosphorylate and regulate signaling networks. These factors include the structure of the active site/catalytic cleft, distal docking sites, conditional docking sites, targeting subunits, localization, scaffolding, and system-level effects.

1.11.1 Catalytic/Active Site

The active site of protein kinases has been shown to be regulated by intrinsic sequences or core motifs on substrates that optimize the ionic and hydrophobic characteristics of the kinase surface for optimal phosphorylation (Kreegipuu, Blom et al. 1998, Taylor, Kim et al. 2005). As mentioned above, roughly 80% of the ePKs phosphorylate at Ser/Thr as opposed to Tyr (Manning, Whyte et al. 2002), and accordingly have conserved residues in the active site which allow for a smaller aliphatic phosphoacceptor (Taylor, Radzio-Andzelm et al. 1995) whereas Tyr kinases utilize a separate group of conserved residues for large, aromatic residue (Pinna and Ruzzene 1996). Furthermore, the Asp-Phe-Gly (DFG) motif, a tripeptide motif within the catalytic site that is highly conserved among kinases (Bayliss, Haq et al. 2015), is followed by a residue that has been shown to be a

major determinant for the preference for Ser or Thr (though not absolutely), termed the DFG+1 residue (Chen, Ha et al. 2014). CaMKII contains a Leu at this site (residue 160 in β, γ, δ numbering); therefore, it predicts a preference for Ser over Thr as the phosphoacceptor. In addition, it was recently found that the composition of the phosphorylation motif, and particularly whether the phosphoacceptor was Ser versus Thr, was a key determinant for mTORC1 "substrate quality"; the intrinsic ability for a phosphorylatable site to act as a substrate in cells. Due to substrate quality and the related concept "relative specificity" (i.e. enzymes have a tendency to differentially and preferentially interact with their substrates), specific phosphorylation motifs of mTORC1 substrates were able to set the sensitivity to various stimuli, thus allowing mTORC1 to selectively phosphorylate substrates even with the same stimuli (e.g. differential phosphorylation following rapamycin inhibition) (Kang, Pacold et al. 2013, Zeng 2014).

Moving outside of the phosphoacceptor site (P-site), a significant amount of substrate recognition and specificity arises from the amino acids generally within 4-7 residues both N- and C-terminally. These sequences which interact proximally to the active site have been shown to confer substrate specificity by their intrinsic chemical composition arranged into ordered motifs that optimize the ionic and hydrophobic characteristics of the kinase surface for optimal phosphorylation (Kreegipuu, Blom et al. 1998, Taylor, Kim et al. 2005). Owing to the differences among kinases on their catalytic surface, consensus sequence motifs for optimal substrate specificity varies among kinases (though with some overlap) and have been identified through various experimental methods. Initially, mutations of known substrate sequences provided information regarding the important residue composition and position (Daile, Carnegie et al. 1975, Kemp, Bylund et al. 1975, Pearson

and Kemp 1991). However, with the advent of oriented peptide libraries, kinases were able to be screened in an unbiased manner phosphorylating a pool of ~2.5 billion soluble peptides (Songyang, Blechner et al. 1994) and subsequently determining the optimal amino acid at each position by correlation to its abundance via Edman degradation sequencing. More recent studies have optimized these oriented library approaches, such that they rely on radiolabeled [γ-^{32}P] ATP, simplifying the process and allowing for a more rapid profiling of kinase specificities (Songyang, Lu et al. 1996, Hutti, Jarrell et al. 2004).

Like a number of other basophilic kinases (e.g. PKA, PKA, and AMPK), the CaM kinase family is classically defined with a preference for an Arg/Lys at the P_{-3} position (i.e. three residues N-terminal to the phosphorylation site). However, neither of the two identified CaMKII phosphorylation sites in GluA1 (a subunit of the AMPA receptor) which are important for these processes (S^{831} and S^{567}) look anything like the typical consensus phosphorylation site of CaMKII. PSD-95, the main scaffolding protein in the PSD, is yet another example of a functionally important CaMKII substrate with a non-consensus CaMKII site (S^{73}); phosphorylation at this site prevents spine growth as well as LTP (Steiner, Higley et al. 2008). Furthermore, sequence analysis of the CaMKII substrates (>200) in PhosphoSitePlus suggests that a majority of the phosphorylation sites would be considered poor substrates given the limited similarity many of them possess to the consensus motif. However, a poor substrate could still be biologically relevant as a high K_m could be overcome by direct targeting and a low V_{max} could be optimized by the fact that small numbers of catalytic events can still produce a biological effect. However, since the PSD is replete with protein phosphatases, it is likely that shifting the equilibrium

towards a phosphorylation state would require mechanisms to enhance the phosphorylation of low-affinity substrates.

1.11.2 Docking Sites/Allosteric Interactions

Beyond the active site, distal regions of a kinase may serve as docking sites for regions of the substrate upstream or downstream of the P-site, leading to an increase in substrate specificity. A number of kinases are known to utilize this type of mechanism including mitogen-activated protein (MAP) kinases, which play essential roles in the signal transduction pathways in the cell. These sites may be quite distant from the phosphoacceptor site. In the case of mitogen-activated protein kinase 2 (MK2), a substrate for the upstream an MAPK kinase (MAPKK) p38α, a 30aa sequence (aa371-400) important for binding is quite removed from the three upstream phosphorylation sites (T^{222}, S^{272}, T^{334}) (Lukas, Kroe et al. 2004). The docking site is essential for the formation of a tight, high-affinity complex with P38α; the removal of this domain leads to a decrease in the catalytic efficiency of MK2 phosphorylation by greater than 2 orders of magnitude (Lukas, Kroe et al. 2004). One consequence of the docking site is allowing for an increase in the effective concentration of the substrate, thereby yielding an increase in phosphorylation. This effect is produced by the bidentate interaction of the substrate with the kinase and has been mapped *in vitro* with other MAPKs (e.g. ERK) using a modified SPOTs synthesis method for the generation of immobilized peptide arrays on derivatized phosphocellulose membranes (Espanel, Walchli et al. 2003). In this study, double peptide synthesis was used to generate both a docking site peptide and a substrate peptide within a single SPOT, resulting in both increased binding and phosphorylation of the substrate

peptide upon the application of the upstream MAPK. In a somewhat analogous study, Naffin et al. showed that bidentate interactions with immobilized peptides had the ability to increase the half-lives for peptide-protein complexes >3 orders of magnitude (Naffin, Han et al. 2003). However, the substrate localization effect of the docking sites is not the only mechanism by which these distal interactions enhance phosphorylation. It was recently shown that the p38α docking site interaction regulates the enzymatic activity through an allosteric mechanism. Binding of the docking peptides led to allosteric structural changes resulting in an increase in the ATP and phosphoacceptor binding affinities, resulting in enhanced catalytic turnover (Tokunaga, Takeuchi et al. 2014). Thus, substrate specificity is maintained through the specific enhancements afforded by the docking site interactions.

Previous literature has suggested that the catalytic surface contains both a targeting site (T-site) and a substrate site (S-site) (Bayer, De Koninck et al. 2001). The T-site includes additional contacts on the catalytic surface which the autoregulatory domain of CaMKII binds to in the autoinhibited state. It is thought that substrates such as GluN2B and the peptide substrate autocamtide-2 (AC-2) which is derived from CaMKII's autoregulatory domain around T^{287} are able to mimic the autoregulatory domain and interact with the T-site; an interaction which is also believed to give rise to their increased affinity (Bayer, De Koninck et al. 2001, Bayer, LeBel et al. 2006). Specific mutants within the T-site have been generated (I205K) which have been shown to only disrupt the targeting of T-site binding substrates; whereas those that only interact with the S-site (e.g. Syntide) are not affected (Bayer, LeBel et al. 2006). This mutant was also found to decrease translocation

to the PSD (Bayer, De Koninck et al. 2001); however, its effect on phosphorylation within the PSD is unknown.

1.11.3 Targeting Subunits and Scaffolds

The docking sites of some kinases resides within the kinase domain while the docking peptide resides within the substrate protein, yet there are other kinases which employ additional proteins to regulate substrate specificity. These enzyme-interacting proteins are classified into various groups with terms such as adaptor (or targeting subunit), docking, anchoring, or scaffolding proteins. However, the defining characteristics between some of these terms are ambiguous and overlapping. For this reason, Langeberg and Scott (Langeberg and Scott 2015) have suggested that adaptor proteins refer to soluble proteins which include protein interaction domains, for example the cyclins which form stable complexes with cyclin-dependent kinases (CDKs) and modulate substrate selectivity (Schulman, Lindstrom et al. 1998, Cheng, Noble et al. 2006). Docking proteins are considered to be similar to adaptor proteins, yet include membrane-associating elements or motifs (e.g. a pleckstrin homology (PH) domain or myristoylation sequence) in their N-terminal region (e.g. insulin receptor substrate (IRS) class (IRS1-4)) (Langeberg and Scott 2015). Scaffolding proteins, having been used often times synonymously with the term anchoring proteins, are defined as having at least one of several attributes: 1) They act as an organizational tether for multiple successive kinases and/or signaling molecules within a signaling cascade; 2) They concentrate and organize enzymatic activity to a defined region of action; or 3) They tether opposing enzymes (e.g. kinases and phosphatases) for the regulated, coordinated control of effectors molecules. One of the key roles of adaptors,

docking proteins, and scaffolding proteins is the localization of kinases; both the localization of kinases to regions of the cell as well as with substrate molecules. One effect this has is decreasing the volume of the spatial searching of substrates, thereby driving substrate selectivity by exclusion of potential substrates.

The rather unique dodecameric holoenzyme structure of CaMKII essentially allows CaMKII to act as its own adaptor protein. As CaMKII is capable of intersubunit autophosphorylation at T^{287}, multimerization allows for a substrate molecule, in this case the autoregulatory domain for another subunit, to be tethered to the kinase through interactions with the association (hub) domains. Like many adaptor proteins which form stable complexes with the kinases they interact with, the association domains form rather stable holoenzymes. In fact, there is little evidence to suggest that subunits exists in monomeric or dimeric forms. Stratton et al. (2014) recently suggest that subunits exchange between holoenzymes under certain activation and autophosphorylation states (Stratton, Lee et al. 2014, Bhattacharyya, Stratton et al. 2016). However, their model of dimeric pair swapping does not necessarily require freely diffusing subunits if the process involves two holoenzymes interacting directly during swapping.

The multimeric architecture of the holoenzyme, sustained by the association domains, allows for several important features for CaMKII function. First, it allows for the intersubunit autophosphorylation at T^{287} to occur as an intraholoenzyme event, thereby reducing the nature of the bimolecular reaction to an intramolecular one in which the concentration of CaMKII and temperature have greatly diminished influences on the rate of the reactions. In this way, CaMKII's unique dodecameric structure and the ability to self-regulate its activity through autophosphorylation allows for the integration of

intracellular calcium transient signals (as during neuronal activation) into graded levels of activation (thereby serving as a "molecular switch" of previous neuronal activation states to lead to a form of molecular memory), regardless of the local concentration of CaMKII. Second, it allows for a genetically encoded mechanism by which to regulate and modulate the threshold for activation/autophosphorylation. Specifically, this has been shown to be accomplished by alternative splicing within the linker region connecting the autoregulatory domains and the association domains (Bayer, De Koninck et al. 2002, Chao, Stratton et al. 2011). Third, the dodecameric assembly of the CaMKII holoenzyme affords the kinase the ability to interact with multiple substrates or targets simultaneously; a feature which may in turn regulate CaMKII enzymatic function and localization. The multivalent interactions occurring concurrently within a given timeframe would be expected to have high avidity; an accumulated measure of the combined affinities of each interaction. Thus, the multimeric nature of the CaMKII holoenzyme would be expected to contribute to the substrate specificity of the kinase.

1.11.4 System-level Effects

The regulatory mechanisms controlling kinase phosphorylation and specificity increase in complexity as one moves beyond the typical *in vitro* methodologies used to study kinase-substrate relationships and considers *in vivo* environments which operate under additional mechanisms referred to as systems-level effects. Typical reaction conditions for *in vitro* assays often utilize activator and substrate concentrations (including ATP) that are not limiting and in which only one phosphorylatable substrate is used. However, many kinases have more than one substrate in the cell, which can produce competitive effects on substrate

phosphorylation. Preferential interactions of kinases with high affinity substrates would tend to limit the available kinase for interactions with lower-affinity substrates. This type of effect would tend to lead to increased specificity and/or temporal ordering of substrate phosphorylation. Cyclin-dependent kinases (CDKs), specifically Cdk1 has been shown to operate under such a mechanism with Wee1 (a nuclear kinase) in yeast and was able to be recapitulated with purified components *in vitro* (Kim and Ferrell 2007). Another system-level effect shown to direct the specific of kinase interactions is multisite phosphorylation, where the combination of numerous nearby phosphorylation events determine the recognition and specificity of an interaction. For example, the recognition of the CDK inhibitor Sic1 by the ubiquitin ligase SCF^{Cdc4} is determined by the summation of multiple low-affinity interaction sites created by multiple phosphorylation events (Tang, Orlicky et al. 2012). Other kinases can controlled by the local concentration of immobilized substrates such that a higher concentration of substrate allows for kinases to effectively outcompete phosphatase activity within a specific environment (Liao, Su et al. 2009).

CaMKII likely encounters these various forms of system-level effects governing kinase specificity. For instance, within the PSD, CaMKII interacts with and phosphorylates >40 known substrates, some involving multiple sites of phosphorylation (Yoshimura, Aoi et al. 2000, Yoshimura, Shinkawa et al. 2002). Based on the sequences of the phosphorylation sites themselves, many of the sites lack much similarity to the consensus CaMKII phosphorylation motif. Thus, it is likely that they are low-affinity substrates and that these sites must compete with other high-affinity substrates within the PSD such as GluN2B. Many of these PSD substrates are immobilized within the cytoskeletal web of the PSD. Thus, the equilibrium between kinase and phosphatase activity would be subject to both

the density of the substrate as well as multivalent avidity of the CaMKII holoenzyme. Interestingly, as activation of the CaMKII holoenzyme produces graded levels of T^{287} autophosphorylation (likely due to different numbers of subunits activated within the holoenzyme) in response to the frequency of Ca^{2+} transients, it is likely that the degree of activation alters substrate phosphorylation within these types of environments.

1.12 Research Goals

CaMKII is a multifunctional kinase with broad substrate specificity involved in many different cellular functions. As such, CaMKII has been shown to phosphorylate a vast number of substrates including >40 substrates identified in the PSD alone (Yoshimura, Aoi et al. 2000, Yoshimura, Shinkawa et al. 2002), with likely many more remaining unidentified. In fact, databases such as PhosphoSitePlus, which include known CaMKII substrates based on *in vivo* and *in vitro* data, list more than 200 unique sites (Hornbeck, Kornhauser et al. 2012). This leads to the question of how a single kinase which is known to regulate many processes (often with opposing effects/outcomes) through the specific phosphorylation of a certain substrate effector, is able to preferentially direct its phosphorylation for its intended target. While it is known that autophosphorylation is required for certain functional outputs (e.g. LTP), the mechanism by which CaMKII turns various activation states into altered substrate selection and therefore disparate forms of synaptic plasticity is not known. Furthermore, whether the multimeric nature of the CaMKII holoenzyme also produces unique regulation and substrate interactions is unknown; however, having multiple catalytic subunits in each holoenzyme could afford enhanced substrate and binding partner interactions leading to altered rules for substrate

selection and phosphorylation compared to the monomeric kinases (Naffin, Han et al. 2003). Understanding the various means by which CaMKII substrate selection is regulated may provide crucial insight into pathological states of the brain, including ischemic stroke and brain trauma, where CaMKII is aberrantly activated and contributes to neurodegeneration.

While CaMKII has been studied for >30 years, the complexity of its holoenzyme structure and autoregulation through multisite phosphorylation within its ARD still leaves some unanswered questions regarding the translation of activation state into multiple downstream effects. The central focus of this work was to explore the impact that T^{287} autophosphorylation and/or degree of activation within the holoenzyme has on kinase activity. Our data presents a functional consequence of the ARD on the enzymatic activity in the absence of T^{287} autophosphorylation; namely, the narrowing of substrate specificity through competition with substrates for access to the catalytic domain. We believe this effect may be further modulated by the extent of holoenzyme activation/autophosphorylation as multivalent effects can also modulate substrate specificity.

CHAPTER 2. Control of CaMKII Substrate Selectivity through ARD Substrate Filtering and Autophosphorylation

2.1 Introduction

Calcium/calmodulin-dependent protein kinase II (CaMKII) is a multimeric holoenzyme (8-14 subunits) generated from four closely related genes (α,β,γ,δ) that is implicated in regulating diverse substrates involved in a host of cellular processes from metabolism and cell cycle control to calcium homoeostasis and excitable cell activity and plasticity (Hudmon and Schulman 2002). Like many CaM-regulated enzymes, binding of the calcium sensor calmodulin (CaM) to a target sequence within an autoregulatory domain (ARD) activates CaMKII through disinhibition of the ARD. As CaMKII does not possess an activation loop as seen in many other kinases, Ca^{2+}/CaM has been considered as a binary switch leading to substrate phosphorylation via ARD disinhibition (Figure 1.3). The unique multimeric architecture of CaMKII permits coincident CaM-binding within the holoenzyme to support an intersubunit autophosphorylation (T^{286} α-isoform and T^{287} β,γ,δ isoforms) event within its ARD that is essential to CaMKII's function *in vivo* (Cho, Giese et al. 1998, Giese, Fedorov et al. 1998, Glazewski, Giese et al. 2000, Gustin, Shonesy et al. 2011). While recent data suggests that Ca_{2+}/CaM alone is not sufficient to fully displace the ARD from the catalytic domain, full displacement occurs following T^{287} autophosphorylation (Hoffman, Stein et al. 2011). This autophosphorylation event produces enhanced CaM-binding affinity (Meyer, Hanson et al. 1992) and autonomous activity (Ca^{2+}/CaM-independent activity) (Schworer, Colbran et al. 1988, Lou and Schulman 1989).

Early knock-out studies in mice found that CaMKIIα is important for both hippocampal long-term potentiation (LTP) (Silva, Stevens et al. 1992) and spatial learning (Silva, Paylor et al. 1992). Later studies using knock-in animal models that mimic or ablate T^{287}

autophosphorylation have clearly shown a functional role for this process *in vivo* (Cho, Giese et al. 1998, Giese, Fedorov et al. 1998, Glazewski, Giese et al. 2000, Gustin, Shonesy et al. 2011). Specifically, removing the ability to autophosphorylate this site ($T^{286}A$) (Giese, Fedorov et al. 1998) or phosphomimetic mutation ($T^{286}D$) (Bach, Hawkins et al. 1995, Mayford, Wang et al. 1995) to generate a constitutive form in the α-isoform impaired both hippocampal LTP and spatial learning, though this could be due to issues with hippocampal development. This led to studies involving temporally controlled expression of the transgenes which further indicate using a $T^{287}D$ mutation that autophosphorylation was important for the hippocampal learning and LTP (Mayford, Baranes et al. 1996).

While the exact functional role of T^{287} autophosphorylation remains debated; recent work suggests that T^{287} autophosphorylation may mediate opposing forms of neuronal plasticity (Shonesy, Jalan-Sakrikar et al. 2014) via differential substrate phosphorylation (Coultrap, Freund et al. 2014). This result is particularly surprising considering that autophosphorylation was shown by this laboratory to possess a very limited influence on catalytic turnover or substrate specificity (Coultrap, Buard et al. 2010, Coultrap, Barcomb et al. 2012). However, given that CaMKII is a multifunctional enzyme which phosphorylates a number of substrates important for synaptic plasticity (as well as many other cellular processes), it seems that changes in kinase output associated with the autophosphorylation could be a direct mechanism underlying the biological data in the literature. In an effort to resolve the functional consequences of autophosphorylation on substrate phosphorylation, we considered the recent electron paramagnetic resonance (EPR) data exploring the impact of this process on ARD interactions with the catalytic domain.

While crystal structures for apoCaMKII and the Ca^{2+}/CaM-activated form of human CaMKIIδ (Figure 1.4) (Rellos, Pike et al. 2010) display autoinhibition (i.e. closed state) versus complete disinhibition and unfolding of the ARD (i.e. open state), in solution, EPR spectroscopy indicates that regions of the ARD continue to interact with the catalytic surface even in the Ca^{2+}/CaM-activated, non-T^{287} autophosphorylated state ($CaMKII_m^{-P}$) (Hoffman, Stein et al. 2011). T^{287} autophosphorylation in the presence of Ca^{2+}/CaM leads to complete destabilization and dissociation of the ARD. Biochemical studies have shown that this allows optimal CaM-binding as evidenced by a 20,000-fold enhancement in Ca^{2+}/CaM binding affinity (Meyer, Hanson et al. 1992); a state known as CaM-trapping.

The functional consequences on substrate phosphorylation stemming from partial ARD disinhibition in the non-T^{287} autophosphorylated state remain unclear. A potential consequence of such a conformeric equilibrium between ARD and catalytic surface in the Ca^{2+}/CaM-bound state (i.e. non-trapped low-affinity state), is that substrate access may be gated as the catalytic surface transitions between open and closed states; an intrinsic inhibitory mechanism disengaged by autophosphorylation. Thus while autophosphorylation and Ca^{2+}/CaM binding maximizes substrate accessibility, substrate binding might be expected to shift the catalytic surface from closed to open states, thereby enhancing Ca^{2+}/CaM binding in the absence of autophosphorylation ($CaMKII_m^{-P}$). We postulated that mutagenesis or inability to control T^{287} autophosphorylation could have previously masked interactions between autophosphorylation and substrate activity/specificity. Therefore, we intended to explore the role of autophosphorylation on the activity of the kinase; specifically focused on potential substrate-dependent effects.

In this study, we use diverse, validated CaMKII substrates in diffusion-limited and diffusion-restricted reactions to show that T^{287} autophosphorylation underlies a switch-like property of the ARD to regulate CaMKII's substrate specificity. While CaMKII's catalytic domain exhibits broad substrate specificity in the absence of its ARD, phosphorylation is restricted to high-affinity substrates in the absence of autophosphorylation. Because T^{287} autophosphorylation (and phosphomimetic substitutions) restores maximal activation and broad substrate selectivity, we find that the ARD of *activated* CaMKII tunes substrate selectivity by competing for substrate binding to the catalytic domain. Our data suggest that calcium-spike frequency encoding (De Koninck and Schulman 1998) into T^{287} autophosphorylation permits an autoregulatory switching mechanism to match substrate selectivity with diverse cellular responses.

2.2 Materials and Methods

2.2.1 Expression and Purification of CaMKII and Calmodulin

Recombinant human CaMKIIδ (NCBI RefSeq: NP_742113.1) with an N-terminal 6xHN tag was integrated into a baculoroviral construct (BacPAK9-6xHN), amplified in Sf9 insect cells, and expressed in Hi5 (*T. ni*) insect cells (Takeuchi-Suzuki, Tanaka et al. 1992) (Brickey, Colbran et al. 1990). Site-directed mutagenesis was used to generate monomeric hCaMKII$\delta_{1\text{-}317}$ (i.e. CaMKII$_m$) (by truncation through the addition of stop codon at aa318) as well point mutants (see Table 2.1 for a list of primers). Kinases were purified under reducing conditions by affinity chromatography (NiNTA resin) followed by size exclusion chromatography (Sephacryl S-400 [holoenzyme] or S-300 [CaMKII$_m$]) using an Äkta Purifier (Amersham) (Bradshaw, Hudmon et al. 2002, Ashpole, Herren et

al. 2012). SDS-PAGE of the purified proteins revealed a single band with purities >98%. A catalytic fragment for hCaMKIIδ was generated by chymotryptic digestion of purified holoenzyme (Kwiatkowski and King 1989, Yoshimura, Nomura et al. 1996), followed by sequential affinity purification utilizing CaM-sepharose to remove any non-proteolyzed subunits with Ni-NTA resin to enrich for the constitutively active catalytic fragment. SDS-PAGE and western blotting with an anti-phospho-$T^{286/287}$ antibody (Millipore) verified that this fragment lacked the region around T^{287}. Recombinant calmodulin (wt or C^{75}-containing mutant) was expressed and purified in E.coli as described previously (Singla, Hudmon et al. 2001, Gaertner, Kolodziej et al. 2004) via boiling, ammonium sulfate precipitation, and phenyl-sepharose affinity chromatography.

Primer Name	Primer Sequence (5' to 3')
hCaMKII-delta-K318Stop_F	5'-aaggaatttctcagcagcctagagtttgttgaagaaacc-3'
hCaMKII-delta-K318Stop_R	5'-ggtttcttcaacaaactctaggctgctgagaaattcctt-3'
hCaMKII-alpha-K317Stop_F	5'-acttctccggagggtagagtgggggaaac-3'
hCaMKII-alpha-K317Stop_R	5'-gtttcccccactctaccctccggagaagt-3'
hCaMKII-delta-T287A_F	5'-tgatgcacagacaggaggctgtagactgcttgaag-3'
hCaMKII-delta-T287A_R	5'-cttcaagcagtctacagcctcctgtctgtgcatca-3'
hCaMKIIdelta-T287V_F	5'-ccatgatgcacagacaggaggttgtagactgcttgaagaaat-3'
hCaMKIIdelta-T287V_R	5'-atttcttcaagcagtctacaacctcctgtctgtgcatcatgg-3'
hCaMKIIdelta-T287N_F	5'-atgatgcacagacaggagaatgtagactgcttgaag-3'
hCaMKIIdelta-T287N_R	5'-cttcaagcagtctacattctcctgtctgtgcatcat-3'
hCaMKII-delta-T287D_F	5'-ccatgatgcacagacaggaggatgtagactgcttgaagaaat-3'
hCaMKII-delta-T287D_R	5'-atttcttcaagcagtctacatcctcctgtctgtgcatcatgg-3'

Table 2.1 Primers for generation of monomeric CaMKII.

2.2.2 Soluble Peptide Substrate Phosphorylation Assays

Soluble peptide substrates (generally 15mers) were obtained (Biopeptide Co., Inc.) and utilized in standard radioactive activity assays. In typical Ca^{2+}/CaM-dependent reactions, 50-200 μM substrate was used in the presence of 50 mM HEPES pH 7.4, 100 mM NaCl, 10 mM $MgCl_2$, 0.2 mM $CaCl_2$, 1 μM CaM, 100 μM cold ATP, 60 μCi/ml [γ-^{32}P] ATP, and 5-10 nM CaMKII (per subunit). In Ca^{2+}/CaM-independent reactions, 5 mM EGTA (or BAPTA) was used to chelate free calcium. This constitutive (i.e. autonomous) activity in the absence of calcium was expressed a percentage of the Ca^{2+}/CaM-dependent activity. Reactions were carried out at 30°C for 1 minute and quenched by spotting onto Whatman Grade P81 ion exchange chromatography paper (Whatman, GE Healthcare, Piscataway, NJ). The filter papers were washed with 75 mM phosphoric acid 3 times for 5 minutes each and subsequently quantified in a scintillation counter (Beckman) via the Cerenkov counting method (Roskoski 1983, Hudmon, Aronowski et al. 1996). AC-2), a CaMKII substrate derived from the CaMKII T^{287} autophosphorylation site was used for standard soluble peptide substrate reactions.

2.2.3 Pre-Autophosphorylation Reactions

For reactions involving T^{287} autophosphorylated CaMKII, a pre-reaction was performed in the presence of 20 mM HEPES pH 7.4, 100 mM NaCl, 10 mM $MgCl_2$, 0.5mM $CaCl_2$, 5 μM CaM, 500 μM cold ATP and 500nM kinase for 10 minutes on ice. In Figure 2.17, autonomous $CaMKII_m$ was allowed to undergo complete "burst" phosphorylation (i.e. rapid phosphorylation of T^{306}/T^{307} associated with the removal of Ca^{2+}/CaM following prior T^{287} autophosphorylation. Therefore, following a standard T^{287}

autophosphorylation pre-reaction described above, Ca^{2+}/CaM was chelated with 10 mM EGTA for 10 minutes at 30°C. Subsequent substrate phosphorylation assays using this form of the kinase included 2 mM EGTA in place of additional Ca^{2+}/CaM.

2.2.4 SPOTs Peptide Substrate Phosphorylation Assay

Peptides were synthesized using the SPOT method (Frank and Overwin 1996, Frank 2002) onto β-alanine derivatized cellulose membranes via a MultiPep synthesizer (Intavis AG, Cologne, Germany). The peptide blots were blocked with 5% BSA in 50 mM HEPES pH 7.4, 100 mM NaCl, 1 mM EDTA, and 0.02% NP-40 for 30 minutes followed by three washes in 100 mM Tris-HCl pH 7.4. Membranes were subjected to a kinase phosphorylation assay in the presence of 50 mM HEPES pH 7.4, 100 mM NaCl, 10 mM $MgCl_2$, 0.2 mM $CaCl_2$, 1 μM CaM, 0.2 mg/ml BSA, 1 mM DTT, 100 μM cold ATP, 6-12 μCi/ml [γ-^{32}P] ATP, and 5-10 nM CaMKII (per subunit). The reactions were incubated at room temperature for 4 minutes unless otherwise noted, terminated with three washes (100 mM sodium phosphate pH 7.0, 1 M NaCl, 10 mM EDTA) and dried. The extent of radioactive phosphate incorporation was quantified using a Fujifilm phosphoimager and expressed as photostimulated luminescence (PSL/mm^2) for a 1.5 mm x 1.5 mm circle centered on each spot. 3-4 replicate spots were averaged for each peptide for a given condition with error bars indicating SD, unless otherwise noted. Substrates were collected from PhosphoSitePlus corresponding to sites shown to be CaMKII substrates (217 in total) via various methods (Hornbeck, Kornhauser et al. 2012). Each 15mer peptide, centered on the confirmed CaMKII phosphorylation site (P_0), was synthesized via SPOTs method and phosphorylated for 10 minutes at room temperature.

2.2.5 GST-Fusion Peptide Substrate Phosphorylation Assays

Short 21mers (55mer for GluN2B) of several CaMKII substrates were subcloned into pGEX-6P-1 (Clontech / AscI-PacI version from Well's lab) and expressed as GST-fusions (Ashpole, Herren et al. 2012) in BL21(DE3) E.coli 4 hours at 37°C using 1 mM isopropyl 1-thio-β-D-galactopyranoside (IPTG). Frozen aliquots of the lysates were made following lysis of the cell pellets in 20 mM Tris, pH 7.4, 200 mM NaCl, 1 mM EDTA, 0.1% Tween-20 and 2X protease inhibitors (Calbiochem, catalog no. 539137). On the day experimentation, lysates of the GST-fusion proteins were bound and purified on glutathione resin in the presence of 2 mM EDTA and additional 2X protease inhibitors. Lysates of the expressed proteins were bound to glutathione beads for 2 hours at 4°C followed by extensive washing in 20 mM Tris, pH 7.4, 200 mM NaCl, 1 mM EDTA, 0.1% Tween-20 and 1× protease inhibitors to remove unbound protein yielding saturating amounts of GST-fusion proteins bound to glutathione resin beads. Phosphorylation of GST-fusion proteins (20 µl bed volume) with 10 nM $CaMKII_m$ in the presence of 50 mM HEPES pH 7.4, 100 mM NaCl, 10 mM $MgCl_2$, 0.5 mM $CaCl_2$, 5 µM CaM, 100 µM cold ATP, 120 µCi/ml [γ-^{32}P] ATP. For the pre-T^{287} autophosphorylated monomer, 1 µM kinase was incubated for 20 minutes on ice in conditions described above. The GST-fusion substrates were phosphorylated for 10 minutes at room temperature with shaking. The reaction was quenched by the addition of 50 mM HEPES pH 7.4, 400 mM NaCl, 50mM EDTA and the beads were washed extensively. Subsequently, the GST-fusions were eluted from the beads in 2X LDS sample buffer (with β-mercaptoethanol) at 70 °C for 5 minutes. SDS-PAGE of the eluted samples followed by Coomassie staining was used to detect and

visualize the total protein while phosphorimaging (FUJIFILM) was used to detect phosphorylation using MultiGauge v3.1. GST-fusions of GluN2B$_{1275-1329}$ (NASTTKYPQSPTNSKAQKKNRNKLRRQHSYDTFVDLQKEEAALAPRSVSLKDK GR), Syntide$_{21mer}$ (MPLARTLSVAGLPGKKDWEDE), GluA1$_{839-859}$ (MKGFCLIPQQSINEAIRTSTL), Serum Response Factor (SRF)$_{93-113}$ (AERRGLKRSLSEMEIGMVVGG), and gp130$_{772-792}$ (PSVQVFSRSESTQPLLDSEER) were used.

2.2.6 Fluorescence measurement of CaM$_{IAEDANS}$

Purified CaM$_{C75}$ was reduced with DTT, dialyzed in 50mM sodium phosphate buffer pH 7.0, and labeled with IAEDANS (Molecular Probes). Excess dye was removed from with a Sephadex G-25 column (Illustra NAP10) yielding CaM$_{IAEDANS}$ labeled with a ratio of 0.8:1 moles of dye per mole of CaM. Fluorescent intensity measurements were acquired with a PTI QuantaMaster 400 with excitation at 336 nm at room temperature with emission maxima at 490 nm. Slit widths for excitation and emission were 4 mm. For steady-state binding, relative intensity measurements, 50 nM CaM$_{IAEDANS}$ in the presence of degassed 50 mM HEPES pH 7.4, 100 mM NaCl, 1 mM $CaCl_2$, 10 mM $MgCl_2$, 1 mM ADP, 0.1 mg/ml BSA was measured for as baseline. For CaMKII binding in the absence of substrate, 100 nM CaMKII$_{holo}$ was added and expressed as the relative intensity change (30 sec steady state average). Substrate-dependent changes in CaM binding were measured via the subsequent addition of soluble peptide substrates at a concentration near the determined K_m value (5 μM for GluN2B and AC2; 50 μM for Syntide). Dissociation rates (K_{off}) were measured following the intensity measurements and initiated via the addition of 2.5 μM

(50-fold excess) unlabeled CaM. All data were background corrected for decay of $CaM_{IAEDANS}$ alone (linear). Data were analyzed using SigmaPlot (v.12.5) and fit to an exponential decay curve [f = y0+a*exp(-b*x)].

2.2.7 Sequence Analysis via Sequence Logo

Sequence logos were generated via WebLogo v.2.8.2 (http://weblogo.berkeley.edu) (Crooks, Hon et al. 2004) using default settings except that 0 pseudocounts were used for small sample correction; each amino acid height is proportional to the sequence conservation at the position relative to the phosphoacceptor site (P_0).

2.2.8 ScanSite Analysis

ScanSite scores were obtained using the ScanSite 3beta algorithm (http://scansite3.mit.edu) (Obenauer, Cantley et al. 2003). Because the algorithm has a minimal length requirement not based on the consensus motif, the residues surrounding the phosphorylation site from the actual protein beyond the optimized/defined peptide was used for AC-2 and Syntide. For all sites not recognized by ScanSite, a score of 0.7 was given.

2.2.9 Data Analysis

One-way analysis of variance (ANOVA) with subsequent Holm-Šídák post-test was performed on log-transformed to account for mean-dependent variances; compared to control (#). For comparisons of two groups, Student's *t* test (*) were used. Statistical

analyses were performed using SigmaPlot 12.5. Statistical significance is denoted by the number of symbols for different P values (e.g. *P < 0.05, **P < 0.01, ***P<0.001).

2.3 Results

2.3.1 Generation and Characterization of Monomeric CaMKII$_{1-317}$ (CaMKII$_m$)

In order to explore the role of autophosphorylation on CaMKII substrate specificity/selectivity in the absence of mutagenesis, we created a monomeric variant (hCaMKIIδ$_{1-317}$, termed CaMKII$_m$) (Figure 2.1, A to C) devoid of the "hub" domain required for multimerization, expressed it in T.ni (Hi5) insect cells, and purified using a combination of Ni-NTA affinity chromatography followed by gel filtration (See Materials and Methods 2.2.1). SDS-PAGE revealed a highly pure band around the expected molecular weight of ~37kDa for CaMKII$_m$ (Figure 2.1C). Because the four CaMKII isoforms exhibit identical substrate binding pockets, we chose the delta variant due to its enhanced stability in our kinase reactions. A desirable feature of CaMKII$_m$, is that unlike the CaMKII holoenzyme (CaMKII$_{holo}^{+P}$) which undergoes a rapid intramolecular intersubunit T^{287} autophosphorylation reaction in saturating Ca^{2+}/CaM conditions (Hanson, Meyer et al. 1994), the bi-molecular T^{287} autophosphorylation event is well-controlled by temperature or enzyme concentration. Using a pre-autophosphorylation reaction with activators (Ca^{2+}/CaM), Mg^{2+}/ATP, and concentrated kinase (See Materials and Methods 2.2.3), CaMKII$_m$ can be autophosphorylated at T^{287} (CaMKII$_m^{+P}$) as indicated by immunoblotting with a phospho-T^{287}-antibody (Figure 2.1D). Autophosphorylation at T^{287} of CaMKII$_m$ also produces the expected increase in Ca^{2+}-independent (i.e. autonomous) activity as measured using standard radiometric assays (See Materials and Methods 2.2.2) when a classical peptide substrate for CaMKII (i.e. autocamtide-2; AC-2) is evaluated (Figure 2.1E).

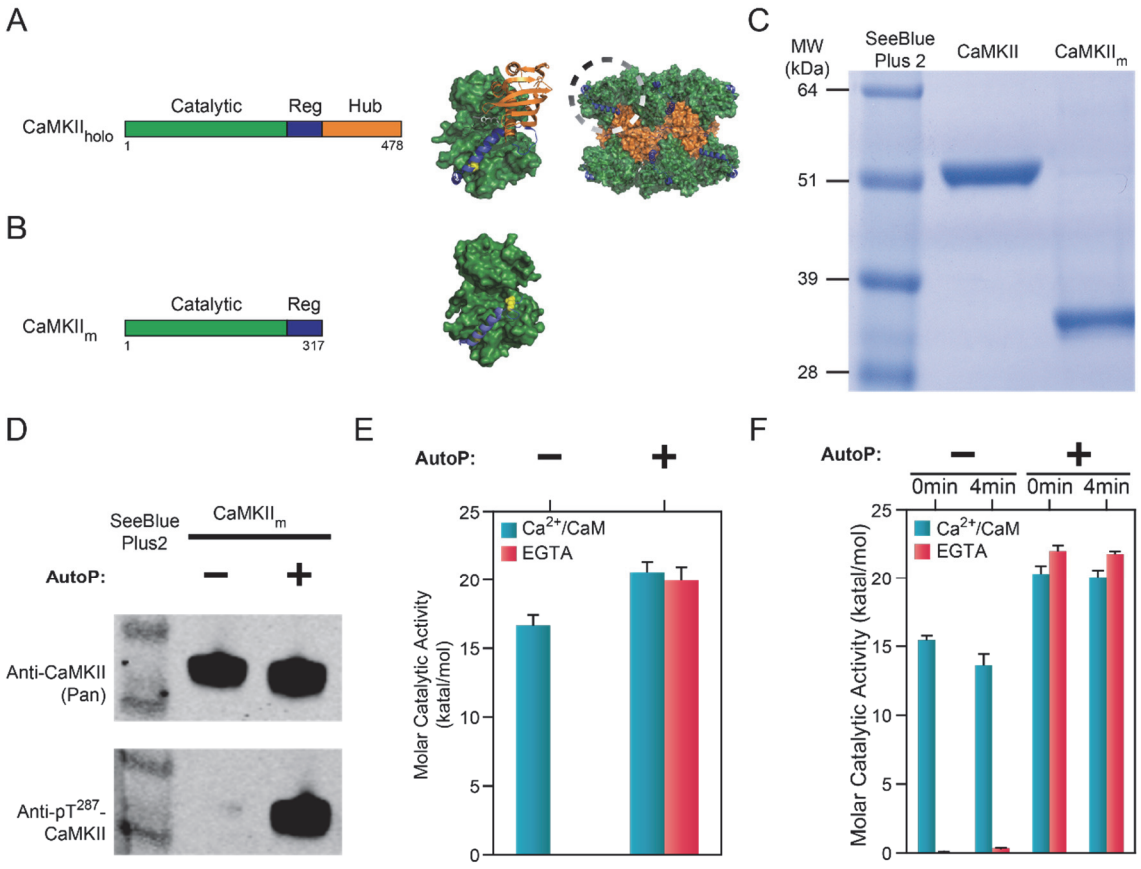

Figure 2.1 Characterization of CaMKII$_m$.
(**A** and **B**) Linear schematic (left) of a single subunit of CaMKII representing the catalytic domain (green), autoregulatory domain (ARD) (blue), and hub domain (orange). X-ray crystal structures of the CaMKII constructs (right). (**A**) Full-length hCaMKII delta with crystal structural depicting a single subunit and holoenzyme (PDB ID: 3SOA) in the autoinhibited state. (**B**) Crystal structure (PDB ID: 2VN9) of monomeric hCaMKII delta residues 1-317 (CaMKII$_m$) in the autoinhibited state. (**C**) Coomassie-stained SDS-PAGE of CaMKII vs CaMKII$_m$. (**D**) Western blot analysis of T^{287} autophosphorylation with (+) or without (-) a pre-autophosphorylation (AutoP) reaction. (**E** and **F**) Enzymatic activity (katal/mol) assays measured via standard soluble peptide (Autocamtide-2) assays with radioactive [γ^{32}P]ATP. Ca^{2+}-dependent (Ca^{2+}/CaM) vs Ca^{2+}-independent (EGTA) assays were measured for kinase with (+) or without (-) a pre-autophosphorylation (AutoP) reaction. (**E**) Activity of CaMKII$_m$ (n = 3). (**F**) Activity of CaMKII$_m$ at the start (0 min) and end (4 min) of the SPOTs assays (n = 3). Error bars in panel (**E** and **F**) denote ±SD.

Given the dodecameric nature of the holoenzyme as well as the molecular weight difference between a single subunit of $CaMKII_{holo}$ and $CaMKII_m$ (See Materials and Methods 2.2.1), protein concentrations and activity measurements are expressed in molar-based units (holoenzyme values are expressed per subunit). $CaMKII_m$ undergoes limited *trans* (i.e., bimolecular) autophosphorylation at T^{287} when activated by Ca^{2+}/CaM at low kinase concentrations used in our assays (5-10 nM). We observed an insignificant increase in the Ca^{2+}-independent activity measured after 4 minutes at room temperature (Figure 2.1F). Thus, the *trans* autophosphorylation event for $CaMKII_m$ can be prevented without having to mutate the ARD even under saturating Ca^{2+}/CaM conditions by reaction time or [$CaMKII_m$].

2.3.2 T^{287} Autophosphorylation is Associated with Decreased CaMKII Substrate Specificity

To investigate the role of T^{287} autophosphorylation on CaMKII activity and substrate selectivity, we gathered a pool of known CaMKII substrates taken from the PhosphoSitePlus database (Hornbeck, Kornhauser et al. 2012). Separated by the CaMKII isoform for which the substrate was identified, this database provides the phosphorylation motif (15mer centered on the phosphorylation acceptor site = P_0) as well as the species information for each substrate. Using SPOTs peptide synthesis, we generated arrays of these CaMKII substrates. The use of peptides over proteins limits the contribution of non-catalytic targeting mechanisms, as well as multi-site phosphorylation. We synthesized 15mer peptide substrates (as typically only 9–12 amino acids make contact with kinase active site) and characterized the phosphorylation of multiple substrates simultaneously via

SPOTs arrays (see Methods). An advantage of this immobilized substrate assay is that diverse substrates can be exposed to identical conditions without high-affinity substrates dominating mixed soluble substrate reactions (Ubersax and Ferrell 2007). Given the limited space available within a given SPOTs array, redundant substrate sequences were removed as well as sites of autophosphorylation within CaMKII. We tested 217 CaMKII substrates (Table 2.2) in all. Since many of the substrates lack kinetic descriptions, we sought for a way to predict a substrate's potential affinity based on sequence information. The strength of the substrate-kinase interaction is dictated by the sequence composition of the phosphorylation motif and its complementarity to the catalytic surface (substrate binding pocket). We reasoned that the relative ability of a substrate to be phosphorylated should therefore be correlated to its similarity to the consensus motif obtained from a degenerate oriented-peptide library (Songyang, Lu et al. 1996). Therefore, we ranked the substrates using a position-specific scoring matrix (ScanSite; http://scansite3.mit.edu (Obenauer, Cantley et al. 2003)) based on a previously defined CaMKII consensus sequence (KRQQSFDLF) obtained from a degenerate oriented-peptide library (Songyang, Lu et al. 1996). This comparison provides a relative measure of substrate sequence similarity to an optimal substrate. Thus, the best substrates (i.e., high-affinity and extent of phosphorylation) should possess lower ScanSite scores (0.0 = identical match); those having limited similarity are predicted to be weak substrates (higher K_m). We defined substrates unrecognized by ScanSite as a value of 0.7.

Figure 2.2 shows the overall sequence composition and diversity of the PhosphoSitePlus CaMKII substrate library, which deviates substantially from the previously described high-affinity CaMKII consensus motif. Specifically, over 50% of the

previously published substrates for CaMKII were not recognized by ScanSite (and therefore given a value of 0.7) as seen in the histogram of ScanSite scores (Figure 2.2A), while a sequence logo for the overall library further illustrates the lack of strong positional sequence determinants for CaMKII substrate utilization (Figure 2.2B). Given the distribution of substrates in Figure 2.2A whereby only a small number of substrates possess sequences similar to the optimal CaMKII phosphorylation motif, we expected that very few substrates would exhibit large amount of phosphorylation by CaMKII.

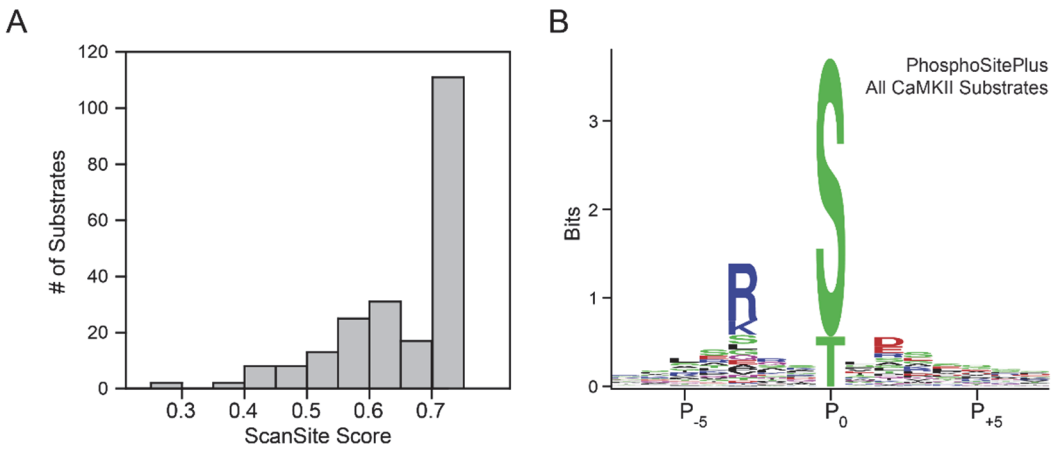

Figure 2.2 Analysis of PhosphoSitePlus library of CaMKII substrates.
(**A**) Histogram of ScanSite scores for all 217 PhosphoSitePlus substrates. CaMKII consensus motif similarity indicated by ScanSite score (lower value = greater similarity) if determinable; otherwise given a value of 0.7. (**B**) Sequence logo (WebLogo) for all 217 PhosphoSitePlus substrate sequences.

Using these peptide substrate arrays, we phosphorylated them under various kinase conditions. Radioactive phosphate [^{32}P] incorporation was used as a measure of the extent of phosphorylation, expressed in terms of photostimulated luminescence per square millimeter (PSL/mm^2). Peptide substrates were considered phosphorylated by a given kinase state if they exceeded a minimal threshold of 11.5 PSL/mm^2, corresponding to the average phosphorylation of 10 CaMKII substrates peptides in which the phosphoacceptor site was mutated to a non-phosphoacceptor residue (i.e. alanine). Under activating conditions of saturating Ca^{2+}/CaM, non-T^{287} autophosphorylatied kinase ($CaMKII_m^{-P}$) phosphorylated only 35 peptides (Figure 2.3A) within the substrate pool. As expected, the best substrates (i.e., greatest phosphorylation) possess lower ScanSite scores. By contrast, pre-autophosphorylated $CaMKII_m^{+P}$ phosphorylates 138 substrates (Figure 2.3B), and native autophosphorylated holoenzyme $CaMKII_{holo}^{+P}$ phosphorylates 118 peptides (Figure 2.3C). While a lack of CaMKII phosphorylation on SPOTs arrays could be influenced by synthesis efficiency and reaction conditions, autophosphorylation elicits a dramatic increase in both number of substrates phosphorylated and the sequence diversity of substrates (Figure 2.4); consistent with a decrease in substrate specificity. This is evident in the increase in the number of substrates not recognized by ScanSite (i.e. value of 0.7) (5-fold for $CaMKII_m^{+P}$ and $CaMKII_{holo}^{+P}$) and the substantial increase in total phosphorylation for these substrates elicited by autophosphorylation (7.4-fold versus 10.1-fold for $CaMKII_m^{+P}$ and $CaMKII_{holo}^{+P}$, respectively) (Figure 2.4).

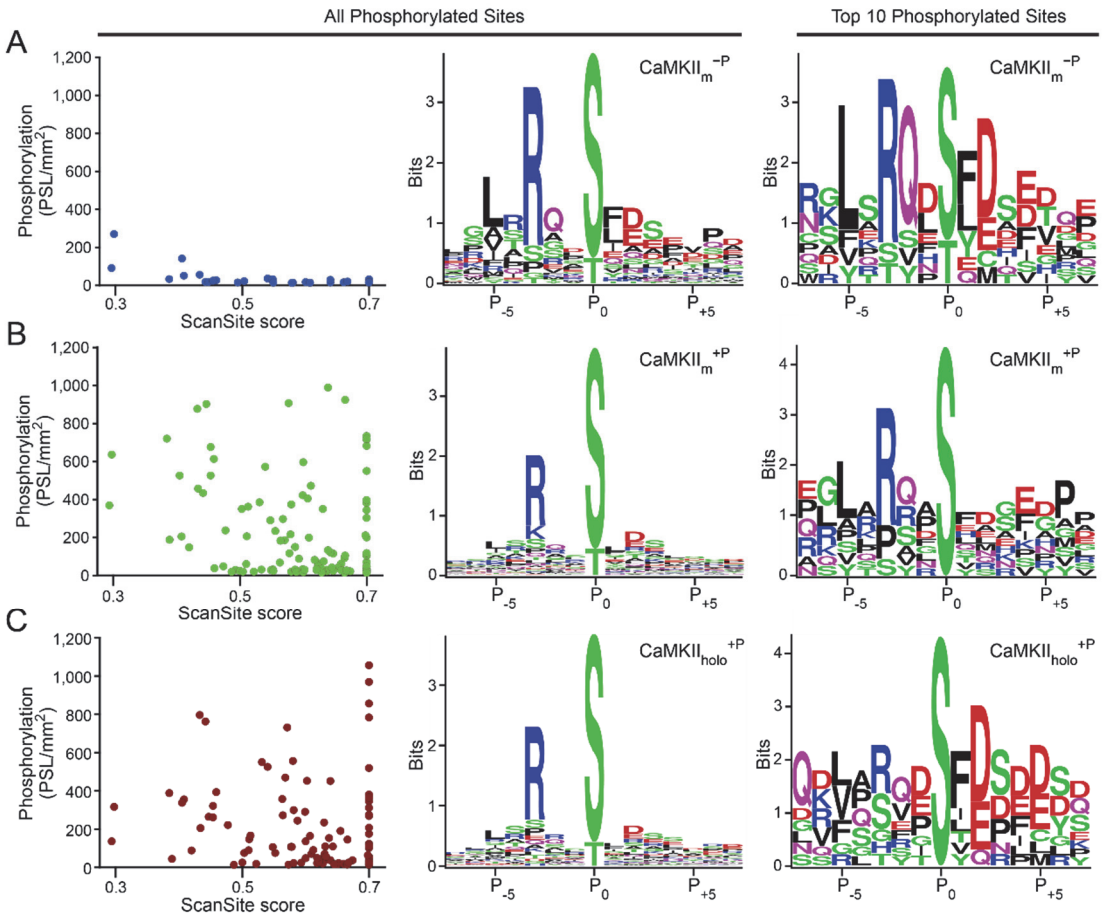

Figure 2.3 Autophosphorylation-associated expansion in CaMKII substrate specificity. (**A-C**), CaMKII substrates from PhosphoSitePlus (n = 217) were synthesized via SPOTs and phosphorylation measured via [γ-^{32}P] phosphate incorporation for various states of the kinase. Substrates phosphorylated above threshold, and their sequences were ranked by ScanSite scores (0.7 = not identified by ScanSite) (left panel). Phosphorylated substrates were analyzed using WebLogo to evaluate position-specific sequence conservation for all phosphorylated substrates (middle) or the top 10 phosphorylated substrates (right). (**A**) Monomeric CaMKII (CaMKII$_m^{-P}$) (blue circles). (**B**) CaMKII$_m^{+P}$ (green circles). (**C**) CaMKII holoenzyme (CaMKII$_{holo}^{+P}$) (red circles).

	Protein	Organism	ACC#	MW (Da)	Residue	Site Sequence	ScanSite Score	$CaMKII_m^{-P}$ Phosphorylation (PSL/mm^2)	$CaMKII_m^{+P}$ Phosphorylation (PSL/mm^2)	$CaMKII_{holo}^{+P}$ Phosphorylation (PSL/mm^2)
1	14-3-3 beta	rat	P35213	28054	S60-p	VVGARRSsWRVISSI	1	2.45	24.04	46.4
2	14-3-3 beta	rat	P35213	28054	S65-p	RSSWRVIsSIEQKTE	0.651	2.65	9.43	15.2
3	5-LO	human	P09917	77983	S272-p	CSLERQLsLEQEVQQ	0.408	26.95	202.45	353.8
4	ADCY3	mouse	Q8VHH7	129085	S1077-p	NVASRMEsTGVMGNI	0.65	0.97	9.49	3.4
5	AMPKA1	human	Q13131	64009	T183-p	SDGEFLRtSCGSPNY	1	0.27	1.09	1.2
6	ANKRD28	human	O15084	112966	S1011-p	TNTSKTVsFEALPIM	0.611	0.5	10.86	0.5
7	APOBEC3G	human	Q9HC16	46408	T218-p	WVRGRHEtYLCYEVE	0.607	0.39	1.6	4.6
8	APP	rat	P08592	86704	T729-p	MLKKKQYtSIHHGVV	0.493	1.09	26.56	5.2
9	ASIC1	rat	P55926	59641	S477-p	QKEAKRSsADKGVAL	0.669	0.56	4.43	1.0
10	BAD	mouse	Q61337	22080	S170-p	KGLPRPKsAGTATQM	0.669	1.07	10.75	4.3
11	BRSK1	rat	BAG28183	85183	T189-p	VGDSLLEtSCGSPHY	1	0.22	1.23	1.7
12	C/EBP-beta	human	P17676	36106	S325-p	EQLSRELsTLRNLFK	1	1.4	24.3	14.3
13	CACNA1B	rat	Q02294	262256	S784-p	RLQNLRAsCEALYSE	1	0.85	11.13	54.9
14	CACNA1B	rat	Q02294	262256	S896-p	ERARPRRsHSKEAPG	1	25.53	712.06	73.4
15	CACNA1B	rat	Q02294	262256	S2126-p	SEKQRFYsCDRFGSR	0.552	2.35	29.16	13.3
16	CACNA1C	mouse	Q01815	240138	S1487-p	DYLTRDWsILGPHHL	1	2.49	19.27	7.4
17	CACNA1C	mouse	Q01815	240138	S1545-p	VACKRLVsMNMPLNS	0.529	2	10.88	6.0
18	CACNA1C	rabbit	P15381	242784	S439-p	GVLSGEFsKEREKAK	1	0.62	4.8	6.4
19	CACNA1C	rabbit	P15381	242784	S1700-p	PEIRRAIsGDLTAEE	0.563	3.92	65.67	355.7
20	CACNA1C	guinea pig	BAA34185.2	242638	T1603-p	RTALRIKtEGNLEQA	1	0.45	10.6	266.0
21	CACNB1	rat	P54283	65680	T499-p	WALSRQDtFDADTPG	0.405	164.78	523.8	335.8
22	CACNB2 iso2	human	Q08289-2	68142	T499-p	RGLSRQEtFDSETQE	0.298	356.13	633.96	314.5
23	caldesmon	chicken	P12957	88747	S26-p	RLEAERLsYQRNDDD	1	3.31	11.64	121.4
24	caldesmon	chicken	P12957	88747	S59-p	QKEEGDVsGEVTEKS	0.593	0.36	1.82	6.5
25	caldesmon	chicken	P12957	88747	S73-p	SEVNAQNsVAEEETK	0.659	0.23	5.67	1.9
26	caldesmon	chicken	P12957	88747	T484-p	QNGERELtTPKLKST	0.638	0.18	1.25	20.1
27	caldesmon	chicken	P12957	88747	S490-p	LTTPKLKsTENAFGR	1	1.06	26.77	1.6
28	caldesmon	chicken	P12957	88747	S602-p	CFSPKGSsLKIEERA	1	0.44	3.49	0.8
29	caldesmon	chicken	P12957	88747	S635-p	AVVSKIDsRLEQYTS	1	0.05	1.27	1.9
30	caldesmon	chicken	P12957	88747	S741-p	RNLWEKQsVEKPAAS	0.618	0.66	9.63	2.1
31	CaMK4	rat	P13234	53151	S332-p	AVKAVVAsSRLGSAS	1	0.9	4.83	3.8
32	CaMK4	rat	P13234	53151	S333-p	VKAVVASsRLGSASS	1	0.71	7.76	3.8
33	CaMK4	rat	P13234	53151	S337-p	VASSRLGsASSSHTN	0.652	0.47	7.48	20.7
34	CaMK4	rat	P13234	53151	S341-p	RLGSASSsHTNIQES	1	0.38	6.07	27.9
35	CARD11	human	Q9BXL7	133284	S116-p	KEPTRRFsTIVVEEG	0.573	0.15	3.67	12.9
36	CD44	human	P16070	81538	S706-p	LNGEASKsQEMVHLV	0.63	0.17	2.23	2.8
37	CDK5R1	rat	P61810	34031	S91-p	ENLKKSLsCANLSTF	0.554	2.94	56.61	1.7
38	ChAT iso3	human	P28329-3	70394	T456-p	VDNIRSAtPEALAFV	1	0.22	1.64	2.9
39	CLCN3	human	P51790	90966	S109-p	ERHRRINsKKKESAW	1	1.58	10.43	29.2
40	CPEB	rat	P0C279	62062	T171-p	VRGSRLDtRPILDSR	1	1.28	18.53	26.0
41	cPLA2	human	P47712	85239	S515-p	SDFATQDsFDDDELD	0.54	54.54	569.23	523.0
42	CREB	rat	P15337	36633	S133-p	EILSRRPsYRKILND	0.42	3.65	61.15	41.5
43	CREB	rat	P15337	36633	S142-p	RKILNDLsSDAPGVP	1	1.12	13.56	4.9
44	CREM iso3	mouse	P27699	38516	S133-p	EILSRRPsYRKILNE	0.623	2.95	47.84	32.4
45	Cx43	rat	P08050	43031	S244-p	KDRVKGRsDPYHATT	1	0.91	5.75	7.1
46	Cx43	rat	P08050	43031	S255-p	HATTGPLsPSKDCGS	1	0.76	2.88	3.0
47	Cx43	rat	P08050	43031	S257-p	TTGPLSPsKDCGSPK	1	1.02	4.04	2.2
48	Cx43	rat	P08050	43031	S296-p	VTGDRNNsSCRNYNK	1	2.44	14.64	15.5
49	Cx43	rat	P08050	43031	S297-p	TGDRNNSsCRNYNKQ	1	2.4	10.73	6.9
50	Cx43	rat	P08050	43031	S306-p	RNYNKQAsEQNWANY	0.647	8.9	112.37	11.1
51	Cx43	rat	P08050	43031	S314-p	EQNWANYsAEQNRMG	1	0.34	2.46	1.1
52	Cx43	rat	P08050	43031	S325-p	NRMGQAGsTISNSHA	1	0.41	1.6	3.4
53	Cx43	rat	P08050	43031	S328-p	GQAGSTIsNSHAQPF	1	0.52	2.89	3.4
54	Cx43	rat	P08050	43031	S330-p	AGSTISNsHAQPFDF	1	0.28	2.03	3.8
55	Cx43	rat	P08050	43031	S364-p	AIVDQRPsSRASSRA	1	1.06	22.77	34.4
56	Cx43	rat	P08050	43031	S365-p	IVDQRPSsRASSRAS	1	1.61	29.68	51.9
57	Cx43	rat	P08050	43031	S369-p	RPSSRASsRASSRPR	1	2.63	34.09	44.1
58	Cx43	rat	P08050	43031	S372-p	SRASSRAsSRPRPDD	1	2.69	67.55	25.8
59	Cx43	rat	P08050	43031	S373-p	RASSRASsRPRPDDL	1	2.31	28.54	25.6
60	Cx45	mouse	P28229	45666	S326-p	AQEQQYGsHEEHLPA	1	1.71	8.84	9.8
61	Cx45	mouse	P28229	45666	T337-p	HLPADLEtLQREIRM	1	1.72	9.44	3.0
62	Cx45	mouse	P28229	45666	S381-p	SKSGSNKsSISSKSG	0.534	1.02	7.05	12.0
63	Cx45	mouse	P28229	45666	S382-p	KSGSNKSsISSKSGD	1	1.63	18.41	9.0
64	Cx45	mouse	P28229	45666	S384-p	GSNKSSIsSKSGDGK	1	1.48	12.62	8.1
65	Cx45	mouse	P28229	45666	S385-p	SNKSSISsKSGDGKT	1	1.17	9.25	9.3
66	Cx45	mouse	P28229	45666	S387-p	KSSISSKsGDGKTSV	1	1.18	13.23	7.6
67	Cx45	mouse	P28229	45666	S393-p	KSGDGKTsVWI____	1	0.4	3.75	3.7
68	DAT	human	Q01959	68495	S2-p	______MsKSKCSVG	1	3.17	5.47	0.8
69	DAT	human	Q01959	68495	S4-p	____MSKsKCSVGLM	1	3.85	5.5	0.7
70	DAT	human	Q01959	68495	S7-p	_MSKSKCsVGLMSSV	1	2.38	6.74	1.0
71	DAT	human	Q01959	68495	S12-p	KCSVGLMsSVVAPAK	1	1.89	8.91	0.8
72	DLG1	rat	Q62696	100571	S39-p	SSIERVIsIFQSNLF	1	0.78	6.46	2.7
73	DRD3	rat	P19020	49516	S229-p	RILTRQNsQCISIRP	0.548	22.11	287.92	104.5

	Protein	Organism	ACC#	MW (Da)	Residue	Site Sequence	ScanSite Score	$CaMKII_m^{-P}$ Phosphorylation (PSL/mm^2)	$CaMKII_m^{+P}$ Phosphorylation (PSL/mm^2)	$CaMKII_{holo}^{+P}$ Phosphorylation (PSL/mm^2)
74	EGFR	human	P00533	134277	S768-p	DEAYVMAsVDNPHVC	0.665	0.94	11.76	729.4
75	EGFR	human	P00533	134277	S1070-p	DSFLQRYsSDPTGAL	1	0.38	3.68	4.7
76	EGFR	human	P00533	134277	S1081-p	TGALTEDsIDDTFLP	1	0.54	10.35	8.3
77	EGFR	human	P00533	134277	S1166-p	QKGSHQIsLDNPDYQ	0.571	10.18	183.49	8.4
78	Ets-1	human	P14921	50408	S251-p	GKLGGQDsFESIESY	0.531	24.06	382.54	548.9
79	Ets-1	human	P14921	50408	S257-p	DSFESIEsYDSCDRL	0.674	2.88	19.72	35.9
80	Ets-1	human	P14921	50408	S282-p	NSLQRVPsYDSFDSE	0.433	128.79	874.23	794.2
81	Ets-1	human	P14921	50408	S285-p	QRVPSYDsFDSEDYP	1	76.92	731.91	854.9
82	Ets-2	human	P15036	53001	S246-p	FPKSRLSsVSVTYCS	0.522	2.62	17.01	16.8
83	Ets-2	human	P15036	53001	S310-p	LDVQRVPsFESFEDD	0.442	33.41	431.82	760.2
84	Ets-2	human	P15036	53001	S313-p	QRVPSFEsFEDDCSQ	1	14.96	197.28	1054.1
85	FAK iso3	mouse	P34152-3	119243	S843-p	DVRLSRGsIDREDGS	1	26.35	378.7	967.7
86	FBX43	human	C9J908	74448	T200-p	FSQQKTStIDDSKDD	0.581	1.01	17.63	20.7
87	FLNA	human	P21333	280739	S2523-p	VTGPRLVsNHSLHET	1	7.33	300.5	378.2
88	GABBR1	mouse	Q9WV18	108216	S867-p	ITRGEWQsEAQDTMK	1	0.45	9.2	15.9
89	GABRB1	mouse	P50571	54100	S409-p	IQYRKPLsSREGFGR	1	1.88	22.27	31.6
90	GABRB1	mouse	P50571	54100	S434-p	GRIRRRAsQLKVKIP	0.66	5.58	60.65	11.2
91	GABRB3	mouse	P15433	54166	S406-p	GIQYRKQsMPKEGHG	0.487	1.64	16.19	12.0
92	GABRG2	mouse	P22723	55099	S381-p	NPLLRMFsFKAPTID	0.503	21.24	347.58	73.6
93	GABRG2	mouse	P22723	55099	S393-p	TIDIRPRsATIQMNN	0.633	1.76	22.24	38.3
94	GFAT	human	Q06210	78806	S261-p	CNLSRVDsTTCLFPV	1	2.62	29.84	173.9
95	GLO1	human	Q04760	20778	T107-p	ELTHNWGtEDDETQS	1	0.22	2.34	4.1
96	GluR1	human	P42261	101506	S567-p	FSPYEWHsEEFEEGR	1	0.92	8.83	34.3
97	GluR1	mouse	P23818	101569	S849-p	FCLIPQQsINEAIRT	0.637	1.5	19.14	151.4
98	GluR1	rat	P19490	101579	S645-p	LTVERMVsPIESAED	0.627	0.68	4.83	17.5
99	GluR4	rat	P19493	100758	S862-p	TRNKARLsITGSVGE	0.593	5.56	85.02	22.6
100	gp130	mouse	Q00560	102452	S780-p	QVFSRSEsTQPLLDS	1	6.59	101.75	781.9
101	GSK3A	rat	P18265	51027	S21-p	SGRARTSsFAEPGGG	0.631	17.11	347.34	107.6
102	GSK3B	rat	P18266	46742	S9-p	SGRPRTTsFAESCKP	0.643	8.1	118.83	107.7
103	H1R	human	P35367	55784	T140-p	LRYLKYRtKTRASAT	1	2.05	21.87	46.5
104	H1R	human	P35367	55784	S396-p	FTWKRLRsHSRQYVS	0.6	1.56	24.24	17.8
105	HDAC4	human	P56524	119040	S210-p	YGKTQHSsLDQSSPP	1	6.58	105.46	99.1
106	HER2	human	P04626	137910	T1172-p	ATLERPKtLSPGKNG	1	2.6	28.94	7.0
107	HSF1	human	Q00613	57260	S230-p	PKYSRQFsLEHVHGS	0.385	28.74	717.79	386.2
108	HSL	rat	P15304	116812	S865-p	ESMRRSVsEAALAQP	1	1.09	18.26	11.8
109	ICAP1	human	O14713	21782	T38-p	GGLSRSStVASLDTD	0.581	38.07	371.85	297.4
110	ITGB1	human	P05556	88415	T788-p	PIYKSAVtTVVNPKY	1	1.79	16.66	2.6
111	ITPKA	human	P23677	51009	T311-p	EHAQRAVtKPRYMQW	1	2.29	9.79	7.1
112	KCNMA1	cow	Q28204	130063	T139-p	PVDEKEEtVAAEVGW	1	1.03	6.16	1.8
113	KIF17	mouse	Q99PW8	116373	S1029-p	SKAKRKKsKNSFGGE	0.474	4.22	45.17	3.7
114	Kv4.2	rat	Q63881	70549	S438-p	ARIRAAKsGSANAYM	1	2.23	26.58	15.4
115	Kv4.2	rat	Q63881	70549	S459-p	LLSNQLQsSEDEPAF	1	0.92	13.88	8.5
116	Kv4.3	rat	Q62897	73513	S569-p	LPATRLRsMQELSTI	1	1.32	15.8	46.0
117	LRP4	rat	Q9QYP1	211880	S1887-p	TTPERRGsLPDTGWK	1	0.9	11.21	10.0
118	LRP4	rat	Q9QYP1	211880	S1900-p	WKHERKLsSESQV__	0.581	2.67	26.88	4.0
119	LRRC7	rat	P70587	166879	S826-p	VPLELEQsTHRHTPE	1	0.54	3.12	8.9
120	LRRC7	rat	P70587	166879	T827-p	PLELEQStHRHTPET	1	0.77	5.09	86.6
121	LRRC7	rat	P70587	166879	S1392-p	IQTKGQRsMDGYPEQ	0.42	5.83	145.21	5.8
122	mAChR M4	rat	P08485	52929	T145-p	TYPARRTtKMAGLMI	1	1.51	9.24	23.0
123	MeCP2	rat	Q00566	53047	S421-p	EKMPRAGsLESDGCP	0.587	1.72	28.75	9.4
124	MOR-1	human	P35372	44779	S268-p	LKSVRMLsGSKEKDR	0.4774	7.93	234.34	219.1
125	MOR-1	rat	P33535	44494	S261-p	LMILRLKsVRMLSGS	0.549	3.34	25.26	11.2
126	myelin P0	cow	P10522	27452	S210-p	HKTAKDAsKRGRQTP	1	1.55	6.91	7.5
127	myelin P0	cow	P10522	27452	S233-p	SRSTKAAsEKKTKGL	1	1.74	11.73	8.6
128	MYH9	rat	Q62812	226338	T1940-p	RRIVRKGtGDCSDEE	0.655	2.57	39.8	188.4
129	myogenin	mouse	P12979	25203	T87-p	VDRRRAAtLREKRRL	0.639	4.38	130.94	35.9
130	NEUROD1	rat	Q64289	40001	S336-p	IPIDNIMsFDSHSHH	0.621	2.49	25.08	7.0
131	NFL	mouse	P08551	61508	S58-p	LSVRRSYsSSSGSLM	0.6	20.64	593.6	8.1
132	NFL	cow	P02548	62646	S67-p	SSGSLMPsLESLDLS	0.647	2.67	22	134.2
133	NMDAR2B	human	Q13224	166367	S1303-p	NKLRRQHsYDTFVDL	0.294	194.03	366.92	134.4
134	nNOS	rat	P29476	160559	S847-p	SYKVRFNsVSSYSDS	0.46	4.32	35.32	8.0
135	NUMB	human	P49757	70804	S276-p	EQLARQGsFRGFPAL	0.447	63.71	899.74	262.3
136	p27Kip1	human	P46527	22073	S10-p	NVRVSNGsPSLERMD	1	1.36	17.53	32.3
137	PEA-15	mouse	Q62048	15054	S116-p	KDIIRQPsEEEIIKL	0.568	16.42	294.65	467.5
138	phosducin	mouse	Q9QW08	28016	S54-p	KEILRQMsSPQSRDD	0.511	7.8	203.17	145.2
139	phosducin	rat	P20942	28129	S6-p	__MEEAAsQSLEEDF	1	0.66	7.62	270.6
140	phosducin	rat	P20942	28129	S36-p	WRKFKLEsEDGDSIP	0.637	3.04	27.58	7.1
141	phosducin	rat	P20942	28129	S73-p	ERMSRKMsIQEYELI	0.564	15.6	180.67	20.2
142	phosducin	rat	P20942	28129	S106-p	QDMHQKLsFGPRYGF	1	1.67	15.99	4.2
143	PLB	human	P26678	6109	T17-p	SAIRRAStIEMPQQA	0.513	21.67	359.19	165.0
144	PLCB3	human	Q01970	138799	S537-p	PSLEPQKsLGDEGLN	0.629	2.01	32.13	232.7
145	PPP1R14A	human	Q96A00	16693	S130-p	GLRQPSPsHDGSLSP	1	0.99	10.3	15.5
146	PPP1R3A	rabbit	Q00756	124170	S48-p	PQPSRRGsESSEEVY	1	1.26	17.77	68.2

	Protein	Organism	ACC#	MW (Da)	Residue	Site Sequence	ScanSite Score	$CaMKII_m^{-P}$ Phosphorylation (PSL/mm^2)	$CaMKII_m^{+P}$ Phosphorylation (PSL/mm^2)	$CaMKII_{holo}^{+P}$ Phosphorylation (PSL/mm^2)
147	PSD-95	rat	P31016	80465	S73-p	ITLERGNsGLGFSIA	1	5.31	115.89	343.4
148	PSMC5	rat	P62198	45626	S120-p	RVALRNDsYTLHKIL	0.553	1.2	21.13	7.1
149	PTPRA	mouse	P18052	93698	S180-p	QAGSHSNsFRLSNGR	1	2.72	44.15	51.3
150	PTPRA	mouse	P18052	93698	S204-p	PLLARSPsTNRKYPP	1	45.19	679.74	116.5
151	rabphilin 3A	rat	P47709	75832	S274-p	QGLRRANsVQASRPA	0.666	104.75	921.48	143.3
152	RCHY1	human	Q96PM5	30110	T154-p	ICLEDIHtSRVVAHV	1	2.37	9.9	6.1
153	RIMS1	rat	Q9JIR4	179655	S241-p	RLQERSRsQTPLSTA	1	4.53	45.02	21.1
154	RIMS1	rat	Q9JIR4	179655	S287-p	KQASRSRsEPPRERK	1	2.97	45.14	29.5
155	RRAD	human	P55042	33245	S273-p	AGTRRREsLGKKAKR	0.5	2.61	21.14	23.5
156	RYR2	human	Q92736	564567	S2808-p	YNRTRRIsQTSQVSV	0.632	4.24	71.23	54.7
157	RYR2	human	Q92736	564567	S2814-p	ISQTSQVsVDAAHGY	0.589	1.35	16.09	10.9
158	SAPAP1	rat	P97836	110178	S389-p	YLKATQPsLTELTTL	0.629	1.51	12.65	5.7
159	SAPAP1	rat	P97836	110178	S691-p	KTSSKFQsVGVQVEE	1	1.53	10.86	8.1
160	SAPAP1	rat	P97836	110178	S947-p	APLIRERsLESSQRQ	0.599	18.91	419.01	288.7
161	SAPAP2	rat	P97837	118978	S1012-p	FPITREKsLDLPDRQ	0.459	86.18	610.98	391.6
162	SAPAP3	rat	P97838	105990	S930-p	GVPVKERsLDSVDRQ	0.599	3.1	30.57	9.2
163	sarcolipin	human	O00631	3762	T5-p	___MGINtRELFLNF	1	0.96	9.84	6.3
164	sarcolipin	mouse	Q9CQD6	3808	T5-p	___MERStQELFINF	1	0.54	7.34	3.9
165	SCN5A	human	Q14524	226940	S516-p	LSLTRGLsRTSMKPR	0.607	17.83	402.89	162.6
166	SCN5A	human	Q14524	226940	T594-p	LHGKKNStVDCNGVV	0.505	2.47	17.03	5.2
167	separase	human	Q14674	233175	S1501-p	TDNWRKMsFEILRGS	0.389	8.9	185.89	42.7
168	SERCA2	rat	P11507	114768	S38-p	KLKERWGsNELPAEE	0.621	2.62	30.72	26.4
169	SHANK1	rat	Q9WV48	226335	S783-p	RLPPPAIsLRSKSMT	0.609	7.82	196.97	68.0
170	SHANK3	rat	Q9JLU4	193258	S769-p	TLTLRSKsMTAELEE	0.51	4.81	57.59	4.9
171	SHANK3	rat	Q9JLU4	193258	S1586-p	QLNKDTRsLGEEPVG	1	1.97	12.75	87.1
172	Smad2	human	Q15796	52306	S110-p	SFSEQTRsLDGRLQV	1	1.67	16.01	309.6
173	Smad2	human	Q15796	52306	S240-p	SDQQLNQsMDTGSPA	0.659	0.44	3.86	3.5
174	Smad2	human	Q15796	52306	S260-p	TLSPVNHsLDLQPVT	0.641	0.56	8.77	2.7
175	smMLCK	chicken	P11799	210446	S1749-p	RAIGRLSsMAMISGM	0.618	3.27	79.41	47.5
176	smMLCK	chicken	P11799	210446	S1762-p	GMSGRKAsGSSPTSP	0.629	1.08	10.21	4.1
177	SNCA	human	P37840	14460	S129-p	NEAYEMPsEEGYQDY	1	1.35	2.41	3.0
178	Spinophilin	rat	O35274	89646	S99-p	RLSLPRAsSLNENVD	1	52.73	716.37	517.3
179	Spinophilin	rat	O35274	89646	S100-p	LSLPRASsLNENVDH	1	13.68	394.62	272.3
180	SPR	human	P35270	28048	S213-p	QQLARETsVDPDMRK	0.58	8.62	213.67	554.1
181	SPR	rat	P18297	28128	S46-p	LLSARSDsMLRQLKE	1	8	341.18	8.3
182	SPR	rat	P18297	28128	S196-p	EPSVRVLsYAPGPLD	0.6	1.6	14.07	362.3
183	SRF	human	P11831	51593	S103-p	RGLKRSLsEMEIGMV	0.639	55.34	986.25	449.5
184	STAT1	human	P42224	87335	S727-p	TDNLLPMsPEEFDEV	1	0.79	9.04	3.8
185	STMN1	mouse	P54227	17274	S16-p	KELEKRAsGQAFELI	1	0.87	8.79	5.3
186	STMN1	human	P16949	17303	S16-p	KELEKRAsGQAFELI	1	1.94	14.45	4.8
187	SYN1	mouse	O88935	74097	S605-p	AGPTRQAsQAGPGPR	0.577	49.64	904.98	105.5
188	SYN1	rat	P09951	73988	S566-p	PQATRQAsISGPAPP	0.434	26.85	454.77	203.9
189	SynGAP	rat	Q9QUH6	144722	S765-p	YMMRDLNsSIDLQSF	1	1.2	13.07	2.5
190	SynGAP	rat	Q9QUH6	144722	S780-p	MARGLNSsMDMARLP	0.66	3.31	24.81	3.0
191	SynGAP	rat	Q9QUH6	144722	S1073-p	PPLQRGKsQQLTVSA	0.612	32.52	469.26	110.0
192	SynGAP	rat	Q9QUH6	144722	S1114-p	QSLSKEGsIGGSGGS	0.625	1.52	10	16.3
193	SynGAP	rat	Q9QUH6	144722	S1118-p	KEGSIGGsGGSGGGG	1	0.71	4.38	88.5
194	SynGAP	rat	Q9QUH6	144722	S1138-p	PSITKQHsQTPSTLN	0.556	7.54	231.67	4.5
195	SYT1	rat	P21707	47399	T112-p	DVKDLGKtMKDQALK	1	0.89	4.95	2.0
196	tau	cow	P29172	46333	S423-p	SNVSSTGsIDMVDSP	0.645	1.99	39.29	14.8
197	tau iso2	human	P10636-2	36760	S307-p	GAEIVYKsPVVSGDT	1	0.78	0.96	2.1
198	tau iso2	human	P10636-2	36760	S315-p	PVVSGDTsPRHLSNV	1	1.81	4.25	5.1
199	tau iso5	human	P10636-5	42603	T231-p	KKVAVVRtPPKSPSS	1	3.23	11.77	6.4
200	tau iso8	human	P10636-8	45850	S262-p	NVKSKIGsTENLKHQ	1	3.53	17.3	6.2
201	TH	human	P07101	58600	S19-p	KGFRRAVsELDAKQA	1	14.59	547.64	205.9
202	TH	human	P07101	58600	S71-p	RFIGRRQsLIEDARK	0.578	5.4	114.31	105.2
203	TH iso5	human	EAX02491	56052	S35-p	AIMVRGQsPRFIGRR	1	1.49	10.83	12.5
204	TNNT2	cow	P13789	33914	T191-p	GYIQKAQtERKSGKR	1	1.91	18.63	11.4
205	TPD52	human	P55327	24327	S176-p	KNSPTFKsFEEKVEN	0.587	8.51	147.78	242.6
206	TPH2	human	Q8IWU9	56057	S19-p	YWARRGFsLDSAVPE	0.454	26.85	523.92	259.7
207	TPH2	mouse	Q8CGV2	55859	S19-p	YWARRGLsLDSAVPE	0.454	24.76	673.01	319.8
208	Trad	rat	P97924	336587	T77-p	DVCKRGFtVIIDMRG	0.402	1.32	11.22	3.7
209	TRPV1	rat	O35433	94948	S502-p	YFLQRRPsLKSLFVD	0.665	3.86	89.96	13.6
210	TRPV1	rat	O35433	94948	T704-p	WKLQRAItILDTEKS	0.666	9.91	102.3	13.8
211	VAMP2	mouse	P63044	12691	S61-p	LERDQKLsELDDRAD	1	6.17	3.96	3.8
212	vimentin	human	P08670	53652	S83-p	GVRLLQDsVDFSLAD	0.602	4.72	27.42	9.6
213	vimentin	mouse	P20152	53688	S39-p	TTSTRTYsLGSALRP	0.698	7.74	208.4	1.8
214	vimentin	cow	P48616	53728	S26-p	GTASRPSsTRSYVTT	0.668	1.68	24.46	450.4
215	vimentin	cow	P48616	53728	S66-p	GVYATRSsAVRLRSG	1	1.51	11.63	23.8
216	vimentin	cow	P48616	53728	S72-p	SSAVRLRsGVPGVRL	1	1.61	7.16	21.4
217	vimentin	cow	P48616	53728	S412-p	EGEESRIsLPLPNFS	1	2.11	0.47	61.8

Table 2.2 PhosphoSitePlus information. List of all 217 peptides used from the PhosphoSitePlus database and phosphorylated by the various activation states of the kinase.

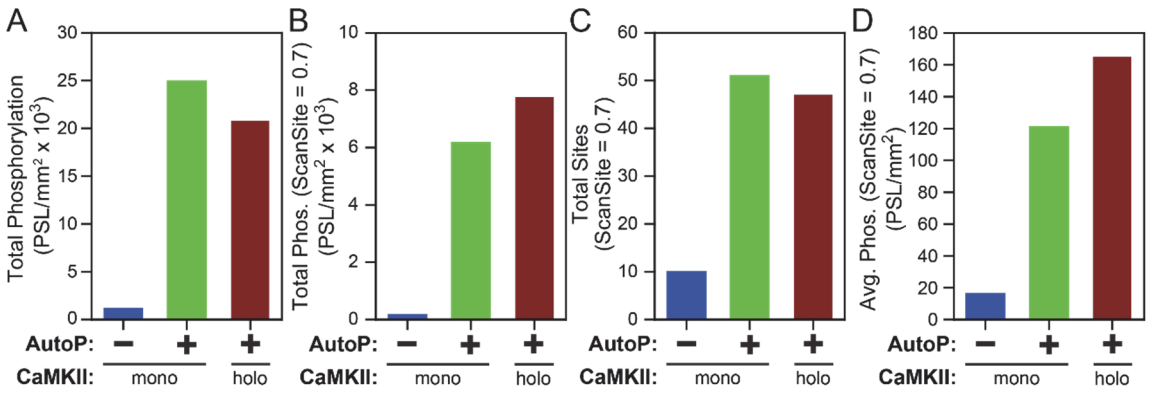

Figure 2.4 Degeneracy in CaMKII substrate selection/preference arising from autophosphorylation or multimerization.
(**A** to **D)** The sum total of phosphoincorporation for all substrates above a threshold (11.5 PSL/mm^2) are shown in (**A**) or for substrates without a ScanSite score (i.e. set to 0.7) in (**B**). The total number of substrates without a ScanSite score (**C**) are used to calculate the average phosphorylation for a non-consensus substrate in (**D**).

Furthermore, the best 5 substrates (i.e. exhibiting the highest extent of phosphorylation) for each state of the kinase possess rather distinct similarities toward the predicted consensus motif (Figure 2.5). Specifically, the average ScanSite scores for these substrates phosphorylated were: 0.368 for $CaMKII_m^{-P}$, 0.602 for $CaMKII_m^{+P}$, and 0.647 for $CaMKII_{holo}^{+P}$. Extending this analysis to include the top ten phosphorylated substrates shows averages of 0.465 for $CaMKII_m^{-P}$, 0.593 for $CaMKII_m^{+P}$, and 0.590 for $CaMKII_{holo}^{+P}$. These scores reflect the large differences in the sequence logos for the top ten phosphorylated substrates for each of these kinase activation states (Figure 2.3, right panels). Though multivalency appears to increase the overall level of phosphorylation, similarity in phosphorylation profiles of $CaMKII_m^{+P}$ and $CaMKII_{holo}^{+P}$ suggests that T^{287} autophosphorylation is a critical driver for this switch-like change in substrate selectivity.

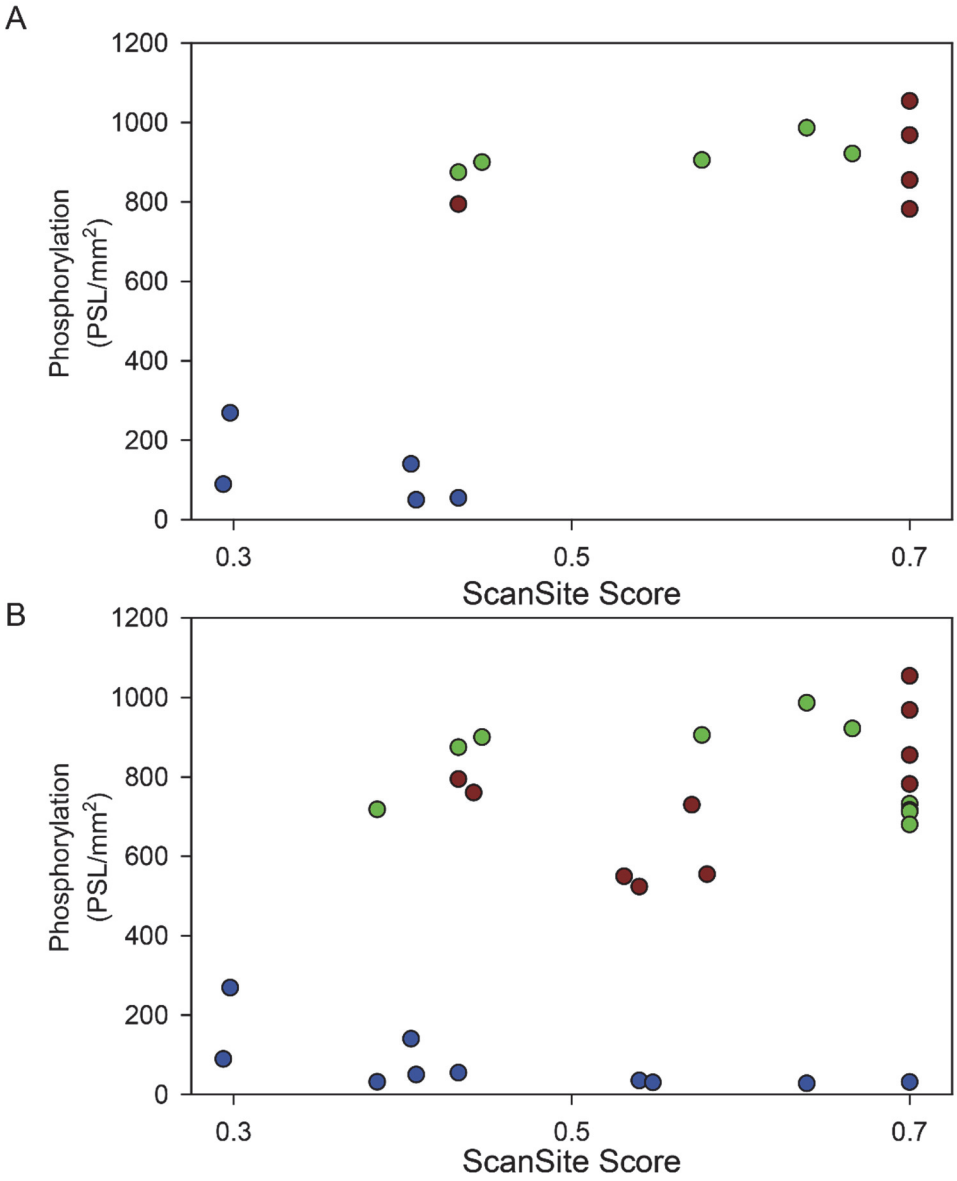

Figure 2.5 Alterations in preferential substrate usage among PhosphoSitePlus.
(**A** and **B**) Comparative phosphorylation data for the substrates with the greatest extent of phosphoincorporation under different kinase conditions. $CaMKII_m^{-P}$ (blue circles), $CaMKII_m^{+P}$ (green circles), and $CaMKII_{holo}^{+P}$ (red circles). (**A**) Top five substrates for each condition. (**B**). Top ten substrates for each condition.

2.3.3 T^{287} Autophosphorylation Produces Switch-like Behavior Toward Poor-consensus Substrates.

To study the role of T^{287} autophosphorylation in more detail, we selected four model substrates—a high-affinity substrate (GluN2B$_{S1303}$, K_m = 4.6±1.1 μM) from a glutamate receptor and three lower-affinity, weak substrates (Syntide, K_m = 43.5±2.3 μM; vimentin$_{S83}$ and GluA1$_{S849}$, K_m > 1 mM) taken from an enzyme (glycogen synthase), a cytoskeletal protein (vimentin) and another glutamate receptor subtype, respectively. When we compared the phosphorylation of CaMKII$_m^{-P}$ for these four substrates in our SPOTs reaction, we observed that the extent of phosphorylation was correlated to substrate affinity (Figure 2.6). Greater substrate affinity led to greater phosphorylation. Upon autophosphorylation (CaMKII$_m^{+P}$), we found that as seen for the PhosphoSitePlus substrates, an enhancement in substrate phosphorylation was observed for all substrates (Figure 2.6B).

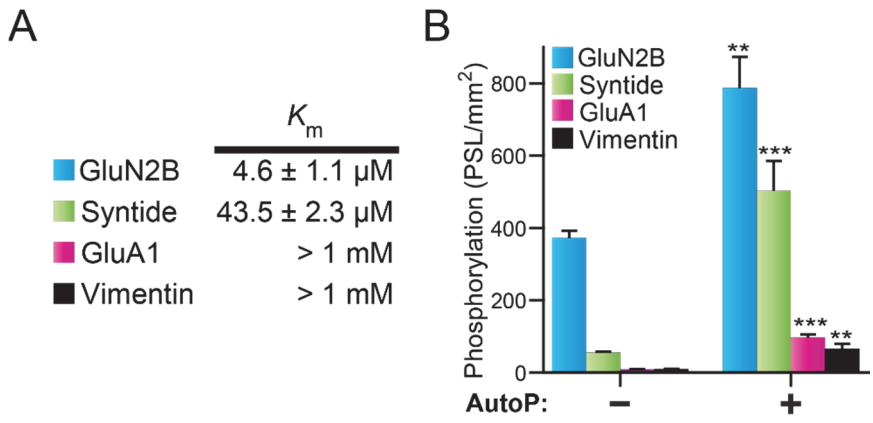

Figure 2.6 CaMKII autophosphorylation enhances the phosphorylation of four diverse CaMKII substrates.

(**A** and **B**) Phosphorylation analysis of four diverse CaMKII substrates (GluN2B, Syntide, GluA1, and vimentin). (**A**) Substrates ranked from lowest to highest K_m obtained via soluble peptide phosphorylation assays. (**B**) Phosphorylation ([γ-^{32}P] phosphate incorporation) of immobilized CaMKII substrates synthesized via SPOTs. $CaMKII_m$ phosphorylation profiles with and without T^{287} autophosphorylation, represented as mean ±SD (n = 3). Unpaired/two-tailed t-test used to compare to $CaMKII_m^{-P}$; (*$P < 0.05$, **$P < 0.01$, ***$P < 0.001$).

It should be noted that autophosphorylation does not generate a linear increase in phosphorylation of all substrates, but rather a preferential increase in phosphorylation of weak substrates. To further address the specificity and potential for preferential changes in substrate phosphorylation with $CaMKII_m^{+P}$, we focused on a small yet diverse subset of our phosphorylated substrate library from PhosphoSitePlus (Table 2.3). We included the well-known CaMKII substrate peptide AC-2 (K_m = 5 μM) and Syntide for comparison as well; 15 substrates were analyzed in all. Table 2.3 (A to C) provides substrate information, representative phosphorimaging of the SPOTs, and absolute phosphorylation values as well as those scaled to the high-affinity substrate GluN2B for the two activation states. Again, as expected for $CaMKII_m^{-P}$, the best substrates (i.e., greatest phosphorylation) possess lower ScanSite scores (Figure 2.7), consistent with being more likely to be high-affinity. To assess relative changes in kinase specificity associated with T^{287} autophosphorylation, we calculated the relative enhancement in phosphorylation for each substrate in the presence versus absence of autophosphorylation ($CaMKII_m^{+P}$ / $CaMKII_m^{-P}$). Because the extent of phosphorylation by $CaMKII_m^{-P}$ correlated with affinity (K_m) of the four substrates previously examined, we plotted the enhancement factor as a function of $CaMKII_m^{-P}$ phosphorylation in lieu of kinetic information for all 15 substrates (Figure 2.8A). These enhancement scores were also presented as function of their ScanSite score (Figure 2.8B). While autophosphorylation ($CaMKII_m^{+P}$) globally increases phosphorylation for all substrates, an autophosphorylation-dependent increase in relative phosphorylation is smaller for high-affinity substrates (i.e., low scores) (Figure 2.8). Weak substrates, exhibiting low phosphorylation or poor consensus motifs (i.e., high ScanSitescores) for the non-autophosphorylated state ($CaMKII_m^{-P}$), show the greatest

enhancement of phosphorylation (Figure 2.8). Furthermore, we find that the altered substrate enhancement is dependent on the affinity of the substrate; the greater the affinity, the lower the enhancement. Taken together, we find that autophosphorylation broadens the target profile to decrease substrate specificity, meaning that the autophosphorylation state of CaMKII determines the substrate specificity of the kinase. Importantly, these effects are not attributable to non-linearity in assays due to limiting substrates or a loss in substrate access/availability as shown in the following section (Results 2.3.4).

A				B			C		
				$CaMKII_m^{-P}$			$CaMKII_m^{+P}$		
Peptide	P_0 Site	ScanSite Score	Sequence	SPOTs	Phos. (PSL/mm^2)	Phos. (Scaled to GluN2B)	SPOTs	Phos. (PSL/mm^2)	Phos. (Scaled to GluN2B)
GluN2B	S1303	0.294	RNKLRRQHsYDTFVD		372.3 ±19.8	100.0 ± 5.3		787.3 ±86.0	100.0 ±10.9
AC-2	T287	0.367	KKALRRQEtVDAL		182.0 ± 5.7	48.9 ± 1.5		485.7 ±56.7	61.7 ± 7.2
Syntide-2	S8	0.605	PLARTLsVAGLPGKK		54.9 ± 2.4	14.8 ± 0.6		503.0 ±82.3	63.9 ±10.5
GluA1	S849	0.637	GFCLIPQQsINEAIR		8.9 ± 1.0	2.4 ± 0.3		97.2 ± 8.2	12.3 ± 1.0
Vimentin	S83	0.602	PGVRLLQDsVDFSLA		9.4 ± 1.3	2.5 ± 0.3		66.5 ±12.7	8.5 ± 1.6
HSF1	S230	0.385	PKYSRQFsLEHVHGS		66.9 ±10.3	18.0 ± 2.8		381.8 ±49.5	48.5 ± 6.3
5-LO	S272	0.408	CSLERQLsLEQEVQQ		91.7 ±17.2	24.6 ± 4.6		274.3 ±34.0	34.8 ± 4 .3
cPLA2	S515	0.54	SDFATQDsFDDDELD		115.5 ± 8.3	31.0 ± 2.2		352.0 ±59.3	44.7 ± 7.5
DRD3	S229	0.548	RILTRQNsQCISIRP		56.6 ± 9.2	15.2 ± 2.5		364.2 ±28.6	46.3 ± 3.6
EGFR	S1166	0.571	QKGSHQIsLDNPDYQ		17.1 ± 1.6	4.6 ± 0.4		138.9 ± 5.8	17.6 ± 0.7
SAPAP1	S947	0.599	APLIRERsLESSQRQ		19.7 ± 2.2	5.3 ± 0.6		226.9 ±10.1	28.8 ± 1.3
mAChR M4	T145	0.700	TYPARRTtKMAGLMI		9.0 ± 0.7	2.4 ± 0.2		57.8 ± 5.8	7.3 ± 0.7
FAK	S843	0.700	DVRLSRGsIDREDGS		29.4 ± 4.3	7.9 ± 1.1		217.8 ±30.8	27.7 ± 3.9
Spinophilin	S100	0.700	LSLPRASsLNENVDH		21.1 ± 4.3	5.7 ± 1.2		220.2 ±33.1	28.0 ± 4.2
gp130	S780	0.700	QVFSRSEsTQPLLDS		13.6 ± 3.4	3.7 ± 0.9		92.0 ±19.0	11.7 ± 2.4

Table 2.3 Monomeric CaMKII phosphorylation of SPOTs substrate peptides.
(**A** to **C**) Table of substrate properties for immobilized SPOTs peptides representing 15 CaMKII substrates; 13 taken from PhosphoSitePlus as well as two classical CaMKII substrates Syntide and Autocamtide-2 (AC-2). (**A**) Phosphoacceptor site (P_0), ScanSite score, and sequence. Substrates unrecognized by ScanSite algorithm given score of 1. (**B** and **C**) Phosphorylated SPOTs images analyzed by phosphoimaging (left), absolute substrate phosphorylation (middle), and phosphorylation scaled to the high-affinity substrate GluN2B (right). (**B**) $CaMKII_m^{-P}$. (**C**) $CaMKII_m^{+P}$. Data represents mean ±SD.

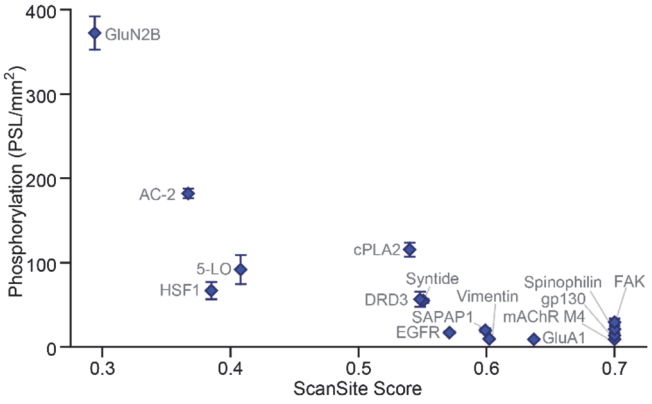

Figure 2.7 Extent of CaMKII phosphorylation is correlated to substrate similarity to consensus motif.
Phosphorylation ([γ-^{32}P] phosphate incorporation) of immobilized SPOTs peptides representing 15 CaMKII substrates; 13 taken from PhosphoSitePlus as well as two classical CaMKII substrates Syntide and Autocamtide-2 (AC-2). Substrate phosphorylation of CaMKII$_m^{-P}$ (blue) as a function of ScanSite score. Error bars denote ±SD.

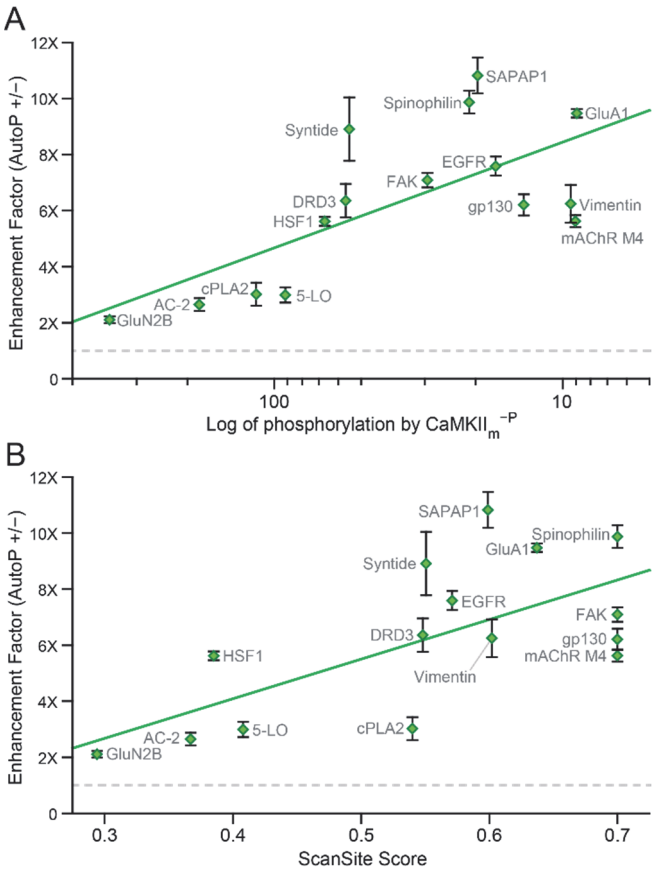

Figure 2.8 Autophosphorylation-associated expansion in CaMKII substrate selectivity. (**A** and **B**) Phosphorylation enhancement for 15 CaMKII SPOTs substrates. Autophosphorylation-induced enhancement of substrates (green) represents the ratio of substrate phosphorylation with and without T^{287} autophosphorylation ($CaMKII_m^{+P}$ / $CaMKII_m^{-P}$). This value is represented either as a function of phosphorylation by $CaMKII_m^{-P}$ on a log scale in (**A**) or as a function of ScanSite similarity score in (**B**). Dashed line indicates no change. Error bars denote ±SD. Data points fit with linear regression (green line) exhibited R^2 coefficient values of 0.48 and 0.47 in (**C**) and (**D**), respectively.

Using this enhancement factor comparison, we reevaluated the PhosphoSitePlus substrates. We compared the phosphorylation of autophosphorylated CaMKII monomer or holoenzyme ($CaMKII_m^{+P}$ and $CaMKII_{holo}^{+P}$, respectively) to the phosphorylation of non-T^{287} autophosphorylated monomer ($CaMKII_m^{-P}$). Like the 15 substrates, enhancement factors were ranked by the extent of $CaMKII_m^{-P}$ phosphorylation in lieu of kinetic information for all substrates or by ScanSite score. We found that the enhanced substrate phosphorylation for autophosphorylated kinase, both $CaMKII_m^{+P}$ and $CaMKII_{holo}^{+P}$ possessed similarities (Figure 2.9). Specifically, enhanced phosphorylation was greatest for substrates poorly phosphorylated in the non-autophosphorylated state ($CaMKII_m^{-P}$) (Figure 2.9, A and B). Furthermore, this similarity in enhancement profile was also observed for substrates as function of their resemblance to a consensus phosphorylation motif (ScanSite score) (Figure 2.9, C and D). Again, enhanced phosphorylation was greatest for substrates that were less similar to the consensus motif. We also analyzed the sequence composition of the 10 substrates with best or worst enhancement factors. We found that while a basic residue at P_{-3} was the strongest determinate for the greatest enhancement in phosphorylation by $CaMKII_m^{+P}$, while an acidic residue at P_{+2} was preferential for $CaMKII_{holo}^{+P}$. Interestingly, basic residues at P_{-3} and P_{+3} were found to be associated with the substrates with the lowest enhancement for $CaMKII_{holo}^{+P}$.

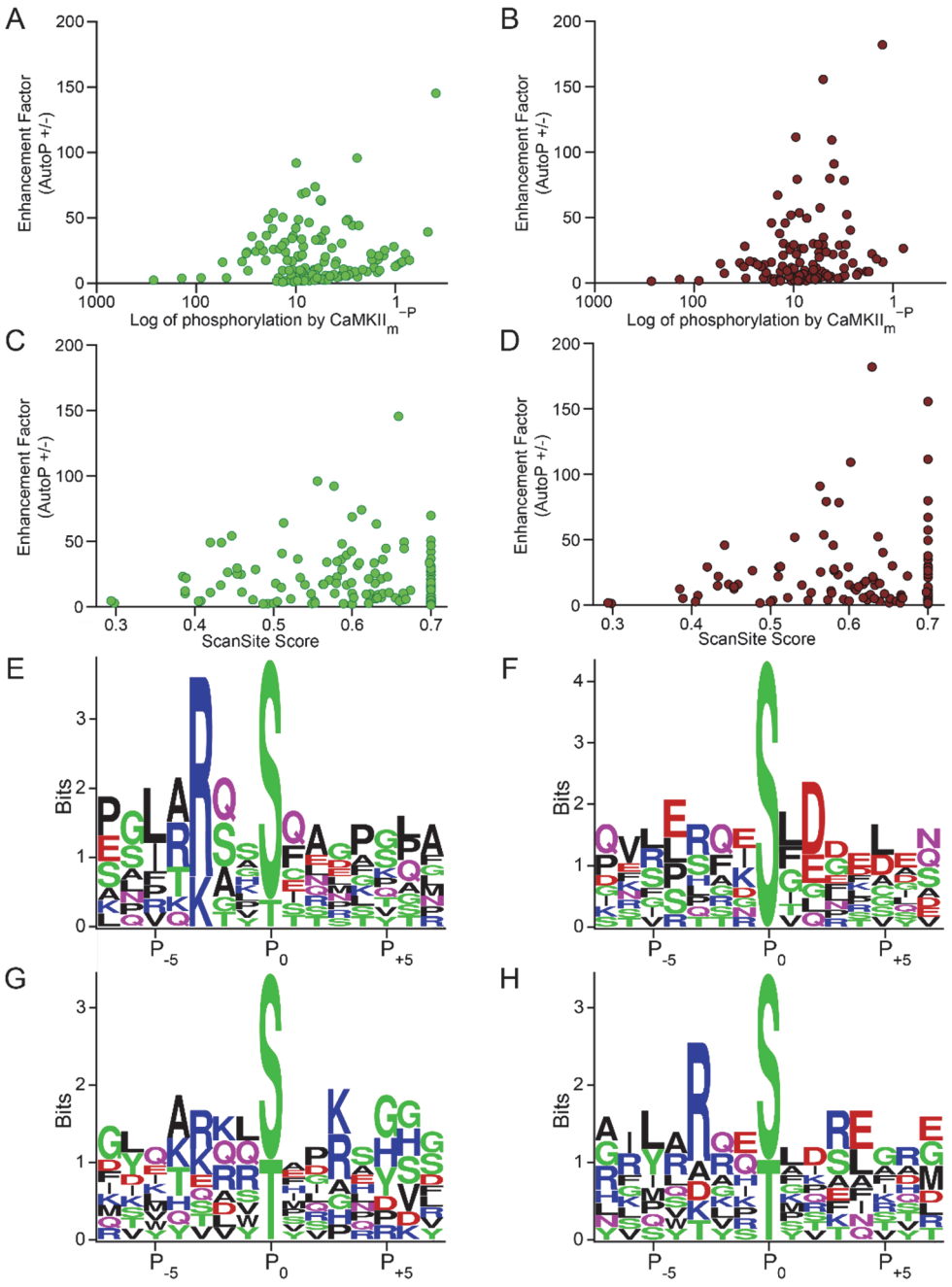

Figure 2.9 CaMKII substrate selectivity changes for PhosphoSitePlus CaMKII substrates. (**A** to **H**) Phosphorylation of CaMKII substrates from PhosphoSitePlus as measured by phosphoincorporation into immobilized SPOTs. (**A** to **D**) Enhancement of substrate phosphorylation representing the ratio of substrate phosphorylation with and without T^{287} autophosphorylation either for monomeric $CaMKII_m^{+P}$ (green) or multimeric $CaMKII_{holo}^{+P}$ (red) compared to $CaMKII_m^{-P}$ ($CaMKII_m^{+P}$ / $CaMKII_m^{-P}$ in **A** and **C** or $CaMKII_{holo}^{+P}$ / $CaMKII_m^{-P}$ in **B** and **D**). Enhancement as a function of phosphorylation by $CaMKII_m^{-P}$ in **A** and **B** or as a function of ScanSite similarity score in **C** and **D**. $CaMKII_m^{+P}$. (**D**) $CaMKII_{holo}^{+P}$. (**E** to **H**) WebLogo to evaluate position-specific sequence conservation in the enhancement of phosphorylation. (**E** and **F**) Top 10 enhanced substrates. (**G** and **H**) Lowest 10 enhanced substrates. (**E** and **F**) Monomeric CaMKII ($CaMKII_m^{+P}$). (**F** and **H**) CaMKII holoenzyme ($CaMKII_{holo}^{+P}$).

2.3.4 SPOTs phosphorylation reactions are linear

The use of the SPOTs membranes is quite different from the typical reactions properties of standard soluble kinase assays typically governed by Michaelis-Menten kinetic parameters. Substrates are diffusion-restricted; the kinase either samples an environment with no substrate (i.e. kinase unbound) or highly saturating (i.e. kinase bound to SPOT). Yet, in comparing the phosphorylation profiles, we aimed for the linear portion of the reaction curve. Extending the reaction time from 4 to 10 minutes, the phosphorylation profiles remained quite similar (Figure 2.10, A and B). While the greatest change was the fold increase in GluN2B phosphorylation, after scaling the data to GluN2B the differences between naïve and T^{287} autophosphorylated $CaMKII_m$ phosphorylation profiles was minimal. Corresponding solution assays indicated that the non-T^{287} autophosphorylated kinase ($CaMKII_m^{-P}$) exhibited less than 3% autonomy by the end of SPOTs reaction. These findings show that these alterations in substrate selectively are observable at longer time points; provided the kinase is not autophosphorylated. Additionally, the decreased enhancement for GluN2B compared to other substrates is not due to limited substrate as less than 2% of the available peptide for each substrate (as compared to a 24 hour reaction for GluN2B , Syntide, GluA1, and Vimentin) was phosphorylated by $CaMKII_m^{+P}$ (Figure 2.10C). This points to the fact the reactions were not saturated. Moreover, nearly identical levels of ^{32}P incorporation are obtained when a secondary reaction (including additional kinase) occurs on the same SPOTs membrane immediately after an initial non-radioactive 4 minute reaction (Figure 2.11D – 1 vs 2). By washing away unbound kinase in a primary reaction and withholding additional kinase in a secondary reaction (Figure 2.11D – 3), we observed that the bound kinase retained lateral-diffusion; phosphorylating any given

substrate at least 25% of a standard reaction. As expected, these percentages were higher for the high-affinity substrate (~70% of control) presumably due to retention of more kinase during the wash step. Therefore, peptides did not act as a sink for the kinase subunits following phosphorylation—subunits were able to phosphorylate multiple substrates. This was also suggested by the fact that no significant loss of enzymatic activity was observed over the course of the experiment (as measured in standard peptide solution assays; Figure 2.1F). Taken together, these data suggest that our reactions involving the SPOTs membrane are linear and that the kinase is mobile within the web of immobilized substrates.

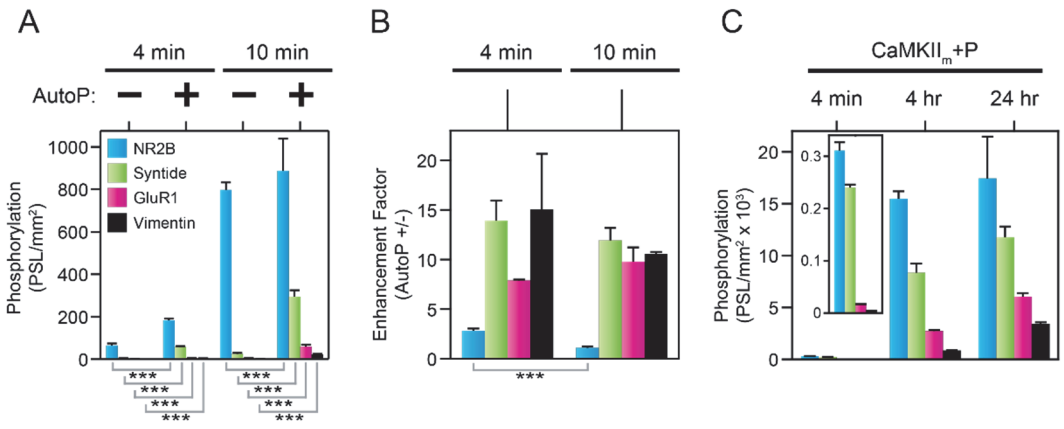

Figure 2.10 Controls for SPOTs phosphorylation reactions.
(**A** to **C**) Substrate phosphorylation profiles ([γ-^{32}P] phosphate incorporation of SPOTs peptides) by CaMKII$_m$. 4 or 10 min reaction in the presence (+) or absence (-) of T^{287} autophosphorylation; absolute phosphorylation values (**A**) or as autophosphorylation-induced enhancement factors representing the ratio of substrate phosphorylation with and without T^{287} autophosphorylation (CaMKII$_m^{+P}$ / CaMKII$_m^{-P}$) (**B**) (n = 3). (**C**) Phosphorylation time-course of T^{287} autophosphorylated CaMKII$_m$ (n = 3); expanded view of 4 min reaction in inset. Error bars in all panels denote ±SD. Unpaired/two-tailed *t*-test, *P < 0.05, **P < 0.01, ***P<0.001.

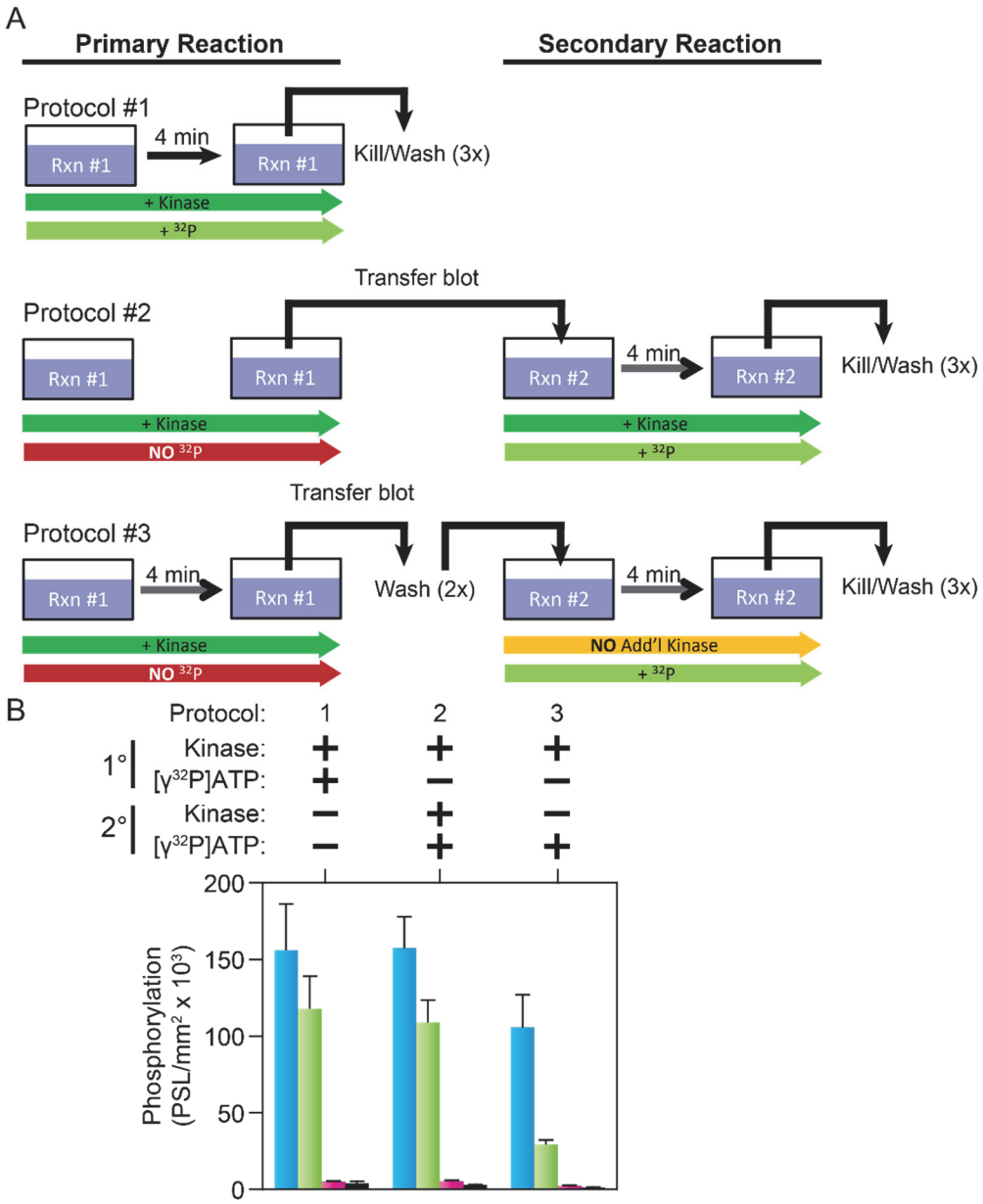

Figure 2.11 CaMKII retains lateral diffusion with SPOTs environment.
(**A** and **B**) Comparisons of SPOTs phosphorylation assays utilizing one or two reactions on a single membrane with or without additional kinase supplemented into the secondary reaction. (**A**) Schematic workflow used in the assay setup for the various protocols. Protocol #1 represents a standard 4 min reaction with both kinase and radioactive ATP (^{32}P) and no secondary reaction. For protocol #2 and #3, a primary reaction was performed with radioactive ATP included. For protocol #2, the membrane was immediately transferred to a standard 4 min reaction with both fresh kinase and radioactive ATP. However, for protocol #3, the membrane was washed twice to remove unbound kinase and then transferred to a secondary reaction which include radioactive ATP but lacked additional kinase. (**B**) Substrate phosphorylation profiles ([γ-^{32}P] phosphate incorporation of SPOTs peptides) by $CaMKII_m$. T^{287} autophosphorylated $CaMKII_m$ phosphorylation of SPOTs comparing a normal 4 min reaction (B – 1) to reactions with only radioactive secondary 4 min reactions with (B – 2) or without (B – 3) additional kinase in the secondary reaction (n = 3).

The substrates in our SPOTs experiments were 15mers; however, we also wanted to see how longer peptides responded. We first compared $CaMKII_m^{-P}$ phosphorylation of GluN2B (a high-affinity substrate) by as a 15mer, 17mer, or 22mer. A significant decrease in the amount of phosphorylation was observed each time the peptide was extended (Figure 2.12A). This could be result of increased substrate affinity of an already high-affinity substrate ($GluN2B_{S1303}$, K_m = 4.6±1.1 μM) such that the catalytic turnover is reduced. It could also be due to less substrate accessibility or degeneration of peptide synthesis as substrate sequence is extended. To try to distinguish between these possibilities, we compared the phosphorylation of the shorter peptides (either 15mer or 17mer) with those that had either an N- or C-terminal linkers. The linkers were composed of alternatively Ala and Gly residues. We found that addition of a linker to extend the total length of the peptide to 22 residues decreased the phosphorylation (though not significantly for an N-terminal addition to the 17mer) (Figure 2.12, B and C). However, there was no significant difference between the N- or C-terminal placement of the linker, suggesting that the decrease was not due synthesis but rather accessibility. Because the decrease in phosphorylation associated with extended the native GluN2B sequence was less than the addition of the linkers, it suggests that this was due to increased affinity. Sequences for all the constructs are shown in Figure 2.12D.

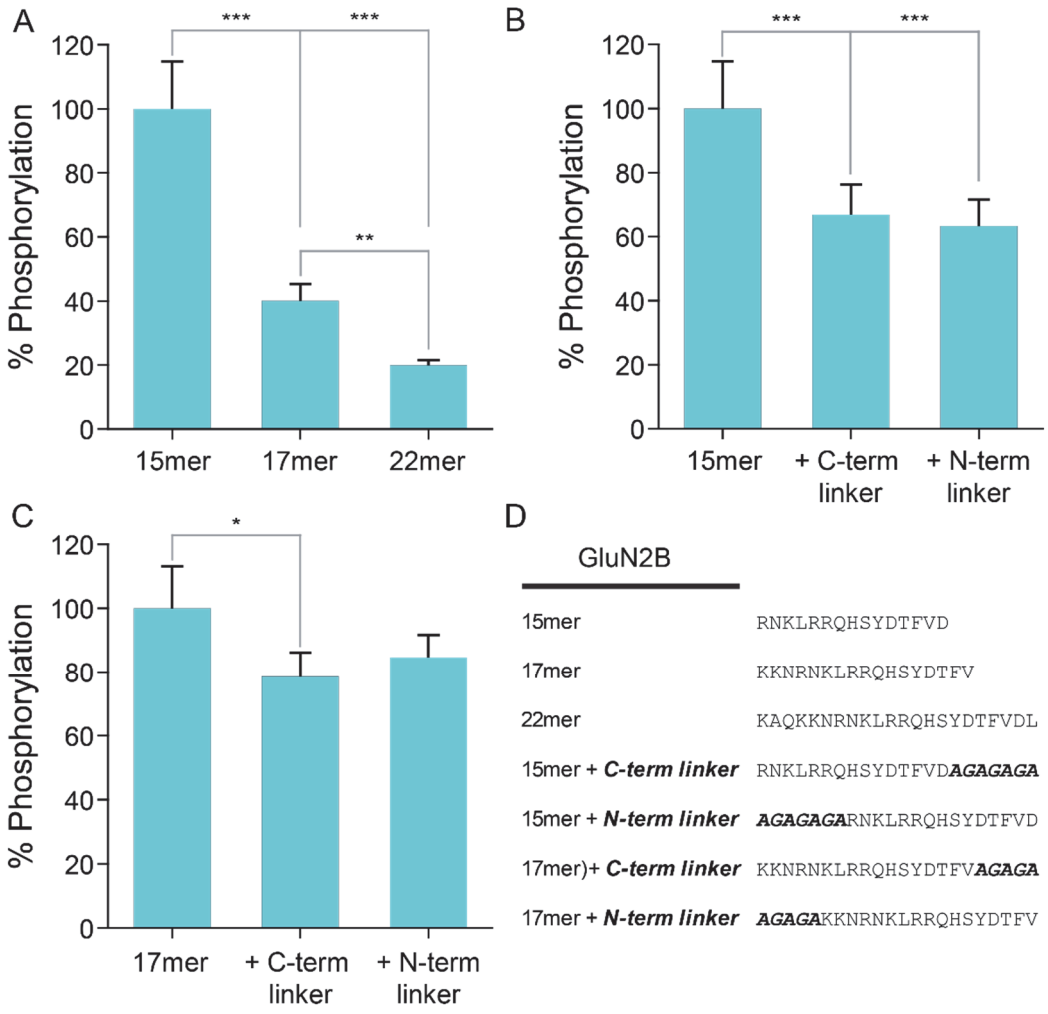

Figure 2.12 Assessments of SPOTs substrate length and accessibility.
(**A** to **C**) Relative phosphorylation of the high-affinity CaMKII substrate GluN2B. (**A**) Comparison of standard 15mer versus longer versions (17mer or 22mer) of GluN2B. (**B** and **C**) Comparison with either an N- or C-terminal linker of Ala-Gly repeats extending total peptide length to 22 amino acids for either the of GluN2B a 15mer in (**B**) or 17mer in (**C**). (**D**) Table of peptide sequences and with linkers italicized in bold.

2.3.5 Autophosphorylation-induced Alterations in Kinase Specificity Does Not Appear to Be Isoform Dependent for $CaMKII_m$

Based on the limited differences seen in the sequence and structures of the catalytic surfaces and regulatory domains for all four CaMKII isoforms (see Figure 1.4) (Rellos, Pike et al. 2010), we predicted that there should be minimal differences in the ability of their ARD to generate substrate filtering for $CaMKII_m$ in the absence of T^{287} autophosphorylation. Though both Syntide and vimentin did exhibit statistical significance, the overall phosphorylation profiles for $CaMKII_m^{-P}$ for both α and δ CaMKII isoforms were quite similar, as expected (Figure 2.13). Similarly, the phosphorylation profiles for $CaMKII_m^{+P}$ were nearly identical for both α and δ CaMKII isoforms, except that GluN2B exhibited greater phosphorylation in the δ isoform (Figure 2.13). These data suggest that substrate filtering is a general mechanism in CaMKII and that isoform differences in the catalytic and autoregulatory domains, at least between α and δ isoforms, do not greatly alter this phenomena.

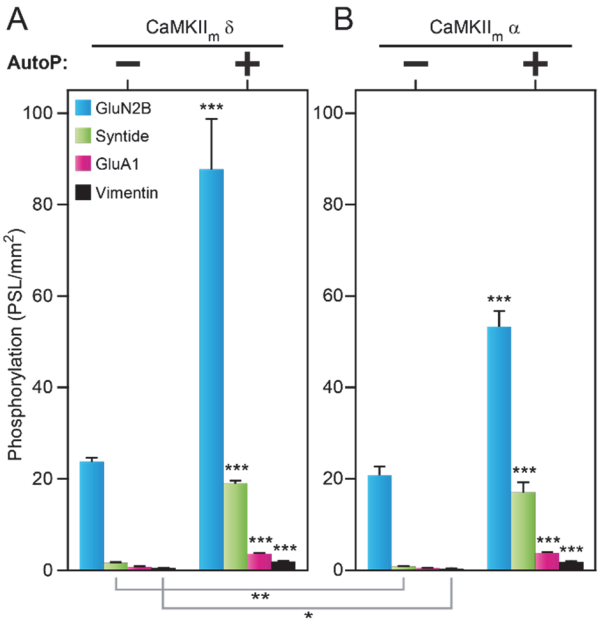

Figure 2.13 Similar phosphorylation profiles between alpha and delta isoforms of CaMKII. (**A** and **B**) Substrate phosphorylation profiles of peptide substrates (SPOTs) by Ca^{2+}/CaM-stimulated $CaMKII_m$ (+/- T^{287} autophosphorylation). $CaMKII_m$ delta isoform in (**A**) or $CaMKII_m$ alpha isoform in (**B**) (n=3). Error bars in all panels denote ± SD. Unpaired/two-tailed *t*-test (*) compared to non-T^{287}-autophosphorylated state (above error bar) or between isoforms (below panels), *P < 0.05, **P < 0.01, ***P < 0.001.

2.3.6 Substrate-dependent Enhancement of Phosphorylation is Not Limited to SPOTs Arrays

The enzymatic properties of CaMKII have historically been studied using solution assays with soluble peptide substrates; therefore, we generated soluble peptide substrates to assess these findings in diffusion-limited reactions. We observed a similar substrate-dependent enhancement seen previously with immobilized, diffusion-restricted SPOTs substrates (Figure 2.14, A and B). Specifically, enhancement increased as substrate affinity decreased, suggesting that this effect is not limited to substrates ability to diffuse. However, our finding were so far limited only to peptides comprised of the phosphorylation motif from known protein substrates. While peptides allow us to specifically dissect the effect of the amino acid composition surrounding the phosphorylation motif, we created a uniform protein backbone deviating only by a substrate adduct to mimic spatial and steric constraints typical of proteins. Thus, this artificial, yet advantageous GST-substrate-fusion model allows differences in substrate utilization by different autophosphorylation states of CaMKII to be attributed directly to substrate-catalytic interactions, rather than the structural diversity inherent to different protein substrates. We observed that autophosphorylation potentiates weak substrate phosphorylation within the context of a larger protein for diffusion-limited (soluble GST fusions) environments (Figure 2.14, C and D). A similar finding was observed for diffusion-restricted (GST-bound fusions) environments, which also was consistent with SPOTs peptides (Figure 2.15). These data support the idea that T^{287} autophosphorylation controls the ability of CaMKII to utilize weak peptide and protein substrates in both diffusion-limited and diffusion-restricted environments.

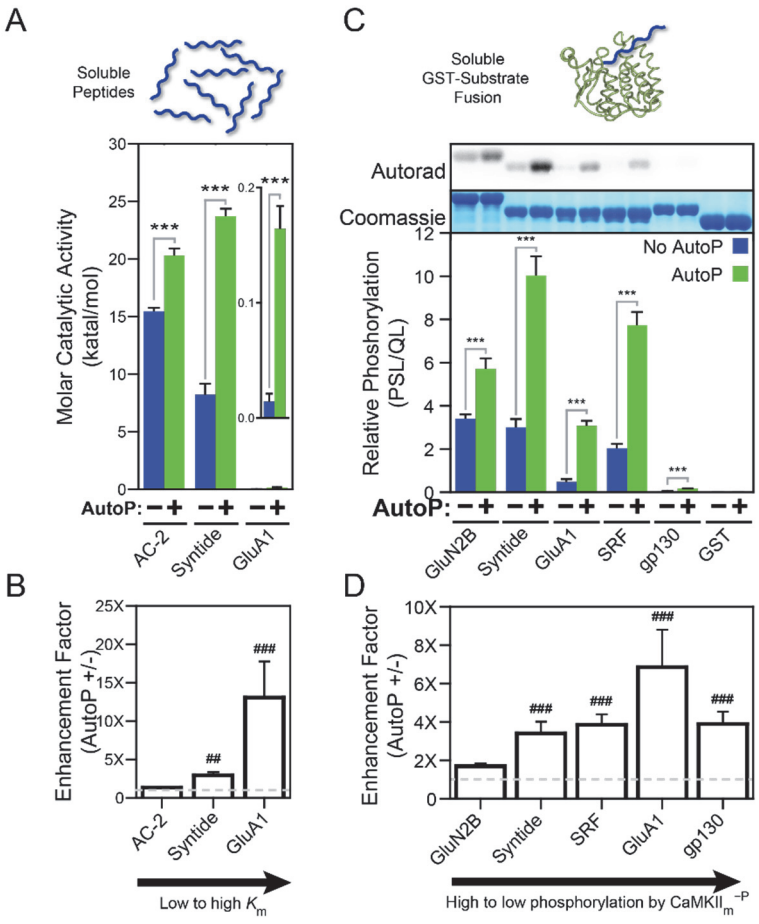

Figure 2.14 T^{287} autophosphorylation alters phosphorylation profile of soluble substrates. (**A** and **B**) Substrate phosphorylation profiles ([γ-^{32}P] phosphate incorporation of soluble peptides by CaMKII$_m$. (**A**) Absolute phosphorylation values for CaMKII$_m^{-P}$ (blue) and CaMKII$_m^{+P}$ (green) (n=3). (**B**) Enhancement factor (white bars) (ratio of +/- T^{287} autophosphorylation) ranked in order of highest to lowest absolute phosphorylation (n = 3). (**C** and **D**) CaMKII phosphorylation of GST-fusion substrates in soluble phosphorylation assays using CaMKII$_m$. (**C**) Representative phosphoimage (top) along with total protein (middle) densitometry of Coomassie stained bands. Relative phosphorylation (lower) values expressed in phosphosignal per total protein (PSL/QL) (n = 4). (**D**) Enhancement factor (n = 4). Results are pooled from three independent experiments with error bars in panels (**A**) and (**B**) denoting ±SEM. Error bars in panel (**B**) denote ±SD for a representative blot.

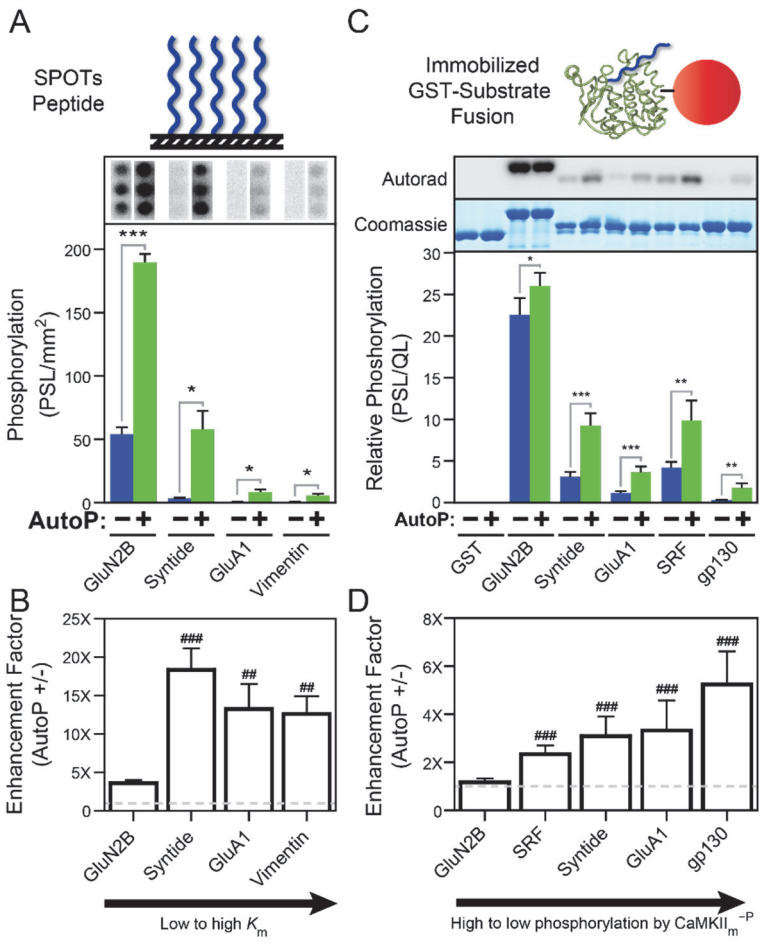

Figure 2.15 T^{287} autophosphorylation alters phosphorylation profile of tethered substrates. (**A** and **B**) Substrate phosphorylation profiles ([γ-^{32}P] phosphate incorporation of SPOTs peptides) by CaMKII$_m$. (**A**) Absolute phosphorylation values for CaMKII$_m^{-P}$ (blue) and CaMKII$_m^{+P}$ (green) (n=3). Representative SPOTs blots (lower) visualized by phosphorimaging. (**B**) Enhancement factor (white bars) (ratio of +/- T^{287} autophosphorylation) ranked in order of highest to lowest absolute phosphorylation (n = 3) with dashed line indicating no change. (**C** and **D**) CaMKII phosphorylation of GST-fusion substrates immobilized onto glutathione resin. (**C**) Representative phosphoimage (top) along with total protein (middle) densitometry of Coomassie stained bands. Relative phosphorylation (lower) values expressed in phosphosignal per total protein (PSL/QL) (n = 4). (**D**) Enhancement factor (n = 4). Results are pooled from three independent experiments with error bars in panels (**A**) and (**B**) denoting ±SEM. Error bars in panel (**C**) and (**D**) denote ±SD for a representative blot.

2.3.7 The ARD of CaMKII is Responsible for Suppressed Phosphorylation of Poor Substrates in the Absence of T^{287} Autophosphorylation

Our results have shown that substrate selectivity is limited in the absence of T^{287} autophosphorylation and that following autophosphorylation, specificity is broadened. The T^{287} residue resides within the R1 segment of the ARD; a region N-terminal to the CaM-target sequence (Figure 1.2A). Since the site of autophosphorylation resides within the ARD, we wanted to explore whether the ARD itself played a role in the altered substrate selectivity. To determine the contribution of the ARD in preventing weak substrate phosphorylation in the activated state, we generated a constitutively active catalytic fragment ($CaMKII_{cf}$) by removing the ARD completely (see Methods 2.2.1 and Figure 2.16). Similarity in the phosphorylation profiles between the $CaMKII_m^{+P}$ and the $CaMKII_{cf}$ (Figure 2.17) indicates that broad substrate specificity is realized upon full ARD displacement from the catalytic domain either from proteolysis of the ARD or upon T^{287} autophosphorylation upon autophosphorylation. Surprisingly, autonomous CaMKII (i.e., Ca^{2+}/CaM-independent activity following T^{287} autophosphorylation) maximizes phosphorylation only of strong substrates (Figure 2.17) suggesting that substrate selectivity is differentially impacted by different activation states of CaMKII. This finding may functionally explain the observation that T^{287} autophosphorylation alone is not sufficient for synaptic plasticity (Barcomb, Buard et al. 2014) suggesting that maximal substrate accessibility associated with coincident Ca^{2+}/CaM binding and T^{287} autophosphorylation underlies the switch-like role of CaMKII in synaptic plasticity. Removal of the ARD via proteolysis exposes the default mode of CaMKII's catalytic domain (i.e., maximal activity

with broad specificity). Autophosphorylation at T^{287} correlates with the high-affinity CaM binding mode termed CaM trapping (Meyer, Hanson et al. 1992, Singla, Hudmon et al. 2001) and yields a similar broadening of substrate specificity consistent with the full disinhibition of the ARD. Thus, while the CaMKII catalytic domain is a classical multifunctional protein kinase with broad substrate specificity, the ARD imparts an intrinsic means of restricting phosphorylation of weak substrates.

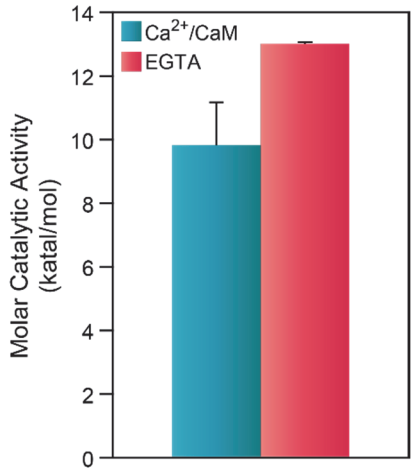

Figure 2.16 Catalytic fragment is constitutively active.
Enzymatic activity (katal/mol) of a catalytic fragment of CaMKII measured via standard soluble peptide assays with radioactive [γ^{32}P]ATP. Ca^{2+}-dependent (Ca^{2+}/CaM) vs Ca^{2+}-independent (EGTA) assays were used to assess the amount of constitutive activity (n = 3). Error bars denote ±SD.

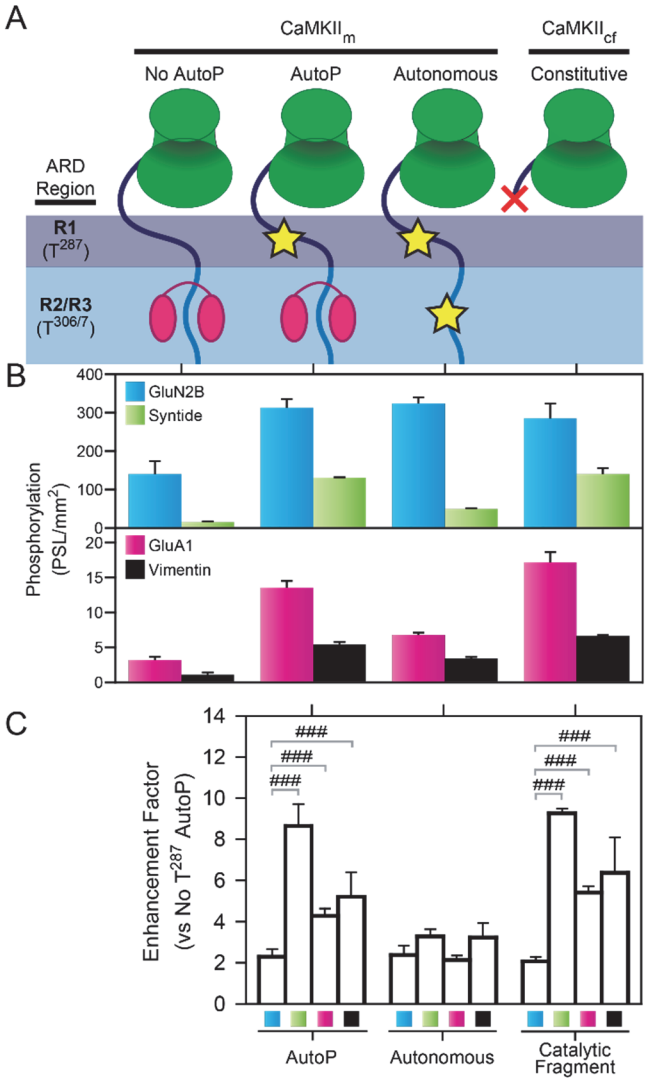

Figure 2.17 Role of the autoregulatory domain (ARD) and T^{287} autophosphorylation in regulating substrate selectivity.
(**A**) Structural representations of $CaMKII_m$: catalytic domain (green) and ARD with subdivisions R1 (dark blue) and R2/R3 (blue) (Chao, Pellicena et al. 2010). Activation state indicated by the presence of calmodulin (CaM) (magenta) and/or autophosphorylation (yellow star) at T^{287} and $T^{306/7}$. Also depicted is a catalytic fragment with truncated ARD. (**B**) Substrate phosphorylation profiles for the catalytic fragment versus Ca^{2+}/CaM-stimulated $CaMKII_m$ (+/- T^{287} autophosphorylation) or autonomous $CaMKII_m$ (n = 3). (**C**) Enhancement factor of phosphorylation profiles compared to $CaMKII_m^{-P}$ (n = 3). **B** shows one-way ANOVA of log-normalized data with Holm-Šídák post-test compared to $CaMKII_m^{-P}$ ($P < 0.001$), while **C** shows comparison to GluN2B ($P < 0.001$).

2.3.8 Differential Ability of Substrates to Enhance CaM Binding Suggests Competition Between Substrates and the ARD in the Absence of T^{287} Autophosphorylation.

Since T^{287} autophosphorylation exposes the default mode of CaMKII's catalytic domain and leads to full displacement of the ARD from the catalytic domain, the data are consistent with a model whereby in the absence of autophosphorylation, Ca^{2+}/CaM activation alone does not displace the ARD sufficiently for catalytic domain access by low-affinity substrates. Because autophosphorylation fully displaces the ARD to allow CaM trapping, we reasoned that a substrate's ability to compete with the ARD for the catalytic domain is reflected by changes in Ca^{2+}/CaM binding affinity. To explore the potential for substrates to influence ARD/catalytic interactions, we used a conformationally sensitive fluorescent reporter of CaM binding ($CaM_{IAEDANS}$) (Figure 2.18A) to test whether substrates differentially enhance Ca^{2+}/CaM binding in the absence of autophosphorylation. We observed that, in contrast to the weak peptide substrate Syntide, high-affinity peptide substrates (AC-2 and GluN2B) increase Ca^{2+}/CaM binding affinity as measured by enhanced fluorescent intensity (Figure 2.18B) and decreased K_{off} (Figure 2.18, B and C). Therefore, the inability of weak substrates to influence Ca^{2+}/CaM binding suggests that weak substrates cannot outcompete the ARD for access to the catalytic domain. Thus, while K_m approximates a substrate's ability to interact with the catalytic domain, a substrate's ability to enhance Ca^{2+}/CaM binding is a reflection of a substrate's ability to displace the ARD from the catalytic domain.

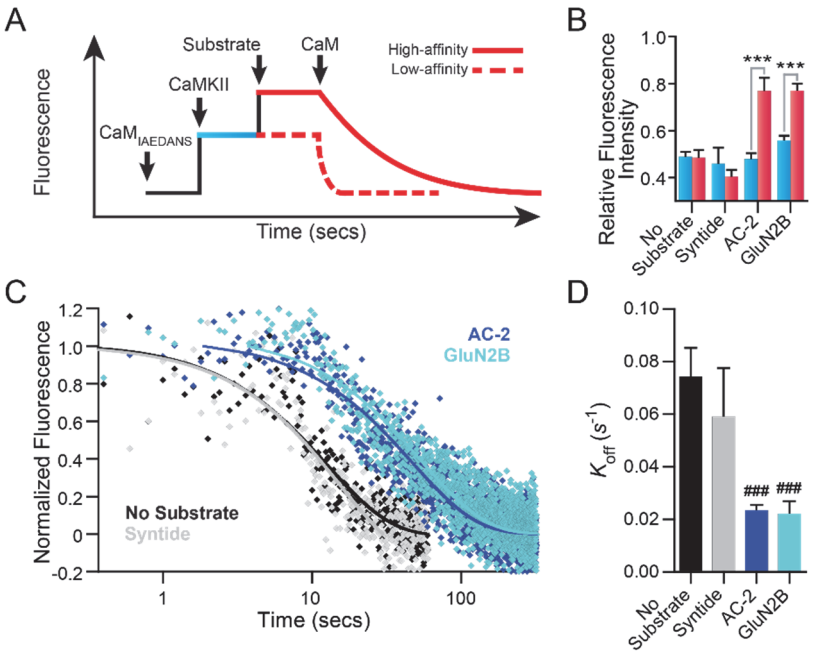

Figure 2.18 The ARD of activated CaMKII competes with substrates for access to the catalytic domain in in the absence of T^{287} autophosphorylation.
(**A**), Schematic of experimental paradigm used to assess the impact of high-affinity (solid red line) versus low-affinity (red dashed line) substrates on CaM binding. (**B**), Relative fluorescence intensity change upon $Ca^{2+}/CaM_{IAEDANS}$ binding to $CaMKII_{holo}$ in the presence of ADP; data normalized to free $Ca^{2+}/CaM_{IAEDANS}$ (0) and $Ca^{2+}/CaM_{IAEDANS}$-bound $CaMKII_m^{+P}$ (10). Data represent mean ±SD (n = 3). Unpaired/two-tailed t-test used to compare to control (no substrate) (***P < 0.001). (**C**), Dissociation kinetics of $CaM_{IAEDANS}$ from $CaMKII_m^{-P}$ were measured by fluorometry initiated by rapid mixing of excess unlabeled Ca^{2+}/CaM. Representative traces without substrate (black diamonds) or with Syntide (white diamonds), AC-2 (light blue diamonds), or GluN2B (dark blue diamonds). Data normalized with intensity difference between kinase-bound $Ca^{2+}/CaM_{IAEDANS}$ and free $Ca^{2+}/CaM_{IAEDANS}$ to be 1.0, with the curve fit to single exponential equation. (**D**), Grouped dissociation data, representing mean ±SD (n = 3). One-way ANOVA of log-normalized data with Holm-Šídák post-test compared to no substrate (###P < 0.001).

2.3.9 CaMKII Substrate Specificity is Differentially Altered by modification of T^{287}

If competition exists between substrates and the ARD for access to the catalytic domain while CaMKII is activated, yet not T^{287} autophosphorylated, and is then disengaged upon autophosphorylation, then weakening ARD binding should yield intermediate phosphorylation profiles. The electronegativity of the autophosphorylated T^{287} residue can be interpreted to create autonomous activity and CaM trapping by preventing re-association with the hydrophobic pocket in which T^{287} resides in the autoinhibited crystal structure (Figure 1.2A) (Singla, Hudmon et al. 2001, Rellos, Pike et al. 2010, Hoffman, Stein et al. 2011). Thus, we manipulated the electronegativity of residue 287 (using site-directed mutagenesis; see Methods 2.2.1) and determined its ability to modulate substrate specificity. Side-chain modification at T^{287} (Val<Ala<Asn<Asp) produces a graded increase in constitutive activity of apoCaMKII (Figure 2.19)—consistent with weakened ARD–catalytic domain interactions. In the Ca^{2+}/CaM-stimulated state ($CaMKII_m^{-P}$), phosphorylation of the weak substrate (Syntide) increases in a graded fashion with mutation electronegativity (Val<Ala<Asn<Asp) (Figure 2.20). In contrast, substitutions less hydrophobic than Val produce maximal phosphorylation of high-affinity substrate GluN2B (Figure 2.20). Consistent with the autonomous form of CaMKII, minimal perturbation of the ARD allows high-affinity substrates to outcompete the weakened ARD in the absence of T^{287} autophosphorylation. In contrast, weak substrates do not have access to the catalytic domain following Ca^{2+}/CaM binding until T^{287} autophosphorylation fully destabilizes the ARD. Interestingly, the non-phospho-acceptor substitution ($T^{287}A$) that classically prevents T^{287} autophosphorylation enhances phosphorylation of weak substrates compared to $CaMKII_m^{-P}$, suggesting that some functional deficits seen in transgenic animal

models and cell-based studies harboring the $T^{287}A$ mutation (Cho, Giese et al. 1998, Giese, Fedorov et al. 1998, Glazewski, Giese et al. 2000, Gustin, Shonesy et al. 2011) may involve unexpected alterations in substrate specificity.

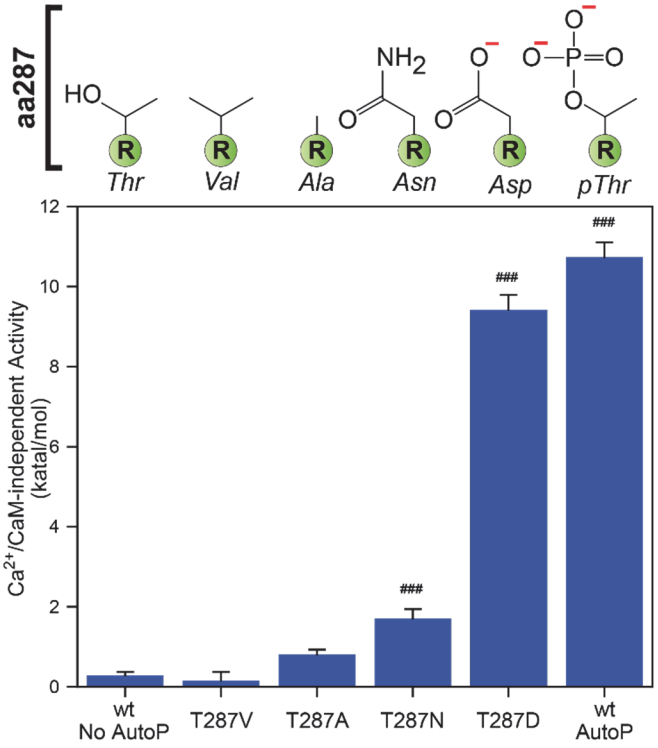

Figure 2.19 T^{287} mutations generate constitutive activity in CaMKII.
Ca^{2+}/CaM-independent activity for $CaMKII_m$ mutants expressed in molar terms (katal/mol) and measured via standard soluble peptide (AC-2) assays with radioactive [γ^{32}P]ATP; mean ±SD (n = 3). One-way ANOVA of log-normalized data with Holm-Šídák post-test (#) used to compare to wt apo$CaMKII_m$ (#$P < 0.05$, ###$P < 0.001$).

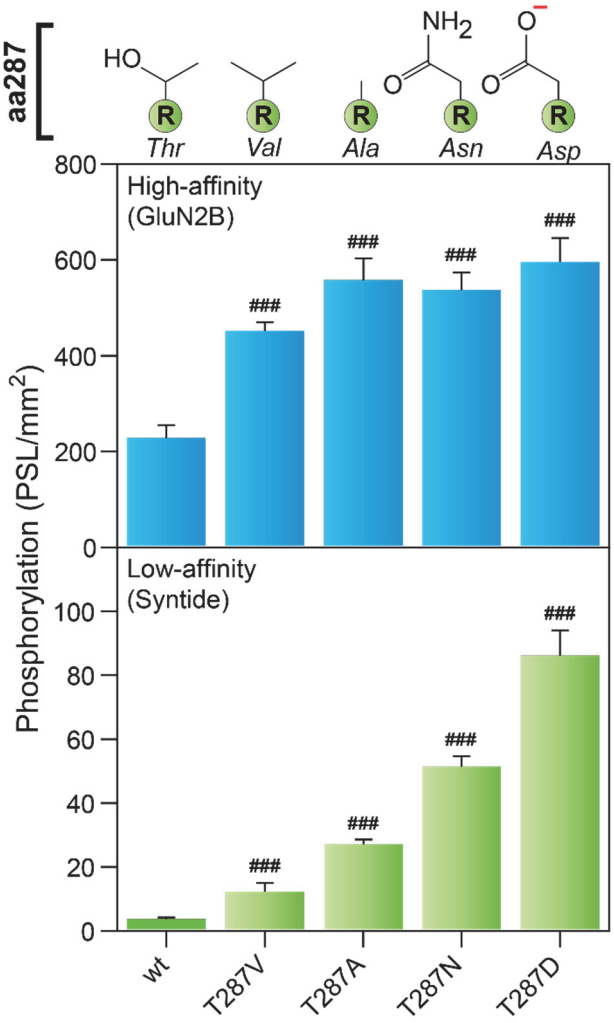

Figure 2.20 T^{287} modification regulates substrate selectivity.
Ca^{2+}/CaM-stimulated phosphorylation of SPOTs substrates for T^{287} mutants of $CaMKII_m$. Data represent mean ±SD (n = 3). One-way ANOVA of log-normalized data with Holm-Šídák post-test compared to wildtype (Thr) (###$P < 0.001$).

2.4 Conclusion

Our data describe a novel and surprising finding for the function of the ARD of CaMKII to act a substrate selective gate regulated by T^{287} autophosphorylation. Initially, we explored the phosphorylation of immobilized peptide substrates made up of 217 known and validated substrate phosphorylation sites. As a way to control the state of T^{287} autophosphorylation without requiring mutagenesis of the site, we utilized a monomeric version of the kinase which retained the ARD, yet was lacking the hub domain. Thus, while activation of this version of the kinase was still Ca^{2+}/CaM-dependent, the autophosphorylation reactions could be controlled by limiting kinase concentration due the now biomolecular, *trans* nature of the reaction. We found that in the absence of autophosphorylation, monomeric CaMKII ($CaMKII_m^{-P}$) exhibited narrow substrate specificity. As such, the best substrates were those most similar in sequence to that of a defined CaMKII consensus motif obtained using a non-biased library screen. This was not the case for autophosphorylated CaMKII, either for monomer ($CaMKII_m^{+P}$) or the multimeric holoenzyme ($CaMKII_{holo}^{+P}$). The best substrates shifted to those with less similarity to the consensus motif consistent with a broadening of substrate specificity. $CaMKII_{holo}^{+P}$ tended to shift the specificity even further towards more diverse substrates, likely the result of multivalent avidity, thereby increasing the relative affinity for normally low-affinity substrates. This change in substrate specificity was very similar between the α- and δ-isoforms of the monomeric kinase, which was consistent with the lack of sequence differences within the ATP and substrate binding grooves. We also confirmed that these findings using SPOTs peptides were not the result of limited peptide availability or accessibility, nor was it a result of limited kinase mobility. Furthermore, we found that this

phenomena was not limited to the SPOTs assays. Instead, we observed similar findings for soluble versions of the peptides. Thus, substrate specificity is broadened following autophosphorylation for substrates in both diffusion-restricted and diffusion-limited environments. By attaching these phosphorylation sites to identical protein fusions, we established that altered substrate specificity based on the state of autophosphorylation can occur in the context of larger proteins. To determine the role that the ARD itself plays in this process, we looked at the phosphorylation of a constitutively active catalytic fragment ($CaMKII_{cf}$) of CaMKII which was generated by chymotryptic digestion of the ARD. This construct should represent the default mode of CaMKII catalytic domain as there is no ARD present to affect to potentially affect the activity and/or specificity. Given that T^{287} autophosphorylation is thought to lead to full displacement of the ARD from the catalytic domain, we expected that that phosphorylation profiles between the $CaMKII_{cf}$ and $CaMKII_m^{+P}$ should be similar. Since they were nearly identical, it suggests that the broadened specificity of $CaMKII_m^{+P}$ is the result of autophosphorylation switching the kinase to its default mode. It also suggests that the ARD itself is responsible for narrowing of substrate specificity by preferentially limiting the phosphorylation of weak, low-affinity and/or poor consensus-like substrates. Importantly, we found that Ca^{2+}/CaM was required to be bound to the ARD in addition to T^{287} autophosphorylation to fully expose the default mode. However, we did find that the autonomous form of the kinase (i.e. T^{287} autophosphorylation followed by removal Ca2+/CaM leading to $T^{306/7}$ autophosphorylation) exhibits a general enhancement of catalytic activity compared to the non-T^{287} autophosphorylated kinase. The strength of CaM-binding in non-T^{287} autophosphorylated state is inversely proportional to the strength of the interaction of the

ARD with the catalytic domain. Thus, we were able to use CaM binding as an indirect readout of whether substrates could compete with the ARD for access to the catalytic domain. Consistent with the ARD limiting the phosphorylation of weaker substrates in the absence of T^{287} autophosphorylation, we found that weak substrates were unable to enhance CaM-binding. We then reasoned that if substrates compete with the ARD, then weakening the ARD-catalytic domain interaction should disrupt the ARD's ability to preferentially limit the phosphorylation of weaker substrates. We found that by incrementally modifying the T^{287} residue from more hydrophobic to more electronegative, substrate specificity could be modulated to produce intermediate phosphorylation profiles.

The ARD has classically been defined as a regulatory gate that prevents substrate accessibility and therefore phosphorylation in the naïve or inactive state. However, our data favors the idea that the ARD of CaMKII continues to modulate substrate accessibility even when activated by Ca^{2+}/CaM. Thus, CaMKII utilizes its ARD to increase the dynamic range between high- and low-affinity substrates, with T^{287} autophosphorylation acting as a switch to disengage the ARD from preventing phosphorylation of weak substrates. One way to envision this process is a competition between the ARD and substrates for access to the catalytic domain. Tighter ARD binding to the catalytic surface prevents the high-affinity binding more of CaM (i.e. trapping). On the other hand, increased displacement of the ARD leads to enhanced CaM binding. Thus, substrates capable of displacing the ARD in the absence of T^{287} autophosphorylation lead to enhanced CaM binding in addition to preferential phosphorylation.

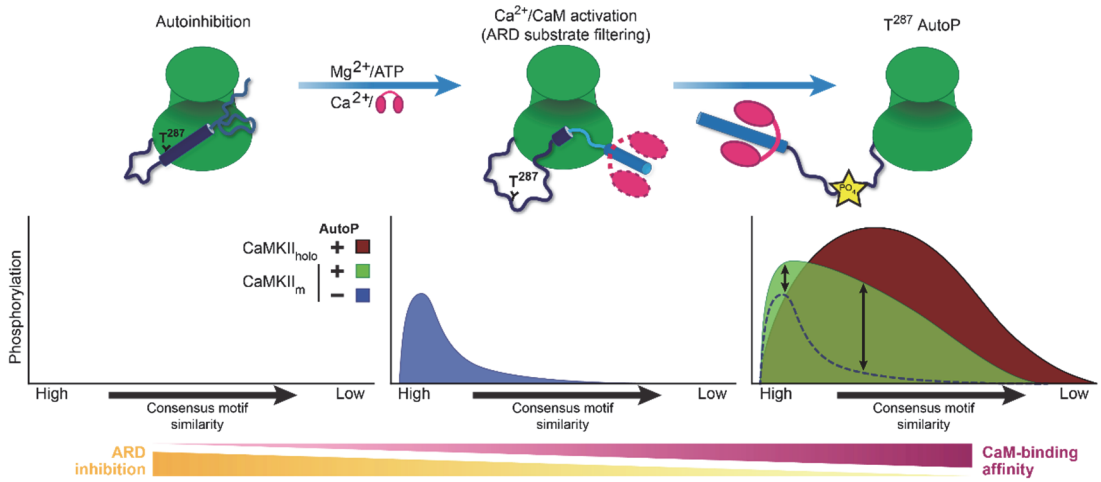

Figure 2.21 Model of ARD selectivity filter.
In the autoinhibited state, the autoregulatory domain (ARD) prevents substrate phosphorylation. Ca^{2+}/calmodulin (CaM) binding partially displaces the ARD, allowing preferential phosphorylation of high-affinity substrates. Partial retention of ARD–catalytic domain contacts in the absence of T^{287} autophosphorylation prevents CaM-trapping, and submaximal catalytic activity results from ARD oscillations between bound and unbound states. Ca^{2+}/CaM-associated T^{287} autophosphorylation fully disengages the ARD, expanding substrate specificity to low-affinity substrates. Model phosphorylation profiles below show how changes in CaMKII state affect substrate phosphorylation. An inverse relationship exists between the amount of ARD inhibition and the affinity of CaM-binding.

Solution EPR studies measuring the conformational changes of the ARD interacting with the catalytic domain indicate a multistep, dynamic process (Hoffman, Stein et al. 2011). More specifically, these analyses on the micro second time-scale show that the region of the ARD defined as the R2 domain, containing F^{294}, actually maintains coupling to the catalytic domain when activated by Ca^{2+}/CaM but does not fully uncouple until T^{287} autophosphorylation (or phosphomimetic substitution) completely destabilizes the R1 region. Such a phenomena likely explains the transition from low- to high-affinity CaM binding and the mechanism by which T^{287} autophosphorylation controls this process. While partial tethering of the ARD appears to serve as the structural mechanism to prevent CaM-trapping, our data show that a novel functional consequence of ARD tethering is to modulate substrate selectivity.

Filtering Model Description

The autoinhibited crystal structures of CaMKII demonstrates that the ARD makes intramolecular contacts within the autoinhibitory-groove (Rellos, Pike et al. 2010, Chao, Stratton et al. 2011); a hydrophobic channel on the catalytic surface whereby the helical ARD makes tertiary contacts around the R1 segment (i.e. T^{287}) and the R2 segment of the ARD (Figure 1.2A). This mode of binding likely prevents the transitioning of the D-helix, which is required for exposure of the active site and substrate binding groove (Figure 2.22). Binding of Ca^{2+}/CaM to the R3 segment of the ARD induces the R1 segment to uncoil for presentation of the T^{287} site for an intermolecular autophosphorylation event (Figure 1.3); a cooperative reaction due to the dual requirement of CaM binding to both subunits acting as kinase and substrate (Hanson, Meyer et al. 1994). Based on crystal structure data of the

naïve versus activated CaMKII, activation induces a shift in the D-helix which deforms the autoinhibitory groove and opens the active site for substrate binding and the phosphotransferase reaction (Figure 2.22).

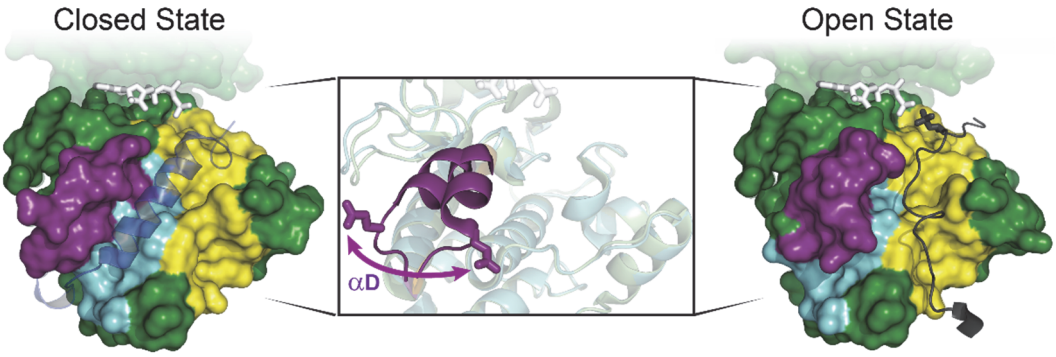

Figure 2.22 Transition of the catalytic surface between closed and open states.
In the closed state (hCaMKII$\delta_{11\text{-}309}$; PDB ID: 2VN9), the substrate binding groove (yellow) of the catalytic domain is autoinhibited by the ARD. The ARD is stabilized in the autoinhibitory groove (cyan) by the αD helix (violet). Full displacement of the ARD in the open state (hCaMKII$\delta_{11\text{-}335}$; PDB ID: 2WEL) following T^{287} autophosphorylation induces the collapse of the autoinhibitory groove as the αD helix shifts toward the substrate binding groove (bound substrate illustrated in black).

The substrate binding groove makes an obvious site to afford the ARD to function as a competitive inhibitor with substrates, thereby preferentially inhibiting low-affinity poor consensus substrates in the activated non-T^{287} autophosphorylated state. However, such a binding interaction would likely promote preferential T^{287} autophosphorylation prior to substrate phosphorylation, due to this motif (T^{287} phosphorylation site) being a high-affinity consensus type substrate. In fact, the ScanSite score of this site is similar to the high-affinity exogenous CaMKII substrate GluN2B (0.388 vs 0.294, respectively). We ruled out interactions of the ARD with the substrate groove based on the fact that, 1) the R3 segment of the ARD is not available in the Ca^{2+}/CaM bound state, 2) a peptide consisting of the ARD ($CaMKII_{281-309}$) is preferentially an inhibitor toward a catalytic fragment of CaMKII (Colbran, Fong et al. 1988), with T^{287} phosphorylation occurring in this peptide only in the Ca^{2+}/CaM bound state, suggesting that the R1 and R2 segments preferentially bind to the autoinhibitory groove in the absence of Ca^{2+}/CaM and 3) T^{287} autophosphorylation has been demonstrated to occur almost exclusively through an intersubunit interaction (Hanson, Meyer et al. 1994, Rich and Schulman 1998); therefore, even though T^{287} is clearly targeted for phosphorylation in the Ca^{2+}/CaM bound state of the ARD, an intrasubunit mode of phosphorylation is not permissible. Direct support for our data indicating that the substrate binding groove is not the binding site for the ARD in producing substrate selection, is that the percent autonomy remained constant from the start to the end of our phosphorylation reactions (Figure 2.1F); evidence that rules out both intra- and intersubunit interactions with the substrate binding groove to mediate substrate selectivity.

In contrast, ARD interactions with the autoinhibitory groove have the distinct advantage of regulating substrate binding without risking dysregulated T^{287} autophosphorylation. Such a mechanism may not be intuitive based on the preconception that CaM binding to the ARD functions to disinhibit autoinhibition. However, T^{287} autophosphorylation requires a CaM-bound ARD to interact with the catalytic surface and active site, indicating that steric constraints induced by CaM's bi-lobed architecture do not prevent the ARD from interacting with the catalytic domain. Thus, stable docking of the ARD with inhibitory groove maintain the autoinhibited state; dynamic contacts between the ARD and autoinhibitory groove could function to limit low-affinity weak consensus substrate access. Such a mechanism maintains a trans-autophosphorylation reaction (i.e. permit high-affinity substrate phosphorylation), while punishing low-affinity substrates. Changes in substrate selectivity are predicted to accompany T^{287} autophosphorylation due to a loss of ARD interactions with the autoinhibitory groove; a process that results from conformational changes in the ARD stabilized by CaM-trapping to the T^{287} autophosphorylated subunit. Elements of this model can be gleaned from EPR solution data (Hoffman, Stein et al. 2011) showing that Ca^{2+}/CaM binding to the ARD (R3 segment) yields a reversible unfolding of the R1 segment associated with increased mobility. These changes in R1 are not accompanied by any major mobility changes in the R2 segment (specifically F^{294}). Furthermore, a phosphomimetic mutation of T^{287} ($T^{287}E$) yielded additional flexibility within the R1 segment, with F^{294} in the R2 region displaying a loss of catalytic surface contacts (Hoffman, Stein et al. 2011); a consequence of F^{294} being required for CaM-trapping (Waxham, Tsai et al. 1998). Therefore, a previously unexplored consequence of this complex interplay between R1 and R2 in the activated and non-T^{287}

autophosphorylated state is that low-affinity substrates should have poor accessibility due to the ARD dynamically binding to the autoinhibitory groove until T^{287} autophosphorylation disables this interaction. Thus, ARD-catalytic surface interactions not only couple CaMKII activity to the Ca^{2+} signal, they also permit T^{287} autophosphorylation to switch substrate phosphorylation preferences from high- to low-affinity targets. As this point, we simply do not have information to separate whether ARD binding to the autoinhibitory groove will be dominated by intra-subunit versus inter-subunit contacts. While our pre-autophosphorylation reactions were designed to control the level of T^{287} autophosphorylation, our exogenous substrate phosphorylation reactions were designed to minimize intermolecular events between CaMKII monomeric subunits (5-10 nM). In fact, previous studies have found that activation of CaMKII through Ca^{2+}/CaM binding yields weak dimeric interactions between subunits (K_D of 50-120 μM) (Rellos, Pike et al. 2010) or were not detected (Hoffman, Stein et al. 2011). These contacts likely reflect the trans-autophosphorylation event occurring through active site interactions and disfavor the possibility of these inter-subunit reactions from dominating in our substrate phosphorylation conditions. However, in the native multimeric holoenzyme, it is conceivable that the ARD might be available to interact in an intrasubunit or an intersubunit mode to produce substrate filtering in the activated, non-T^{287} autophosphorylated state by dynamically interacting with the autoinhibitory groove.

CHAPTER 3. Multimeric Control of Substrate Specificity in CaMKII

3.1 Introduction

CaMKII is a multifunctional serine/threonine kinase which plays a role in maintaining neuronal viability and integrating intracellular Ca^{2+} transients. The most well-known role of CaMKII is the regulation of synaptic plasticity, particularly within the post-synaptic neuron as signals from the presynaptic neuron are integrated in the macromolecular signaling complex known as the post-synaptic density (PSD). CaMKII targets, phosphorylates, and regulates a large number of substrates within the PSD to direct distinct outcomes (e.g. LTP and LTD). However, what substrate selectivity mechanisms govern the ability of CaMKII to perform these crucial functions in this macromolecular structure are unknown.

CaMKII exists as a multimeric holoenzyme generally thought to be a dodecamer, though some studies have suggested it may also form tetradecamers (Kolb, Hudmon et al. 1998, Rellos, Pike et al. 2010 Hoelz, 2003 #981, Chao, Stratton et al. 2011, Stratton, Lee et al. 2014, Bhattacharyya, Stratton et al. 2016). This multimeric architecture is rather unique among kinases and gives CaMKII some interesting properties. First, T^{287} autophosphorylation occurs through a *trans*, intersubunit reaction requiring coincident Ca^{2+}/CaM binding to both subunits (contributing either the kinase or the ARD substrate) (Hanson, Meyer et al. 1994, Rich and Schulman 1998). Thus, intersubunit intraholenzyme autophosphorylation functions as a Ca^{2+} spike frequency encoder (De Koninck and Schulman 1998). Such a feature has been viewed as a critical property of CaMKII in synaptic plasticity, where the frequency of cellular activity in neurons is directly related to Ca^{2+} frequency which tunes the strength of synaptic contacts (Lisman, Schulman et al. 2002, Lisman, Yasuda et al. 2012). Second, the multimeric assembly of the CaMKII

holoenzyme affords the kinase with the ability to interact with multiple substrates simultaneously; a feature which may in turn regulate CaMKII enzymatic function and localization. We postulate that in macromolecular complexes such as the post-synaptic density (as well as at the plasma membrane, sarcolemma, and endoplasmic reticulum) where many substrates exist in a diffusion-restricted environment, that these multivalent interactions in conjunction with T^{287} autophosphorylation alter phosphorylation patterns and provide a temporal regulatory function that is dependent on the affinity of the substrate. Thus, there are several fundamental questions about CaMKII signaling that we would like to address: 1) What role does the multimeric structure play in the substrate selection? 2) Can substrates in a complex environment affect CaMKII localization and/or activity?

In this study, we used inhibitory autophosphorylation to titrate the number of activatable subunits within the holoenzyme to explore how limited holoenzyme activation alters substrate specificity. Using immobilized peptide substrates (SPOTs), we found that an individual subunit within the holoenzyme behaves like a monomer in the absence of autophosphorylation, displaying narrowed substrate specificity similar to that observed in Chapter 2. Further activation of subunits within the holoenzyme preferentially enhanced the phosphorylation of weaker substrates beyond simply the contribution of T^{287} autophosphorylation alone. We found that the holoenzyme led to a large increase in the total amount of phosphorylation in purified rat PSDs as assessed by ^{32}P-incorporation. Subsequent analysis by mass spectrometry also displayed similar increases in the number of substrates detected by the holoenzyme. These findings are consistent with enhanced phosphorylation of weaker substrates by T^{287} autophosphorylation and was further

increased by multivalent avidity, which as we show affords high-affinity targeting substrates to broaden specificity through localization.

3.2 Materials and Methods

3.2.1 Expression and Purification of CaMKII and Calmodulin

Recombinant human CaMKIIδ (NCBI RefSeq: NP_742113.1) with an N-terminal 6xHN tag was integrated into a baculoroviral construct (BacPAK9-6xHN), amplified in Sf9 insect cells, and expressed in Hi5 (*T. ni*) insect cells (Takeuchi-Suzuki, Tanaka et al. 1992) (Brickey, Colbran et al. 1990). Site-directed mutagenesis was used to generate monomeric hCaMKII$\delta_{1\text{-}317}$ (i.e. CaMKII$_m$) (by truncation through the addition of stop codon at aa318) as well point mutants. Kinases were purified under reducing conditions by affinity chromatography (NiNTA resin) followed by size exclusion chromatography (Sephacryl S-400 [holoenzyme] or S-300 [CaMKII$_m$]) using an Äkta Purifier (Amersham) (Bradshaw, Hudmon et al. 2002, Ashpole, Herren et al. 2012). SDS-PAGE of the purified proteins revealed a single band with purities >98%. Recombinant sea-urchin calmodulin was expressed and purified in E.coli as described previously via boiling, ammonium sulfate precipitation, and phenyl-sepharose affinity chromatography (Singla, Hudmon et al. 2001, Gaertner, Kolodziej et al. 2004).

3.2.2 CaMKII Holoenzyme Inactivation via Inhibitory Pre-Autophosphorylation

CaMKII$_{holo}$ [600 nM] was exposed to inhibitory autophosphorylation ($T^{306/7}$ capping) for 0, 5, or 15 minutes in the presence of 50 mM HEPES pH 7.4, 100 mM NaCl, 10 mM $MgCl_2$, and 500 μM ATP. Inactivated states of CaMKII were then diluted to 60 nM for SPOTs substrate phosphorylation reactions (described below). For all states of pre-inactivation (0, 5, or 15 min), the SPOTs phosphorylation was normalized to the number of active subunits per holoenzyme. The number of active subunits per holoenzyme was

assessed by measuring the Ca^{2+}/CaM-dependent activity of each inactivation condition in standard soluble peptide substrate phosphorylation assays using AC-2 peptide. These activity assays were performed at the beginning and end (4 min) of the SPOTs phosphorylation assay, their values averaged together. The activity from naïve $CaMKII_{holo}$ (i.e. 0 min pre-inactivation) was considered to maximal (i.e. all 14 subunits activated) and was thus used to calculate the average enzymatic activity per subunit.

3.2.3 Pre-Autophosphorylation Reactions

For reactions involving T^{287} autophosphorylated CaMKII, a pre-reaction was performed in the presence of 20 mM HEPES pH 7.4, 100 mM NaCl, 10 mM $MgCl_2$, 0.5 mM $CaCl_2$, 5 μM CaM, 500 μM cold ATP and 500 nM kinase for 10 minutes on ice. To achieve varying numbers of T^{287} autophosphorylated subunits, similar pre-reactions were used with 50nM kinase incubation times of 0, 5, or 20 minutes on ice, or 10 minutes at 30°C (Figure 3.6A; states 1-4, respectively).

3.2.4 Post-Synaptic Density Purification

PSDs were acquired from female adult rats (Sprague-Dawley) using previously defined procedures involving differential centrifugation with various sucrose gradients followed by Triton X-100 extraction and collection of the Triton-insoluble fraction (Ehlers 2003, Swulius, Kubota et al. 2010). Several steps were taken to limit and reduce the Ca^{2+}/CaM stimulated and autonomous activity of endogenous CaMKII within the PSDs. Rat brains were extracted and snap-frozen in liquid nitrogen within 90 secs after sacrificing the animal, as CaMKII is known to activate and translocate to the PSDs within minutes in

response to cell death (Suzuki, Okumuranoji et al. 1994). In order to dephosphorylate T^{287} to prevent autonomous activity of endogenous CaMKII as well as to reduce the phosphorylation state of endogenous substrates, purified PSDs were dephosphorylated with 1.5 μM PP1α (6xHis purified) overnight at 4°C or at RT for 2 hours with shaking in the presence of 50 mM HEPES pH 7.4, 100 mM NaCl, 1 mM $MnCl_2$, 0.015 Brij 35, 2.5 mM DTT, 10 μM KN-93, and 2X Calbiochem Protease Inhibitor Cocktail Set V.

3.2.5 Post-Synaptic Density Dephosphorylation and Phosphorylation

The PSDs were dephosphorylated to prevent autonomous activity of endogenous CaMKII (resulting from prior T^{287} autophosphorylation), as well as to reduce the phosphorylation state of endogenous substrates. This was accomplished with 1.5 μM PP1α (6xHis purified) overnight at 4°C or at RT for 2 hours with shaking in the presence of 50 mM HEPES pH 7.4, 100 mM NaCl, 1 mM $MnCl_2$, 0.015 Brij 35, 2.5 mM DTT, 10 μM KN-93, and 2X Calbiochem Protease Inhibitor Cocktail Set V. Phosphorylation reactions were carried out on dephosphorylated PSDs in the presence of 2X phosphatase inhibitor cocktail (Calbiochem) as well as the small molecule CaMKII inhibitor KN93 which only inhibits the autoinhibited kinase (naïve). PSD phosphorylation reactions were carried out on ~50 μg of dephosphorylated PSDs (see above) in the presence of 20 mM HEPES pH 7.4, 100 mM NaCl, 10 mM $MgCl_2$, 0.5 mM $CaCl_2$, 5 μM CaM, 100 μM cold ATP, 120 μCi/ml [γ-^{32}P]-ATP, and 350 nM CaMKII (per subunit). For reactions involving T^{287} autophosphorylated CaMKII, a pre-reaction was performed in the presence of 20 mM HEPES pH 7.4, 100 mM NaCl, 10 mM $MgCl_2$, 0.5mM $CaCl_2$, 5 μM CaM, 500 μM ATPγS, and 3.5 μM kinase for 10 min at 30°C (for monomer) or on ice (for the holoenzyme). PSD

phosphorylation reactions (60 µl total) were incubated at room temperature for 4 min unless otherwise noted. Reactions were terminated with the addition of 500 µl of 100 mM sodium phosphate pH 7.0, 1 M NaCl, 10 mM EDTA) followed by centrifugation to obtain a PSD pellet. Pellet was three times in the same termination buffer. The PSD pellet was resuspended in 2X LDS sample buffer and resuspended using a horn sonicator. SDS-PAGE was performed followed by Coomassie staining and drying of the gel. Total protein was assessed by densitometry of the Coomassie signal while the extent of radioactive phosphate incorporation was quantified using a Fujifilm phosphorimager and profiles measured as photostimulated luminescence (PSL/mm^2). The densitometric intensity data was converted to area under the curve (AUC) to determine to protein or total phosphorylation.

3.2.6 Mass Spectrometric Analysis for Phosphorylation of Post-Synaptic Density

PSD phosphorylation reactions similar to those using ^{32}P incorporation were performed (see Method 3.2.5). Instead of both ATP and [γ-^{32}P]-ATP in the phosphorylation reaction, ATPγS was used. The reactions were incubated at room temperature for 4 min, 30 min, or 24 hours with shaking and were terminated by the addition of 50 mM EDTA. The samples were then alkylated via the addition of 2.5 mM *p*-nitrobenzyl mesylate/5% DMSO (Abcam #ab138910), incubated for 1 hr at room temperature, and analyzed by western blotting using a Thiophosphate Ester specific RabMAb (Abcam #92570) at 1:5,000 in TBST/5% Milk visualized using IRDye® 800CW goat anti-mouse secondary antibody and quantified using LI-COR. For mass spectrometry, following the termination of the phosphorylation reaction with EDTA, samples were snap frozen and transferred to Indiana University Bloomington (Dr. Jon Trinidad) for analysis.

3.2.6 Double Synthesis SPOTs (DS-SPOTs)

In experiments where the addition of a targeting peptide along with a substrate peptide in a single spot was required, we utilized a technique called Double Synthesis SPOTs (DS-SPOTs) which takes advantage of differentially protected amino acids. During the first amino acid coupling, a mixture of differentially-protected alanine (Fmoc-Ala and Alloc-Ala) was spotted on the membrane. Synthesis of the first peptide follows normal solid-state synthesis from the Fmoc-Ala. After completion of the peptide synthesis on the blot, the blot was removed from the apparatus and deprotection of the Alloc-Ala in tributyltin hydride and palladium is performed overnight (Espanel, Walchli et al. 2003). Subsequently, the blot is washed and carefully realigned in the synthesizer, where a second round of peptide synthesis will be performed using standard Fmoc chemistry to form the second peptide. This technique allows two different peptides be created within a single spot by sequential solid-phase synthesis reactions.

3.3 Results

3.3.1 The Effect of Multimerization in CaMKII Substrate Selectivity

In our studies concerning the phosphorylation of CaMKII substrates from the known pool of substrates from PhosphoSitePlus, we observed that while autophosphorylation alone ($CaMKII_m^{+P}$) led to decreased substrate specificity, the specificity of autophosphorylated holoenzyme ($CaMKII_{holo}^{+P}$) appeared be even further diminished. To further explore the effect of the holoenzyme assembly of CaMKII on substrate specificity, we focused on the phosphorylation of a set of 15 CaMKII substrate peptides. Table 3.1 shows representative SPOTs for each substrate as well as both the absolute phosphorylation values as well as those scaled to the high-affinity CaMKII substrate GluN2B. Similar to our analysis of the effect of T^{287} autophosphorylation on substrate phosphorylation, we measured an enhancement factor for each substrate compared to the non-T^{287} autophosphorylated monomeric CaMKII ($CaMKII_{holo}^{+P}$ / $CaMKII_m^{-P}$). Then, in lieu of kinetic information for all substrates, we expressed these enhancement factors as a function of the extent of phosphorylation by non-T^{287} autophosphorylated CaMKII monomer ($CaMKII_m^{-P}$). This metric correlates to the relative substrate affinity as well as similarity to a non-biased consensus motif represented by a ScanSite score. Similar to the PhosphoSitePlus data, the enhanced substrate phosphorylation for autophosphorylated kinase, both $CaMKII_m^{+P}$ and $CaMKII_{holo}^{+P}$ were greatest for substrates poorly phosphorylated $CaMKII_m^{-P}$ (i.e. weak, low-affinity substrates) (Figure 3.1A). Furthermore, the enhancement profile for substrates as function of their similarity to a consensus phosphorylation motif (ScanSite score) showed that enhanced phosphorylation

was greatest for substrates that were less similar to the consensus motif (Figure 3.1B). However, to concentrate only the added effect of multimerization, we instead compared the phosphorylation of the autophosphorylated CaMKII holoenzyme to the autophosphorylated CaMKII monomer ($CaMKII_{holo}^{+P}$ / $CaMKII_{m}^{+P}$) (Figure 3.2). Beyond the effect of T^{287} autophosphorylation alone, preferential phosphorylation was exhibited towards weak, non-consensus substrates. Thus, our findings indicate that the multimeric holoenzyme complements the effect of T^{287} autophosphorylation in broadening substrate specificity.

A

Peptide	P_0 Site	ScanSite Score	Sequence
GluN2B	S1303	0.294	RNKLRRQHsYDTFVD
AC-2	T287	0.367	KKALRRQEtVDAL
Syntide-2	S8	0.605	PLARTLsVAGLPGKK
GluA1	S849	0.637	GFCLIPQQsINEAIR
Vimentin	S83	0.602	PGVRLLQDsVDFSLA
HSF1	S230	0.385	PKYSRQFsLEHVHGS
5-LO	S272	0.408	CSLERQLsLEQEVQQ
cPLA2	S515	0.54	SDFATQDsFDDDELD
DRD3	S229	0.548	RILTRQNsQCISIRP
EGFR	S1166	0.571	QKGSHQIsLDNPDYQ
SAPAP1	S947	0.599	APLIRERsLESSQRQ
mAChR M4	T145	0.700	TYPARRTtKMAGLMI
FAK	S843	0.700	DVRLSRGsIDREDGS
Spinophilin	S100	0.700	LSLPRASsLNENVDH
gp130	S780	0.700	QVFSRSEsTQPLLDS

B

SPOTs	Phos. (PSL/mm^2)	Phos. (Scaled to GluN2B)
	103.1 ± 7.4	100.0 ± 7.2
	390.0 ± 18.6	378.4 ± 18.0
	553.5 ± 20.5	537.0 ± 19.9
	122.8 ± 26.3	119.1 ± 25.5
	154.3 ± 18.1	149.7 ± 17.6
	570.1 ± 26.1	553.2 ± 25.4
	310.4 ± 24.1	301.1 ± 23.3
	657.0 ± 59.7	637.4 ± 57.9
	141.7 ± 22.3	137.4 ± 21.6
	690.1 ±114.0	669.5 ±110.6
	400.7 ± 53.8	388.7 ± 52.2
	40.9 ± 5.1	39.7 ± 5.0
	517.7 ±181.8	502.3 ±175.8
	943.0 ±118.8	914.9 ±115.2
	621.8 ±136.4	603.2 ±132.4

Table 3.1 Multimeric CaMKII phosphorylation of SPOTs substrate peptides.
(**A** to **C**) Table of substrate properties for immobilized SPOTs peptides representing 15 CaMKII substrates; 13 taken from PhosphoSitePlus as well as two classical CaMKII substrates Syntide and Autocamtide-2 (AC-2). (**A**) Phosphoacceptor site (P_0), ScanSite score, and sequence. Substrates unrecognized by ScanSite algorithm given score of 0.7. (**B**) Phosphorylated SPOTs images analyzed by phosphoimaging (left), absolute substrate phosphorylation (middle), and phosphorylation scaled to the high-affinity substrate GluN2B (right) for T^{287} autophosphorylated CaMKII holoenzyme ($CaMKII_{holo}{}^{+P}$). Error bars denote ±SD.

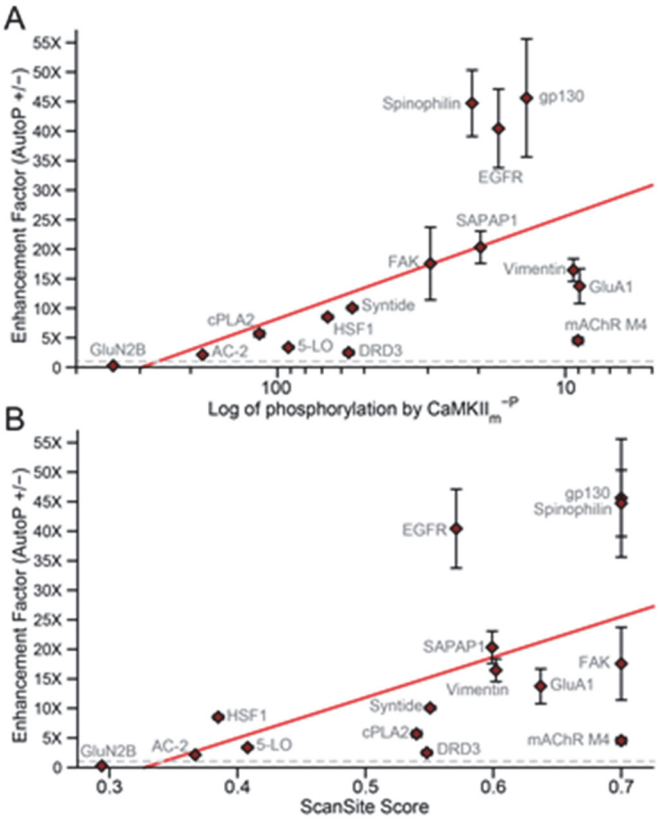

Figure 3.1 T^{287} autophosphorylation of multimeric CaMKII broadens substrate specificity. (**A** and **B**) Phosphorylation ([γ-^{32}P] phosphate incorporation) of immobilized SPOTs peptides representing 15 CaMKII substrates; 13 taken from PhosphoSitePlus as well as two classical CaMKII substrates Syntide and Autocamtide-2 (AC-2). Enhancement in phosphorylation of the T^{287} autophosphorylated CaMKII holoenzyme compared to non-T^{287} autophosphorylated CaMKII monomer (CaMKII$_{holo}^{+P}$ / CaMKII$_m^{-P}$). This value is represented either as a function of phosphorylation by CaMKII$_m^{-P}$ on a log scale in (**A**) or as a function of ScanSite similarity score in (**B**). Dashed line indicates no change. Error bars denote ±SD. Data points fit with linear regression (red line) exhibited R^2 coefficient values of 0.34 and 0.31 in (**C**) and (**D**), respectively.

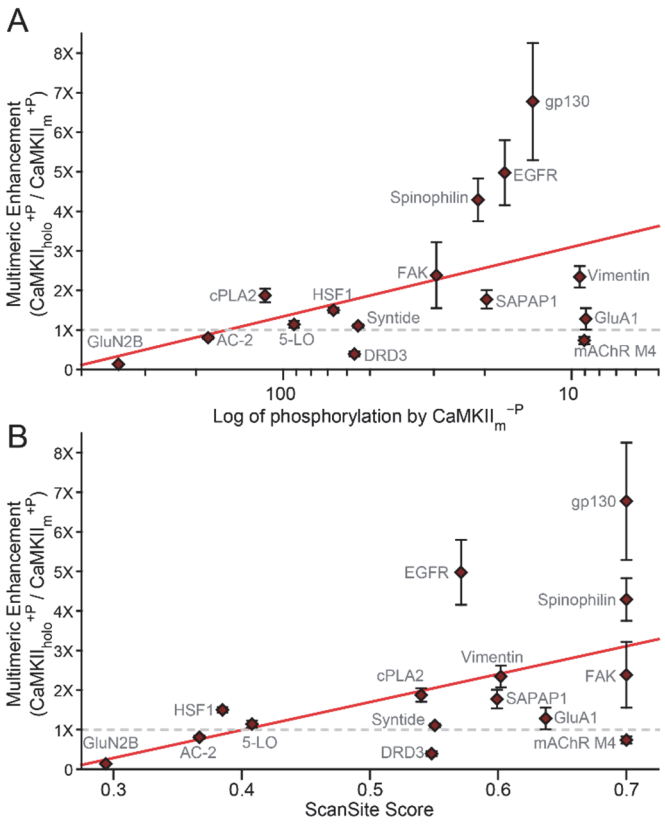

Figure 3.2 Multimeric CaMKII broadens substrate specificity beyond T^{287} autophosphorylation alone.

(**A** and **B**) Phosphorylation ([γ-^{32}P] phosphate incorporation) of immobilized SPOTs peptides representing 15 CaMKII substrates; 13 taken from PhosphoSitePlus as well as two classical CaMKII substrates Syntide and Autocamtide-2 (AC-2). Multimerization-induced enhancement represented as the ratio of substrate phosphorylation between the T^{287} autophosphorylation states of holoenzyme and monomeric CaMKII (CaMKII$_{holo}^{+P}$ / CaMKII$_m^{+P}$). This value is represented either as a function of phosphorylation by CaMKII$_m^{-P}$ on a log scale in (**A**) or as a function of ScanSite similarity score in (**B**). Dashed line indicates no change. Error bars denote ±SD. Data points fit with linear regression (red line) exhibited R^2 coefficient values of 0.26 and 0.23 in (**A**) and (**B**), respectively.

To confirm that these findings were not due to limited substrate availability (due to poor synthesis, inaccessibility, etc.), we generated a phosphorylation time-course for a set of immobilized SPOTs peptides. We found that like the phosphorylation by $CaMKII_m^{+P}$ (Figure 2.10C), $CaMKII_{holo}^{+P}$ phosphorylation at 4 min (or standard reaction time) was less than 4% of the extent of a 24hr phosphorylation (Figure 3.3). Thus, substrates do not appear to be limiting under our assay conditions. In addition, the kinase concentrations used in our assays were within the linear range for both a high-affinity substrate ($GluN2B_{S1303}$, K_m = 4.6±1.1 μM) and a lower-affinity substrate (Syntide, K_m = 43.5±2.3 μM (Figure 3.4).

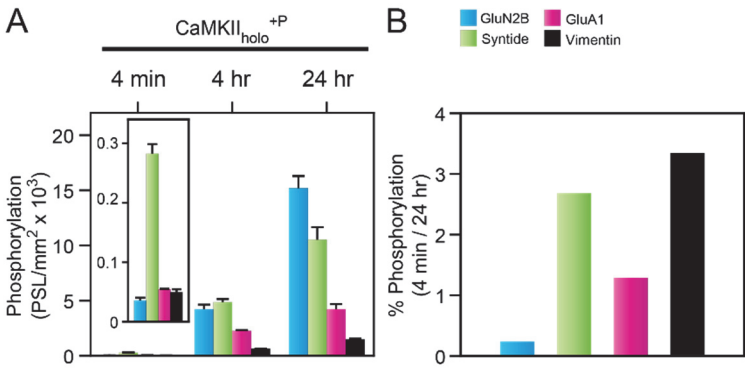

Figure 3.3 CaMKII holoenzyme SPOTs phosphorylation time-course.
(**A** and **B**) Substrate phosphorylation profiles ([γ-^{32}P] phosphate incorporation of SPOTs peptides). (**A**) Phosphorylation time-course of T^{287} autophosphorylated CaMKII holoenzyme ($CaMKII_{holo}^{+P}$) (n = 3); expanded view of 4 min reaction in inset. Error bars in all panels denote ±SD. (**B**) Percent of substrate phosphorylated of a standard 4 min reaction versus a 24 hr phosphorylation reaction.

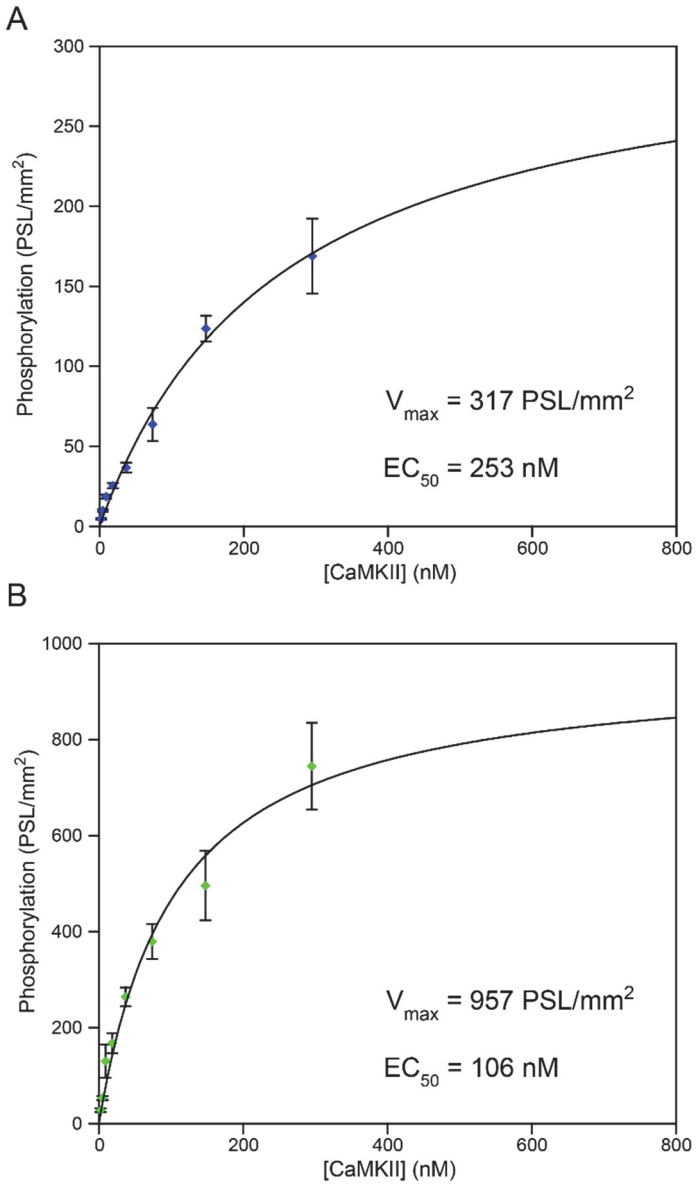

Figure 3.4 Autophosphorylation-associated expansion in CaMKII substrate specificity. Kinase concentration dependent phosphorylation curve for T^{287} autophosphorylated CaMKII holoenzyme ($CaMKII_{holo}^{+P}$). Substrate phosphorylation profiles ([γ-^{32}P] phosphate incorporation of SPOTs peptides) comparing the high-affinity substrate GluN2B (**A**) and lower-affinity substrate Syntide (**B**). Error bars denote mean±SD.

3.3.2 Graded Subunit Activation within CaMKII Holoenzymes

The unique structure and autoregulation make CaMKII an ideal sensor to encode calcium-spike frequency into graded levels of activity and T^{287} autophosphorylation within the holoenzyme (Hudmon and Schulman 2002, Smedler and Uhlen 2014). This process is influenced by calcium-spike duration and amplitude (De Koninck and Schulman 1998) as well as phosphatase activity (Colbran 2004), alternative spliced linker length and CaM availability (Estep, Alexander et al. 1989, Persechini and Stemmer 2002). Each of these factors described in previous studies should contribute to production of different numbers of activated subunits per holoenzyme depending the frequency and amplitude of the Ca^{2+} transient associated with cellular activity. Thus, our goal was to test how the number of activated subunits and/or extent of autophosphorylation elicits different functional outputs.

To determine how graded CaMKII activity influences substrate phosphorylation and selectivity, we prepared holoenzymes in which different numbers of subunits remained activatable (human CaMKIIδ holoenzyme is tetradecameric (Rellos, Pike et al. 2010)). This was accomplished using the natural mechanism by which non-activatable CaMKII subunits are generated in vivo, namely through basal, inhibitory (Ca^{2+}/CaM-independent) autophosphorylation in the CaM binding domain (T^{306} in CaMKIIδ) that blocks subsequent Ca^{2+}/CaM binding/activation (see Methods 3.2.2). Autophosphorylation at $T^{306/7}$ was induced by the addition of Mg^{2+}/ATP and allowed to proceed in a time-dependent manner in order to titrate the level of $T^{306/7}$ autophosphorylation. This is a biological mechanism to limit the ability of Ca2+/CaM to bind to its target sequence to disinhibit the ARD (Colbran 1993). We then activated these holoenzyme preparations with saturating Ca^{2+}/CaM which led to different levels of activity to a soluble peptide substrate (AC-2) (Figure 3.5). Using

these activities, the average number of activated subunits per holoenzyme was calculated by dividing by the activity of a naïve subunit (see Method 3.2.3).

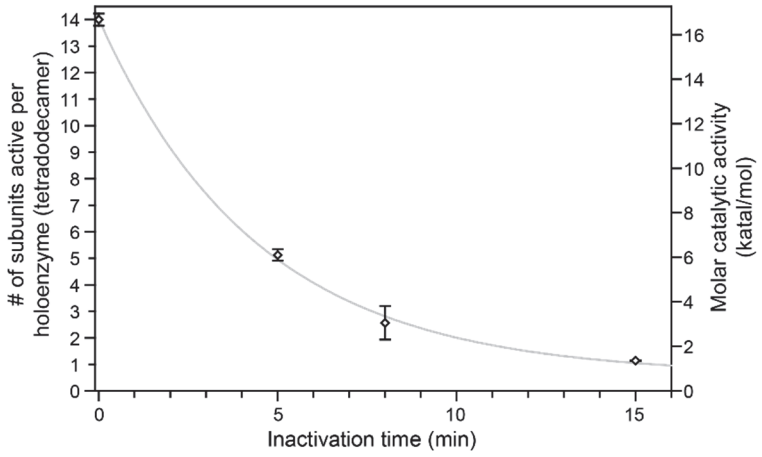

Figure 3.5 Time-dependent inactivation of CaMKII by basal autophosphorylation.
Ca^{2+}/CaM-stimulated activity of $CaMKII_{holo}$ expressed in molar terms (katal/mol) and measured via standard soluble peptide (AC-2) assays with radioactive [γ^{32}P]ATP. Enzymatic activity was measured following 0, 5, or 15min pre-inactivation reactions (see Methods) both at the start (0 min) and end (4 min) of the SPOTs assays; mean±SD (n = 3).

We estimated that if the autophosphorylation reaction to cap CaM binding was stochastic, then we should have prepared holoenzymes in which on average 1, 5 or all 14 subunits remained activatable. We then characterized the phosphorylation of multiple substrates simultaneously via SPOTs arrays (see Methods) using the four peptide substrates as before (GluN2B$_{S1303}$, Syntide, vimentin$_{S83}$ and GluA1$_{S849}$). CaMKII with one active subunit per holoenzyme (CaMKII$_{holo}^{1/14}$) displays preferential phosphorylation for the high-affinity substrate GluN2B (Figure 3.6A). Compared to GluN2B, increasing the number of activatable subunits per holoenzyme significantly increases relative phosphorylation of weak substrates. Scaling factors for different substrates are shown in Figure 3.6B compared to CaMKII with one active subunit per holoenzyme (CaMKII$_{holo}^{1/14}$). While minimal changes in GluN2B phosphorylation were seen, we observed a 20-fold increase in Syntide phosphorylation by submaximally-activated CaMKII$_{holo}^{5/14}$. Maximally-activated CaMKII$_{holo}^{14/14}$ produced the greatest increase (12-fold) in phosphorylation of the weakest substrates, GluA1 and vimentin. Again, these effects are not attributable to non-linearity in assays due to limiting substrates (Figure 3.3). Importantly, the relative substrate phosphorylation profile for maximally-activated CaMKII$_{holo}^{14/14}$ remained consistent even when diluted to possess the same number of active catalytic subunits as CaMKII$_{holo}^{1/14}$ (Figure 3.6A – CaMKII$_{holo}^{14/14}$ vs Figure 3.3A – 4 min reaction). This again argues that our assays are linear within the range of 5-60nM kinase. More importantly, it augments our previous data (Chapter 2) on monomeric CaMKII to show that the substrate phosphorylation profile is also governed by the activation state of CaMKII for the native, multimeric holoenzyme. Because the number of activatable subunits per holoenzyme could influence this intraholenzyme, intersubunit

reaction occurring between neighboring Ca^{2+}/CaM-activated subunits (Hanson, Meyer et al. 1994), this furthers the concept that broadened substrate specificity is attributed to the state of T^{287} autophosphorylation (as established in Chapter 2). Thus, this data suggests that individual subunits within the holoenzyme operate via similar substrate selective mechanisms compared to the individual subunits and that differences observed when greater number of subunits are activated are the result of multimeric avidity.

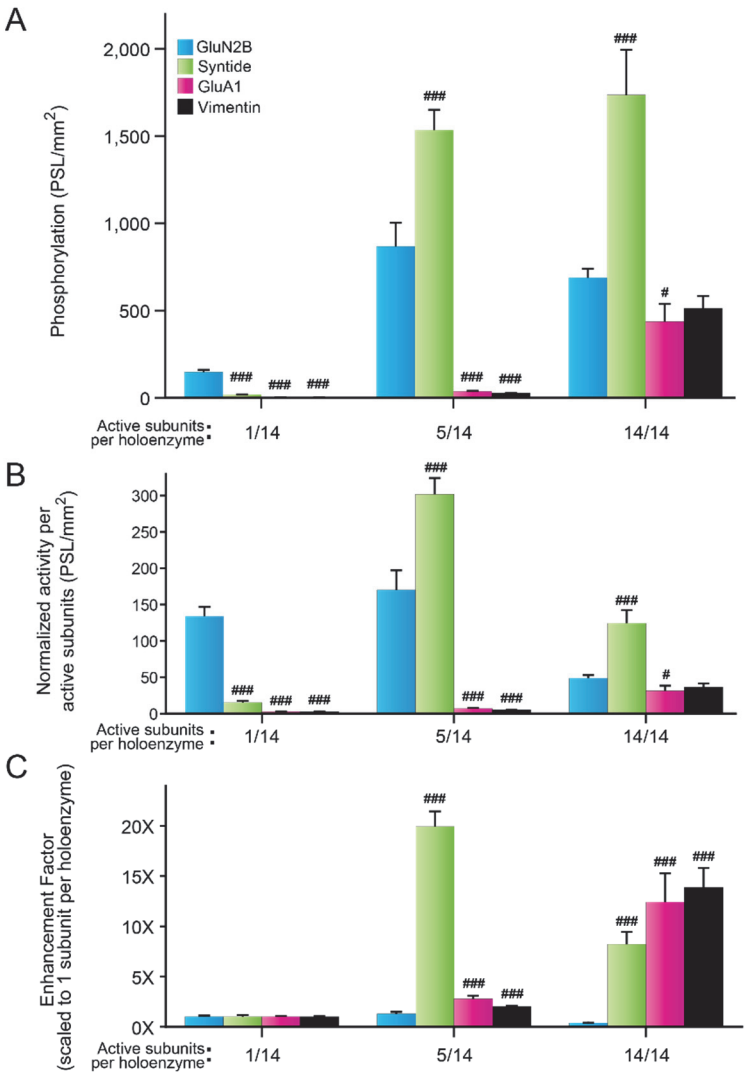

Figure 3.6 Enhanced phosphorylation of weak substrates with increasing number of active subunits per holoenzyme.
(**A** to **C**), Phosphorylation ([γ-^{32}P] phosphate incorporation) of immobilized CaMKII substrates (GluN2B, Syntide, GluA1, and vimentin) synthesized via SPOTs. (**A**) Phosphorylation profiles of $CaMKII_{holo}$ exhibiting varying numbers of activated subunits per holoenzyme (see Method 3.2.3). Substrates ranked from lowest to highest K_m. Raw phosphorylation (PSL/mm^2) represented as mean ±SD ($n = 3$). (**B**) Phosphorylation normalized by the number of subunits activated per holoenzyme and represented as mean ±SD ($n = 3$). (**C**) Enhancement of substrate phosphorylation representing the relative change in substrate phosphorylation scaled to the phosphorylation of a given substrate by a holoenzyme with 1 active subunit ($CaMKII_{holo}^{1/14}$); mean ±SD ($n = 3$). One-way ANOVA of log-normalized data with Holm-Šídák post-test used to compare to GluN2B (#$P < 0.05$, ###$P < 0.001$).

3.3.3 CaMKII Substrate Specificity is Differentially Altered by Extent of T^{287} Autophosphorylation.

To further explore how degrees of activated/autophosphorylated subunits within the holoenzyme affect substrate specificity, we utilized monomeric CaMKII ($CaMKII_m$) to allow us to maintain tight control over the ratio of T^{287} autophosphorylated to non-T^{287} autophosphorylated subunits (i.e. $CaMKII_m^{-P}$: $CaMKII_m^{+P}$). To establish this ratio, we utilized soluble substrate peptide phosphorylation assays to measure the increase in Ca^{2+}-independent activity associated with T^{287} autophosphorylation (i.e. autonomous activity). We used the high-affinity substrate AC-2, as it generates 100% autonomous activity (Figure 2.1A) and exhibits a 1:1 correlation with the number of T^{287} autophosphorylated subunits (Ikeda, Okuno et al. 1991). Using varying time and temperature for pre-autophosphorylation assays with concentrated $CaMKII_m$, we generated submaximal T^{287} autophosphorylated subunits within the population of Ca^{2+}/CaM activated subunits (see Methods 3.2.3 and Figure 3.7A). Using the populations of $CaMKII_m$, we compared their ability to phosphorylate immobilized peptide substrates (SPOTs). Importantly, the percentage of autophosphorylated subunits did not change over the course of the SPOTs reaction (Figure 3.7A, 0 min vs 4 min). Substrate-selective enhancement of weak substrates was observed, with the level of enhancement directly correlated to proportion of T^{287} autophosphorylated subunits (Figure 3.7, B and C).

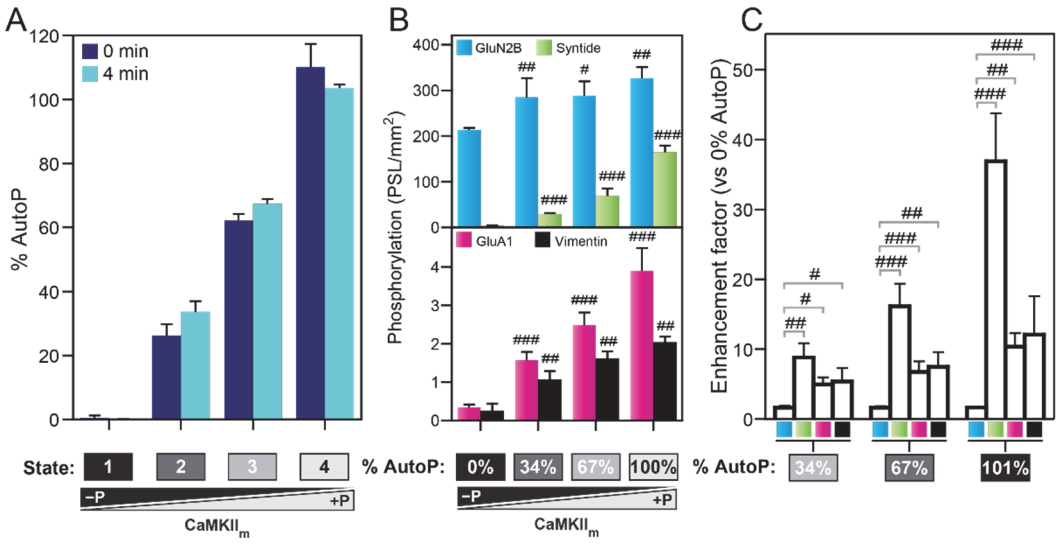

Figure 3.7 Phosphorylation profile of CaMKII is differentially altered by extent of T^{287} autophosphorylation.

(**A**) Percent autonomy of calcium-independent CaMKII activity compared to maximal activity corresponding to the beginning (0 min) or end (4 min) of SPOTs assays was used as a readout of T^{287} autophosphorylation (n = 3). Error bars denote ±SEM. (**B**) Phosphorylation profiles for T^{287} autophosphorylation states generated in (A). Error bars denote ±SD for a representative blot. (**C**) Enhancement factor of phosphorylation profiles compared to $CaMKII_m^{-P}$ (n = 3). Error bars denote ±SEM. Results represent one-way ANOVA of log-normalized data with Holm-Šídák post-test compared to 0% autonomy (**B**) or to GluN2B (**C**). #$P < 0.05$; ##$P < 0.01$; ###$P < 0.001$.

3.3.4 Activation States of CaMKII Alter the Phosphorylation of Substrates within the Post-Synaptic Density

CaMKII is known to play a major role in the regulation of a number of important targets with the post-synaptic density (PSD), a macromolecular complex contain the machinery involved in the transmission of neuronal activity. Within the web of proteins, CaMKII phosphorylates greater than 40 known targets (Yoshimura, Aoi et al. 2000, Yoshimura, Shinkawa et al. 2002). While numerous reports have studied CaMKII enzymology using classical solution kinetics experiments, the role of the multimeric structure to influence the phosphorylation of diffusion-restricted substrates (e.g. PSD) has remained largely unstudied. In order to begin to understand these relationships, we first examined the global ability of CaMKII to phosphorylate substrates within the PSD.

PSDs were acquired from female adult rats (Sprague-Dawley) using previously defined procedures involving differential centrifugation with various sucrose gradients followed by Triton X-100 extraction and collection of the Triton-insoluble fraction (See Methods 3.2.4) (Figure 3.8) (Ehlers 2003, Swulius, Kubota et al. 2010). Figure 3.8A shows a Coomassie stained SDS-PAGE of a typical PSD preparation. We further characterized our PSDs with the help of Dr. Neal Waxham (University of Texas – Houston) who verified their structural integrity of our preparations using cryo-transmission electron microscopy (Figure 3.8B). Because our intent was focus on characterize exogenously added CaMKII in PSD phosphorylation reactions, several steps were taken to limit and reduce the Ca^{2+}/CaM stimulated and autonomous activity of endogenous CaMKII within the PSDs. First, rat brains were extracted and snap-frozen in liquid nitrogen as rapidly as possible (~90 secs) after animal sacrifice, as CaMKII is known to activate and translocate to the

PSDs in response to ischemic insult produced by decapitation (Suzuki, Okumuranoji et al. 1994). Second, in order to dephosphorylate T^{287} to prevent autonomous activity of endogenous CaMKII as well as to reduce the phosphorylation state of endogenous substrates, purified PSDs were dephosphorylated with PP1α (6xHis purified) overnight. This allows for a greater dynamic range in the phosphorylation measurement in the assay. Finally, the small molecule CaMKII inhibitor KN93 which only inhibits the autoinhibited kinase (naïve, non-T^{287} autophosphorylated) was included in the PSD phosphorylation reaction itself. This, in combination with dephosphorylation of the PSD preps serves to limit activation of endogenous kinase and since the exogenously added kinase was first pre-autophosphorylated at T^{287}, only the activity of endogenous, co-purified CaMKII within the PSD.

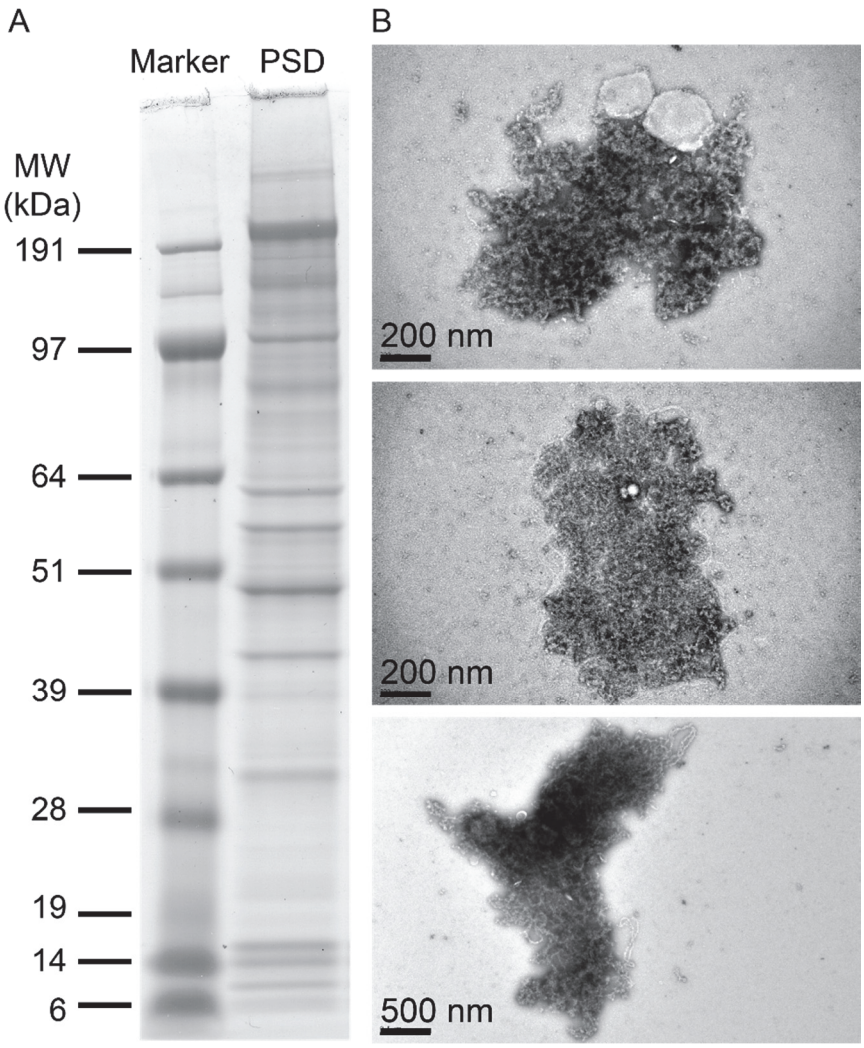

Figure 3.8 Characterization of purified PSDs.
(**A**) SDS-PAGE and Coomassie staining of a typical PSD preparation. (**B**) Cryo-transmission electron microscopy showing several examples of our isolated rat PSDs imaged by Dr. Neal Waxham (University of Texas – Houston).

To explore the effect of the of the multimeric structure of the CaMKII holoenzyme, we phosphorylated the PSDs (see above) with T^{287} autophosphorylated $CaMKII_{holo}^{+P}$ or $CaMKII_{m}^{+P}$ in the presence of [γ-^{32}P]-ATP. The amount of enzymatic activity (both Ca^{2+}/CaM stimulated and autonomous) was confirmed for the reactions before and after the experiment a standard radioactive assay with a soluble peptide substrate to verify that any instability of the monomer/multimer did not account for the observed phosphorylation differences (Figure 3.9). Similar amounts of catalytic activity of the monomer and multimer were added to the PSD reactions (4 min) and subsequent SDS-PAGE gels were quantified by phosphorimaging of the ^{32}P-incorporation. Our PSDs preparations are by definition the Triton-insoluble fraction of a synaptosomal preparation. This makes them especially difficult to process, transfer, etc. Great care was taken to ensure that equal amounts of PSD were loaded onto SDS-PAGE. We observed nearly identical levels of protein as well as profiles of the Coomassie stained samples (Figure 3.10A). Regardless, we still scaled the corresponding phosphorylation data (autoradiography of ^{32}P incorporated bands) (Figure 3.10B) to the total PSD protein in a given sample based on the area under the curve (AUC). Under these conditions, the addition of Ca^{2+}/CaM alone produced less than a 2-fold increase in the total phosphorylation (measure as AUC) compared to other Ca^{2+}/CaM-independent kinases (Figure 3.10). The inclusion of exogenous $CaMKII_{m}^{+P}$ produced ~2-fold increase in the phosphorylation compared to Ca^{2+}/CaM activated PSDs alone, suggesting that phosphorylation sites were available to exogenously added kinase (Figure 3.9). When then added $CaMKII_{holo}^{+P}$, which produced a 6.4-fold increase in phosphorylation compared to Ca^{2+}/CaM activated PSDs (Figure 3.10). More importantly, compared to the T^{287} autophosphorylated monomer, there was a 4.4-

fold increase in total phosphorylation when corrected for endogenous Ca^{2+}/CaM stimulated phosphorylation (Figure 3.10). Thus, even though the holoenzyme might be expected to have less accessibility to substrates in the PSD compared to the monomer because of their size difference (~750kDa vs 35kDa, respectively), the multimeric assembly of native CaMKII significantly enhances the ability to phosphorylate substrates. As mentioned above, these two kinases produce the same level of activity at the end of the PSD phosphorylation assay when assessed by the phosphorylation of a soluble, high-affinity peptide substrate (AC-2) in a classical diffusion-limited reaction environment (Figure 3.9). Overall, these findings indicate that a feature related to the multimeric nature of the holoenzyme alters its ability to interact many of the substrates within this diffusion-restricted environment.

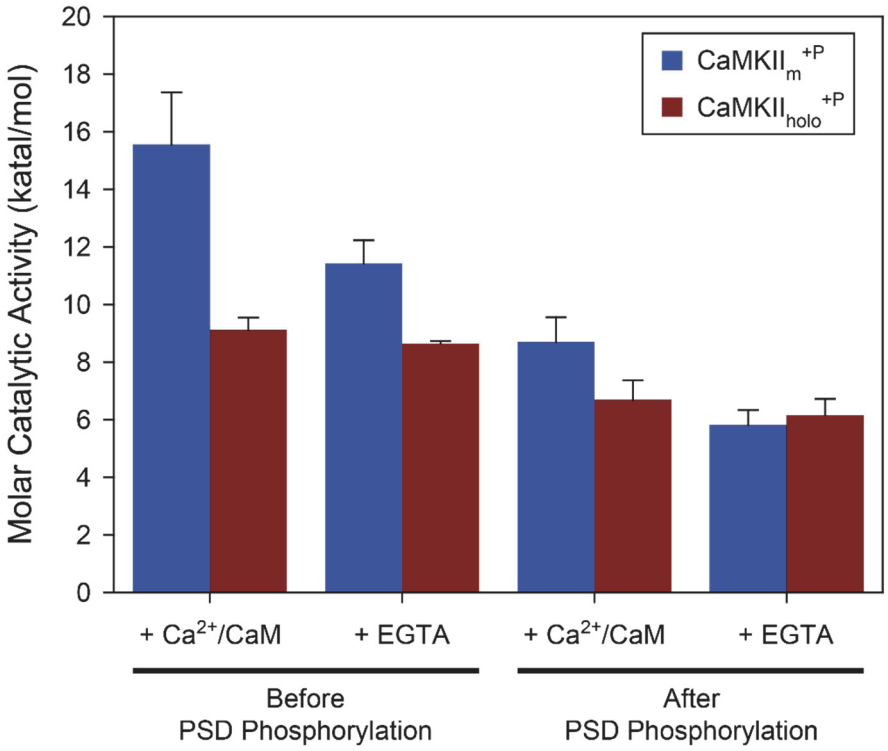

Figure 3.9 CaMKII activity measurement before and after PSD phosphorylation.
Enzymatic activity (katal/mol) assays measured via standard soluble peptide (Autocamtide-2) assays with radioactive [γ^{32}P]ATP. Measurements taken as secondary assays from the PSD phosphorylation reactions. Ca^{2+}-dependent (Ca^{2+}/CaM) vs Ca^{2+}-independent (EGTA) assays were measured for kinase. CaMKII, monomer or holoenzyme was pre-T287 autophosphorylated prior to the PSD phosphorylation (and activity measurement). Activity of $CaMKII_m$ at the start (0 min) and end (4 min) of the PSD phosphorylation assay (n = 3). Error bars denote ±SD.

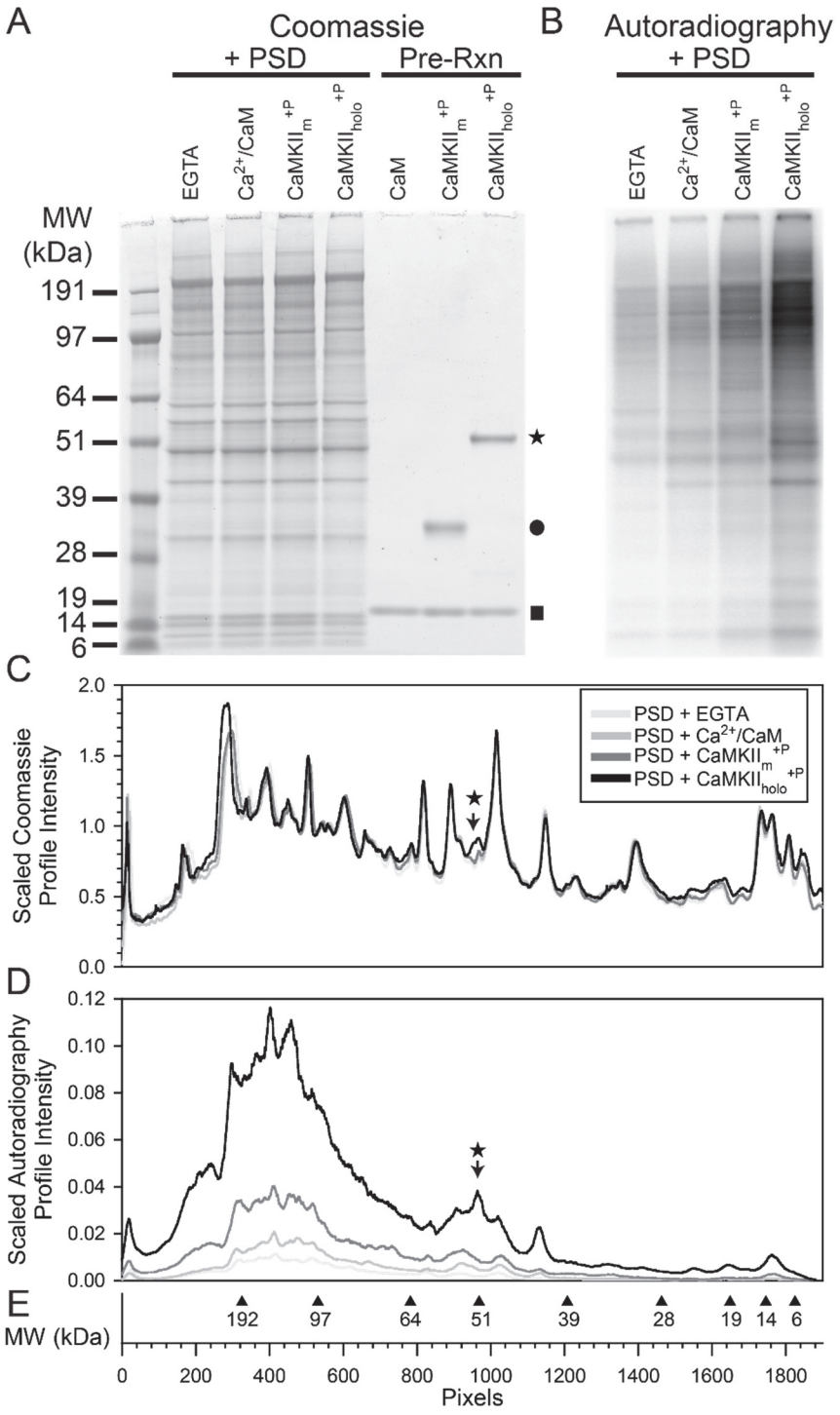

F

	PSD + EGTA	PSD + Ca^{2+}/CaM	PSD+ $CaMKII_m^{+P}$	PSD+ $CaMKII_{holo}^{+P}$
AUC (arbitrary units)	0.16	0.27	0.59	1.72
AUC (Corrected for endogenous CaM-activated kinase)	N/A	0	0.33	1.46

Figure 3.10 CaMKII phosphorylation of PSD proteins.

(**A** to **F**) Isolated rat PSDs were phosphorylated under various conditions. These included low (EGTA) or high calcium (Ca2+/CaM) to assess endogenous, co-purified kinases. PSDs were also phosphorylated exogenous addition of equal molar catalytic subunits of T^{287} autophosphorylated CaMKII holoenzyme ($CaMKII_{holo}^{+P}$ = star) or monomer ($CaMKII_{m}^{+P}$ = circle). (**A**) Coomassie-stained gel illustrating the PSD profile and the purified proteins used in the reaction. Square indicates CaM. (**B**) Phosphorimaging of the SDS-PAGE showing ^{32}P-phosphoprotein bands. (**C** and **D**), Quantification of the PSD phosphoprotein profile using phosphorimaging to assess either the total protein (**C**) or phosphorylation signal (**D**). The diamond indicates purified δCaMKII potentially complexed to the PSD. (**E**) Molecular weight markers indicated along the scaled axis (pixels) representing the scaled lane of the SDS-PAGE. (**F**) Total phosphorylation for each condition assessed using the area under the curve (AUC) as arbitrary intensity units.

To explore the phosphorylation of individual substrates within the PSD, reactions similar to the ^{32}P incorporation assay (above) were performed. Instead of both ATP and [γ-^{32}P]-ATP in the phosphorylation reaction, ATPγS was used. To first address the linearity of the reaction, we compared a time-course of phosphorylation. To assess these phosphorylation reactions, the samples were alkylated with 50mM (PNBM) and western blotting was performed using a thioesters-specific antibody to visualize the sites of thiophosphate incorporation (Figure 3.11A). We found that background kinase phosphorylation (i.e. in the presence of EGTA) was linear for the 4, 15, and 30 min (Figure 3.11B). Addition of exogenous $CaMKII_{holo}^{+P}$ drastically increased the total PSD phosphorylation for all timepoints, but was not completely linear at 30 min (Figure 3.10B). This analysis provides a general overview of the linearity of the phosphorylation reaction for substrates; however, we recognize that this analysis will not likely hold for all CaMKII substrates. Individual substrates would be affected not only by the rate of the reaction but also their individual concentrations.

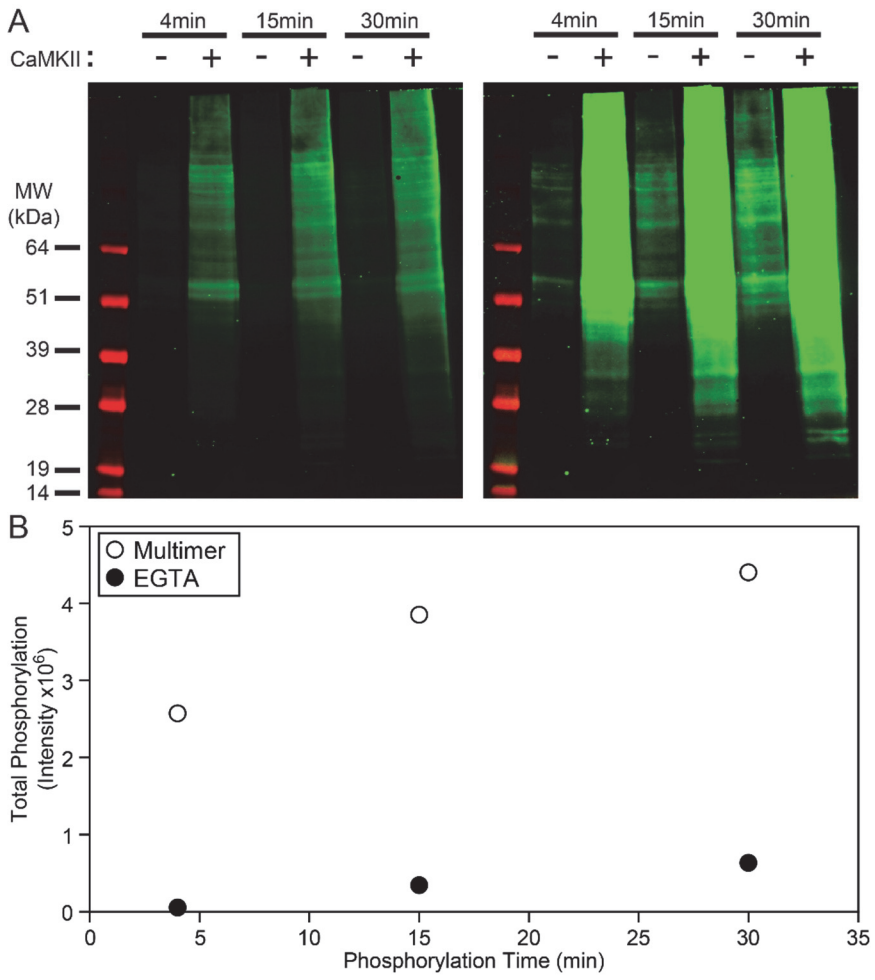

Figure 3.11 CaMKII phosphorylation of PSD proteins using thiolATP.
(**A** to **F**) Isolated rat PSDs were phosphorylated either with low calcium (EGTA) or exogenously added T^{287} autophosphorylated CaMKII holoenzyme ($CaMKII_{holo}^{+P}$) in the presence of thiolATP (ATPγS) for 4, 15, or 30 min. (**A**) Western blotting of alkylated samples with a thiophosphate ester specific antibody and visualized via LI-COR with intensities scaled differentially between left and right image. (**B**) Quantification of the total PSD phosphorylation signal.

We selected a 15 min reaction for subsequent analysis by mass spectrometry through collaboration with Dr. Jon Trinidad, Director of Biological Mass Spectrometry in the Department of Chemistry at Indiana University (Bloomington). In our initial comparisons (and analysis by Dr. Jingwei Meng in the Hudmon lab), we found that $CaMKII_m^{+P}$ phosphorylated 74 proteins covering 193 different regions while $CaMKII_{holo}^{+P}$ phosphorylated 240 proteins covering 475 different regions (Figure 3.12). Between the two, 28 protein we common including 144 regions. Similar to the fold-change in total phosphorylation assessed via ^{32}P-incorporation for the multimeric holoenyzme, a 3.2-fold increase in the number of proteins phosphorylated was observed. Based on overlapping individual peptides, a 2.5-fold increase in the number of phosphorylated regions.

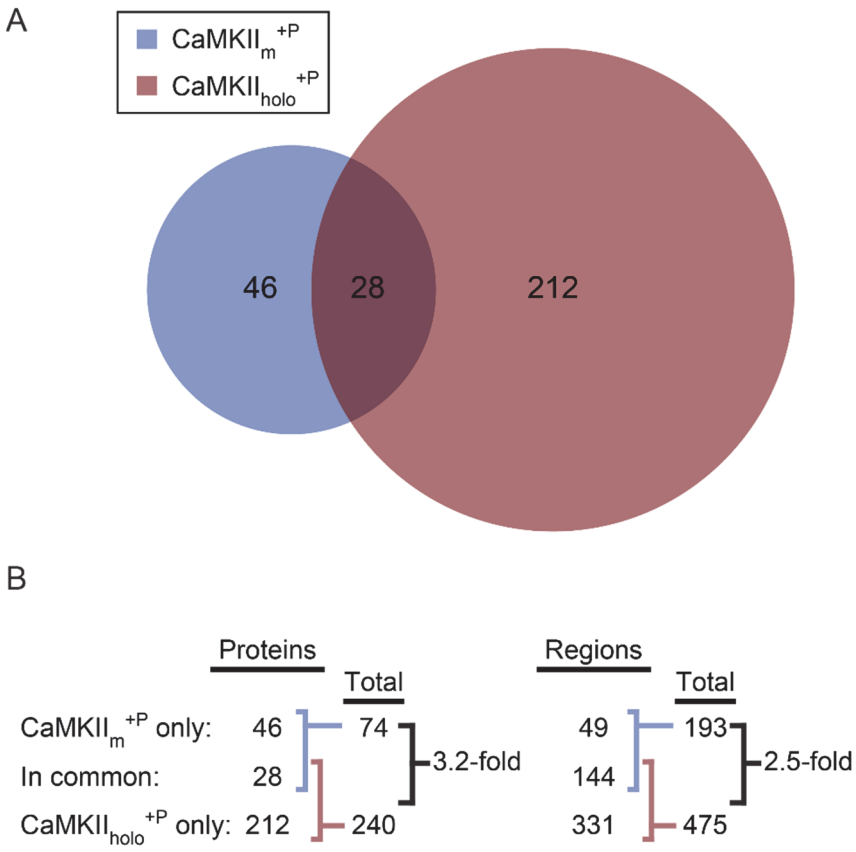

Figure 3.12 Enhanced phosphorylation of substrates in the PSD by the CaMKII holoenzyme measured by mass spectrometry.
(**A** and **B**) Mass spectrometry analysis of isolated rat PSDs phosphorylated with either equimolar amounts of exogenously added T^{287} autophosphorylated CaMKII monomer ($CaMKII_m^{+P}$) or holoenzyme ($CaMKII_{holo}^{+P}$) in the presence of thiolATP (ATPγS). Peptides were considered putative substrates if they exhibited thiophosphorylation. (**A**) Venn-diagram of the overlapping proteins phosphorylated by $CaMKII_m^{+P}$ or $CaMKII_{holo}^{+P}$. (**B**) Tabulated numbers of phosphorylated proteins and/or regions of proteins (peptides harboring potential thiophosphorylation on the same site) for the two kinase states. The total multimeric enhancement (fold) for the holoenzyme is calculated as the ratio of total substrates ($CaMKII_{holo}^{+P}$ / $CaMKII_m^{+P}$).

3.3.5 Role of Targeting on CaMKII Substrate Phosphorylation

Localization of protein substrates into diffusion-restricted subcellular compartments enhances the importance of targeting and translocation of enzymes to execute their function. Kinases are often targeted to specific regions through secondary interaction sites, whether they be docking sites, targeting domains, or scaffolds (see Chapter 1). Previous studies have shown that GFP-CaMKII translocates to the PSD and that CaMKII binding to GluN2B within this compartment is required for maintaining CaMKII levels in the PSD (Shen and Meyer 1999, Shen, Teruel et al. 2000, Gleason, Higashijima et al. 2003, Otmakhov, Tao-Cheng et al. 2004, Halt, Dallapiazza et al. 2012). However, unlike other kinases with require accessory domains/subunits, the oligomeric architecture of CaMKII could allow the catalytic domains to function as a targeting domains for the holoenzyme. We hypothesize that the targeting of CaMKII to the PSD by high-affinity attractors ultimately enhances the phosphorylation of low-affinity substrates by maintaining the dwell time of the kinase within this compartment. Based on our PSD phosphorylation experiments, we observed a unique band in the multimer phosphorylation of PSDs that was of similar molecular weight to the exogenously added $CaMKII_{holo}^{+P}$ (Figure 3.10); consistent with previous data for an association of the multimeric holoenzyme with the PSD. However, no band similar to the size of exogenously added monomeric CaMKII was detected. These findings suggest the enhanced binding of the CaMKII holoenzyme is a result of avidity interactions possibly created between multiple active subunits per holoenzyme and that while monomer is quite capable of transiently interacting with targets

for the phosphotransferase reactions, monomeric CaMKII does not bind with sufficient affinity to pull-down with the PSD during wash steps.

The PSD experiments are limited in that we cannot specifically test the contribution of a substrate protein versus another protein or domain that is not a substrate but functions to attract or target CaMKII to impact its localization. To study this in a highly-reduced yet controllable system, we implemented a modified SPOT synthesis protocol whereby two different peptides are synthesized within a single spot on the membrane in order to study the effects of targeting of the kinase by a high-affinity substrate and its effect on phosphorylation of a locally-tethered, low-affinity substrate. Previous studies have used this strategy to identify docking domains important for the selectivity of extracellular signal-regulated kinase (ERK2), a mitogen-activated protein kinase (MAPK) (Espanel, Walchli et al. 2003). Using this technique with CaMKII phosphorylation, we show that a high-affinity targeting peptide (a phosphomimetic peptide of a CaMKII substrate, $GluN2B_{S1303D}$) enhances the phosphorylation of low-affinity substrates for both $CaMKII_m^{-P}$ and $CaMKII_{holo}^{+P}$ (Figure 3.13). Interestingly, Syntide, a substrate with intermediate affinity and some sequence similarity to CaMKII's consensus motif exhibited a moderate increase in phosphorylation with the $CaMKII_m^{-P}$ when the targeting peptide was present. However, $CaMKII_{holo}^{+P}$ showed an 80% decrease in phosphorylation when the targeting peptide was present. We believe this phenomenon likely results from the high-affinity targeting peptide locking down the kinase to prevent lateral diffusion and hindering the phosphorylation by the holoenzyme. We expect that within a certain range, the holoenzyme would exhibit phosphorylation increases for intermediate- and low-affinity

substrates multivalent avidity counteracts the lower-affinity of individual substrate molecules.

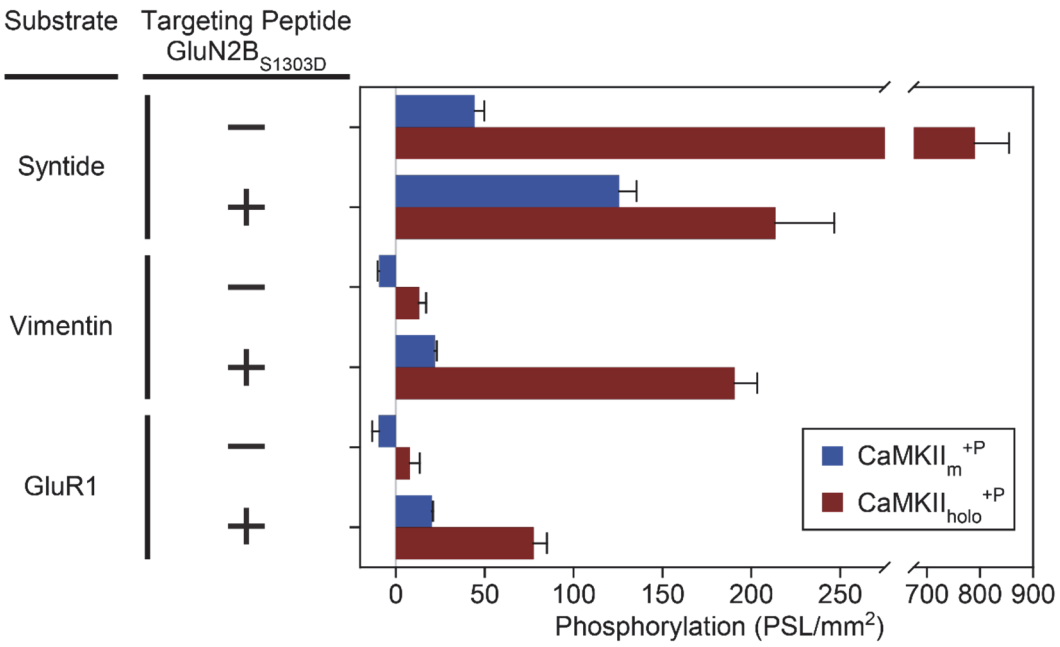

Figure 3.13 Enhanced phosphorylation of poor substrates in the presence of a targeting peptide/substrate.
Immobilized substrate phosphorylation in the absence (−) or presence (+) of a targeting peptide. The targeting peptide is a phosphomimetic version of the high-affinity CaMKII substrate GluN2B ($GluN2B_{S1303D}$). Two peptides were synthesized within a single SPOT using the double synthesis SPOT method (DS-SPOTs) described in Method 3.2.6. Phosphorylation reactions and quantification were performed as described for a standard SPOTs reaction (see Method 2.2.4.

3.4 Conclusion

In these studies, we focused on the role of that holoenzyme architecture plays on the phosphorylation of substrates. We began by exploring the extent to which substrate phosphorylation increased above and beyond that of autophosphorylated CaMKII monomer ($CaMKII_m^{+P}$). Therefore, to test the full contribution of the multimeric effect, we maximally activated CaMKII. We used a set of 15 diverse CaMKII substrates and found that the specificity of the kinase was further broadened such that low-affinity, non-CaMKII consensus-like substrates were preferentially phosphorylated. These findings were not due to poor access to substrates by the holoenzyme, as substrates were not limiting in these assays. While the broadened pattern of phosphorylation was nearly identical for the various concentrations used in our assays under maximal holoenzyme activation, a very different pattern was observed when holoenzymes were generated such that only one subunit was activated. In that case, the phosphorylation was very similar to the limited, narrow substrate specificity produced by non-T^{287} autophosphorylated monomer. We clearly demonstrate that individual subunits within holoenzyme operate in a manner similar to separated subunits. The changes in substrate specificity as more subunits were activated are produced by a combination of both autophosphorylation and multimeric effects. Based on our knowledge of the role of autophosphorylation to function as a switch to change substrate specificity (Chapter 2), we were interested in how graded levels of autophosphorylated subunits within the holoenzyme might contribute to substrate specificity. However, as T^{287} autophosphorylation occurs through a rapid intersubsunit process within the holoenzyme (Hanson, Meyer et al. 1994, Rich and Schulman 1998), controlling this process within the native holoenzyme is not possible with current technology. We elected to again reduce the

complexity by again using the monomeric CaMKII ($CaMKII_m$) to model the process in holoenzymes. We clearly observed an incremental broadening of substrate specificity in response to intermediate levels of autophosphorylation (i.e. mixed populations of $CaMKII_m^{+P}$ and $CaMKII_m^{-P}$).

While our previous experiments focused on individual substrates, we were also interested in how this multimeric effect contributes to the phosphorylation of actual PSDs. Rat PSDs were isolated and purified in our lab and then verified for structural integrity using cryo-transmission electron microscopy by Dr. Neal Waxham's lab (University of Texas – Houston). Using ^{32}P-incorporation as measure of phosphorylation, we found the multimeric structure of the native CaMKII holoenzyme led to a considerable increase in the overall phosphorylation of the PSDs. We attempted to gain a more detailed understanding of the specific substrates phosphorylated and therefore turned to mass spectrometry. We observed increases in both the total number of proteins phosphorylated and more importantly the regions of the protein, even though the amount of active kinase added to the reaction was controlled for. Thus, not only is this consistent with the general increase in phosphorylation that we observed using ^{32}P-incorporation, but more importantly, it also is indicates that substrate selectivity is broadened by maximal activation/autophosphorylation of the holoenzyme within the subcellular compartments in which CaMKII plays a critical function. This is interesting in light of the role of CaMKII in the generation of LTP. High-frequency Ca^{2+} spikes associated with higher neuronal activity would not only produce greater numbers of subunits activated and T^{287} autophosphorylated within each holoenzyme, but would in turn lead to the preferential enhancement of phosphorylation of weaker substrates; some of which are known to be

important for LTP (e.g. GluA1). Additionally, the targeting peptide data argues that even when different substrates are in close proximity and must compete for access to the kinase, this type of mechanism is able to regulate selectivity.

CHAPTER 4. Discussion

4.1 General Conclusions

Like other multifunctional protein kinases, CaMKII exhibits broad substrate specificity, targeting many different substrates involved in a host of cellular functions. These include diverse processes such as carbohydrate, amino acid and lipid metabolism, neurotransmitter synthesis and release, ion channels, receptors, transcription and translation, cytoskeletal organization and dynamics, cell cycle control and calcium homoeostasis (Hudmon and Schulman 2002). CaMKII is found throughout the cell including the nucleus, cytoplasm and cytoskeletal domains. Thus, mechanisms must be in place which allow for proper signaling and substrate specificity. While it is believed that CaMKII autophosphorylation encodes Ca^{2+} spike frequency into graded levels of activity/autophosphorylation, how this process impacts substrate selectivity and processing remains unclear. Given the unique multimeric structure of the holoenzyme and the well-studied forms of autophosphorylation that are known to control the kinase, we endeavored to understand how these features might contribute to the enzymatic output of the kinase.

Overall, our data suggest a model whereby CaMKII utilizes its ARD to increase the dynamic range between high- and low-affinity substrates, with T^{287} autophosphorylation acting as a switch to disengage the ARD from preventing phosphorylation of weak substrates (Figure 2.21). We find that this mode of substrate specificity generation occurs for substrates in both diffusion-limited and diffusion-restricted environment, suggesting that this mechanism may function in with various subcellular locations in which CaMKII operates. In the context of the majority of known CaMKII sites (i.e. PhosphoSitePlus), our data argues that T^{287} autophosphorylation is the major contributor of altered substrate

specificity, while effects related to the multimeric holoenzyme structure tends to broaden the specificity further for diffusion-restricted substrate environments.

Structurally, while our data indicates that T^{287} autophosphorylation functions to regulate substrate selectivity, we hypothesize that the origins of this mechanism are rooted in preventing intrasubunit autophosphorylation of this site. While other CaM kinases (CaMKI and CaMKIV) have an autoregulatory domain, they also have activation loops that require phosphorylation by an upstream kinase, CaMK kinase (CaMKK), to allow for full activation (Swulius and Waxham 2008). They can undergo autophosphorylation at various sites; however, they do not occur within the autoinhibitory portion of their ARD in a manner similar to CaMKII. CaMKII's activation loop is already in the active conformation and therefore does not require phosphorylation by an upstream kinase. Without partial tethering of CaMKII's ARD following Ca^{2+}/CaM activation, one might expect that autophosphorylation of T^{287} (which conforms closely to the consensus phosphorylation motif) would be autophosphorylated in an intrasubunit fashion. This would limit the ability of CaMKII to function as a Ca^{2+} spike frequency detector. Thus Partial ARD tethering is likely responsible for establishing a threshold of sustained activation to allow for coincident CaM binding on neighboring subunits that is required for intersubunit autophosphorylation. As a byproduct of retained interactions of the ARD, substrate phosphorylation is limited such that high affinity substrates are preferentially phosphorylated.

We hypothesize that this mechanism: 1) enables a unique form of autoregulation to counteract multivalency and mass action consequences of CaMKII's unique multimeric structure in substrate-rich environments; 2) allows calcium-spike frequency detection by

CaMKII to translate into substrate selectivity (De Koninck and Schulman 1998); 3) utilizes the ability of different CaMKII isoforms/splice variants harboring unique thresholds for T^{287} autophosphorylation to differentially regulate substrate selectivity (Bayer, De Koninck et al. 2002, Gaertner, Kolodziej et al. 2004, Chao, Stratton et al. 2011); and 4) functions as a switch to allow CaMKII signaling to generate complex patterns of substrate phosphorylation in response to graded levels of autophosphorylation within the holoenzyme. Thus, the potential unique characteristics of CaMKII in regulating substrate selection appears to afford this kinase with a dominant role in regulating synaptic plasticity and learning, possibly functioning as an overall facilitator of global phosphorylation.

4.2 Historical Perspectives of T^{287} Autophosphorylation

Our data describe a new and surprising finding for the function of the ARD of CaMKII to act a substrate selective gate regulated by T^{287} autophosphorylation. Classically, the phenomena most studied concerning the function of T^{287} autophosphorylation was the generation of autonomous activity (Schworer, Colbran et al. 1988, Lou and Schulman 1989). Autonomous activity (i.e. substrate phosphorylation in the absence of Ca^{2+}/CaM following T^{287} autophosphorylation) has been used as an indirect readout of T^{287} autophosphorylation for over 30 years (Saitoh and Schwartz 1985). Autonomous (Ca^{2+}-independent) activity can reach 100% of the Ca^{2+}-dependent activity in *in vitro* assays for certain substrates. While autophosphorylation of CaMKII has been studied for over three decades in regards to the autoregulation of CaMKII, the role this post-translational modification plays on substrate phosphorylation has been inconclusive. Nearly 25 years ago, Katoh and Fujisawa reported a lag-phase in substrate phosphorylation in the absence

of prior autophosphorylation (Katoh and Fujisawa 1991) suggesting that autophosphorylation may proceed substrate phosphorylation. However, others have argued against this lag-phase at higher ATP concentrations (100μM, which is an order of magnitude below measured cellular ATP concentrations) (Coultrap, Barcomb et al. 2012). In fact, the same lab subsequently showed that autothiophosphorylation at T^{287} produced no change in the kinetic parameters for the total, Ca^{2+}/CaM-dependent activity (i.e. $CaMKII^{-P}$ versus $CaMKII^{+P}$) of the kinase for several different substrates with saturating ATP (100 μM) (Ikeda, Okuno et al. 1991). Around the same time, Yasugawa et al. found that there was no change in the total activity, though subsequently they showed that autophosphorylation increased the activity for certain substrates (including Syntide) (S., K. et al. 1988, Yasugawa, Fukunaga et al. 1991). More recently, autophosphorylation has been shown to have only a small effect on the dependent activity (Coultrap, Buard et al. 2010, Coultrap, Barcomb et al. 2012). Specifically, when the phosphoacceptor site was mutated to prevent autophosphorylation, the activity was similar to the autophosphorylated kinase. It was therefore concluded using this $T^{287}A$ mutant that T^{287} autophosphorylation contributes minimally to the phosphorylation of substrates (Coultrap, Barcomb et al. 2012). However, our data suggests that the $T^{287}A$ mutation itself produces Ca^{2+}/CaM-dependent substrate phosphorylation patterns much different than the wild-type kinase (Figure 2.20). Thus, it remains unclear how animal models harboring these knock-in mutations should be interpreted in terms of the role of T^{287} autophosphorylation (Cho, Giese et al. 1998, Giese, Fedorov et al. 1998, Glazewski, Giese et al. 2000, Gustin, Shonesy et al. 2011). We postulate that ARD mutagenesis, an inability to control T^{287} autophosphorylation, or the use of limited/biased substrates likely masked the ability of previous studies to report

confounding conclusions regarding T^{287} autophosphorylation and substrate specificity. Our data provide compelling evidence for the ARD restricting substrate phosphorylation in the absence of T^{287} autophosphorylation. However, while all substrates benefit from T^{287} autophosphorylation, our data clearly show that low-affinity, weak substrates benefit from a disproportional enhancement in their phosphorylation.

Although autonomous activity (which has been used as an indirect measure of T^{287} autophosphorylation) can reach 100% *in vitro*, for *in situ* measurements, the level of autonomous activity generated in neurons by various stimulation protocols appears to be 15-50% of the total CaMKII activity (Gorelick, Wang et al. 1988, MacNicol, Jefferson et al. 1990, Molloy and Kennedy 1991, Lengyel, Cammarota et al. 2001). Submaximal T^{287} autophosphorylation/autonomy of CaMKII may be attributed to: 1) limiting free CaM in cells (Estep, Alexander et al. 1989, Persechini and Stemmer 2002), 2) phosphatase activity, and 3) $T^{306/7}$ capping. Thus, it appears that *in vivo*, there exists the dynamic range in which subunits of CaMKII are or are not T^{287} autophosphorylated such that new stimuli capable of producing autophosphorylation are therefore able to direct changes in substrate specificity. Furthermore, prior activity levels such as those that could lead to $T^{306/7}$ autophosphorylation (i.e. CaM binding domain capping that prevents subsequent Ca^{2+}/CaM activation of the subunit) would also be expected to affect future activation/autophosphorylation (T^{287}) within the holoenzyme, and therefore contribute to selectivity (Figure 4.1).

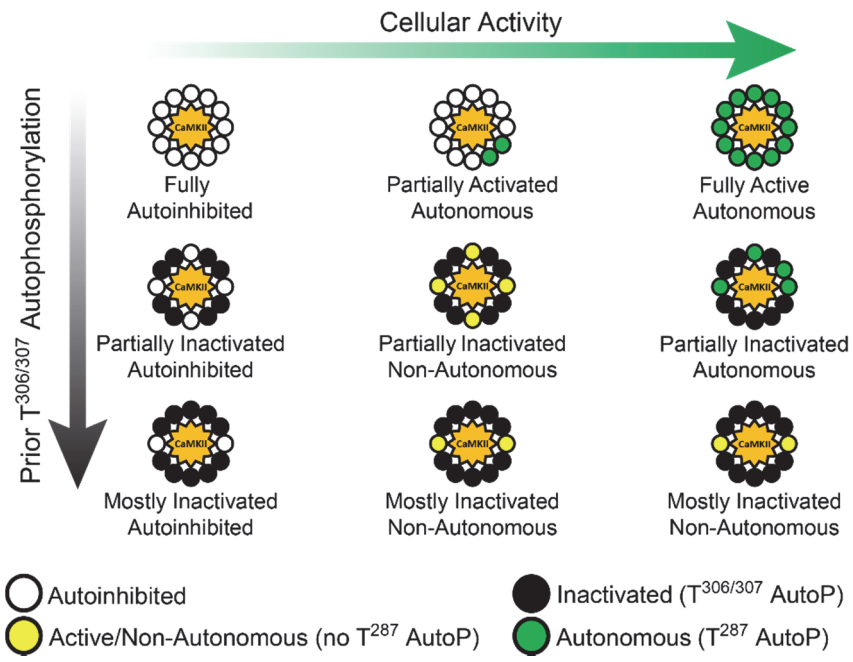

Figure 4.1 Autophosphorylation-associated expansion in CaMKII substrate specificity. Schematic representations of CaMKII holoenzymes depicting variable states of activation/autophosphorylation as a function of both prior inhibitory autophosphorylation ($T^{306/307}$) and cellular activity (i.e. Ca^{2+} spike frequency).

4.3 SPOTs Model of Phosphorylation

As much of the work described here involved exploring changes in substrate specificity, it was critical that I establish a direct and cost efficient means of assessing these changes using diverse substrates. The SPOT technique for peptide synthesis was the perfect solution to our quest to explore many substrates simultaneously. For a single synthesis run, we could easily generate 600 peptides per membrane in an automated fashion with our robotic peptide synthesizer. This allowed for flexibility in the number of substrates synthesized, the number of individual replicate SPOTs, and the number of replicate arrays to be assayed under varying kinase conditions to all be generated within the same synthesis run to minimize potential variations. Since these peptides were synthesized directly on the derivatized cellulose membranes, peptides were not able to be purified away from degenerate peptides. This limitation is inherent to any micro-scale solid state chemistry. We therefore enacted multiple precautions to ensure the maximal efficiency throughout the synthesis, including storing reagents under argon, replacing activators through the synthesis (typically 60-72hr for 15mers), using slightly smaller initial deposition of first amino acid to prevent degenerate peptides at the outer edge, and repeated couplings for each round of synthesis. We found that even between membranes, phosphorylation profiles were rather robust. It should be noted that even though the SPOTs peptides may be susceptible to substrate availability issues stemming from synthesis or access to the substrates, comparisons between kinase states would have the same issues for an individual substrate. Therefore, individual enhancement factors for a given substrate provide a good measure of the changes associated with the state of the kinase.

To assess substrate specificity, we compared both the absolute and relative enhancement of phosphorylation between substrates. We consistently found that the greater the phosphorylation in the non-T^{287} autophosphorylated state, the lower the enhancement associated with autophosphorylation. This same finding could be achieved if only a general enhancement to kinase activity was produced by T^{287} autophosphorylation. It addition, it could have been compounded by limiting amounts of substrate within a given SPOT peptide which would tend to depress the observed enhancement in high-affinity substrates. However, we ruled out a simple interpretation of a general enzymatic enhancement by showing that substrates were in fact not limiting (< 2% of a 24hr phosphorylation; Figure 2.10C) and that there were no differences in the relative phosphorylation profiles for a 4 vs 10 min phosphorylation reaction (Figure 2.10, A and B). Furthermore, repeated phosphorylation reactions on a single membrane, which was transferred at the end of an initial phosphorylation reaction to a second reaction with new kinase exhibited a nearly identical phosphorylation profile (Figure 2.11). By comparing SPOTs data to other kinase reaction formats, we were able to complement the high-throughput strengths of SPOTs substrates with other classical strategies for studying kinase interactions. Using soluble peptides as well as soluble and immobilized versions of GST-fusion substrates, we clearly observed similar changes in substrate specificity in response to changes in the autophosphorylation state of the kinase. Thus, we believe that the SPOT peptide method, when used in conjunction with proper control reactions, provides an effective method for rapidly assessing changes in the substrate specificity of an enzyme.

4.4 CaM Trapping and the Autonomous State of CaMKII

The classical function of an ARD is to couple enzyme activity with second messenger signaling or its upstream effectors. CaMKII is an unusual enzyme in that it has a modulatory (not required for is activity) autophosphorylation site within the R1 segment of CaMKII's ARD ($T^{286/287}$) that can uncouple its activity from its second messenger and activator (Saitoh and Schwartz 1985, Lou and Schulman 1989, Waxham, Aronowski et al. 1990). Thus, Ca^{2+}-independent autonomous activity (i.e. CaMKII substrate phosphorylation following the removal of bound CaM) has been used *in vitro* as a direct readout of this uncoupling associated with T^{287} autophosphorylation (Saitoh and Schwartz 1985). Our functional data showing that following T^{287} autophosphorylation, bound CaM is required for the broadening of substrate specificity is consistent with previous structural EPR data which showed that bound CaM was also required for the full ARD displacement associated with T^{287} autophosphorylation. Based on our understanding of CaM dynamics and intracellular Ca^{2+} concentrations and fluctuations, it seems that CaM would tend to remain bound to the ARD following T^{287} autophosphorylation. The fact that T^{287} autophosphorylation leads to a 20,000-fold enhancement in Ca^{2+}/CaM binding affinity (Meyer, Hanson et al. 1992, Singla, Hudmon et al. 2001) along with concomitant changes in the Ca^{2+}-binding properties of CaM (Gaertner, Putkey et al. 2004), is consistent with CaMKII attempting to enhance, not eliminate its coupling to its second messenger. Even as calcium levels return to basal levels in the cell, the rate of dissociation for trapped CaM seems sufficiently slow such that it would be unlikely for "autonomous" (T^{287} + $T^{306/7}$ autophosphorylated) subunits to be generated, especially in regions such as the PSD where

one might expect more regular elevations in Ca^{2+} signaling associated with neuronal activity.

4.5 Implications

CaMKII is critical to a number of cellular processes and as such is connected to many different pathophysiological conditions including neurodegenerative and cardiac disease as well as cancer. Often, CaMKII contributes to these aberrant processes due to dysregulated calcium signaling. Therapeutic strategies which target CaMKII are potentially promising. Recent advances stemming from structural characterizations of CaMKII through crystallography as well as dynamic changes throughout the various activation states through the use of EPR provide valuable information for developing inhibitors/activators through rational drug design methods. However, beyond simply the understanding the three-dimensional structure and dynamics, understanding how the various activation states contributes to the output of the kinase is key to determining the structure-function relationship. Our studies provide valuable insight into the translation of activation and autophosphorylation into distinct changes in substrate specificity. Specifically, our model of ARD substrate filtering can be viewed as a functional outcome of the partial tethering of an activated CaMKII ARD in the absence of T^{287} autophosphorylation described in solution via EPR. In addition, we find that mutagenesis of this autophosphorylation site alone is able to disrupt the ARD. Specifically $T^{287}A$, a mutation frequently used as a non-phosphorylatable substitution in animal models, was found in our studies to significantly alter the substrate specificity of the kinase.

4.6 Future Directions

While our studies focused on the effects of autophosphorylation and holoenzyme structure in terms of its effects on substrate specificity, many of the same techniques could be used to study how other regulatory processes might contribute (Figure 4.2). Though CaMKII has been studied for over three decades, the interplay between holoenzyme architecture, multisite autoregulatory phosphorylation, other PTMs, and isoform/alternative splicing differences have contributed to the complexity of CaMKII's regulation. For example, it is interesting to speculate that other post-translational modifications in the ARD of CaMKII that also generate an form of autonomous activity, including oxidation, nitrosylation, and glycosylation (Mattiazzi, Bassani et al. 2015), may also function independently or in conjunction with T^{287} autophosphorylation to regulate substrate selectivity. Most of the sites shown to be important in generating these non-canonical forms of autonomous activity are within close proximity to the T^{287} in the R1 segment of the ARD. Therefore, one might expect that these PTMs would generate similar increases on CaM binding affinity and broadened substrate specificity. Such convergence of post-translational modifications associated with diverse signaling pathways could make a powerful set of modulators to produce a gain of signaling as well as to direct the specificity and targets for multifunctional kinases like CaMKII. We recognize that ARD domains for other CaM-kinases may also provide intrinsic selectivity gates to maintain substrate specificity. Thus, future endeavors should look at how these and potential other non-CaM-dependent kinase regulate specificity through post-translational modification.

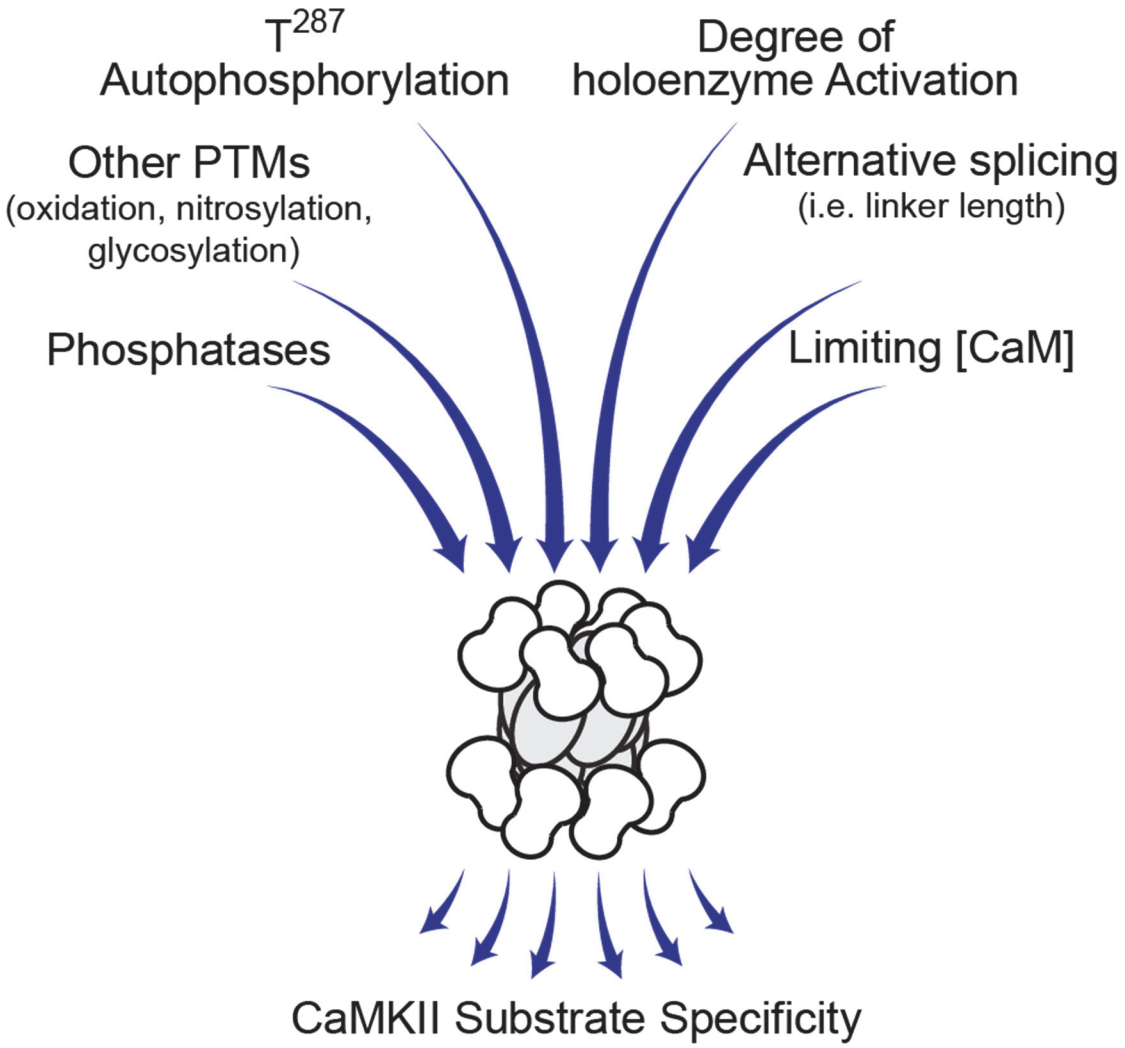

Figure 4.2 Mechanisms contributing to CaMKII substrate specificity.
Schematic depicting some of the actual and potential mechanisms important for controlling substrate utilization and specificity in CaMKII.

One of the interesting potential functions of alternative splicing in CaMKII is the ability to regulate sensitivity to CaM and thus T^{287} autophosphorylation. This centers on the fact that most of the variants (close to 40 variants across the four isoforms) come from changes in the length of the linker between the region between the ARD and the hub domain (Figure 1.2A). Thus, models were developed such that the length of the linker determined to the equilibrium of the catalytic domain's proximity to the hub domain (either compact or extended) (Chao, Stratton et al. 2011). Longer linkers yielded more extended structures with greater access for CaM (and lower EC_{50}) and thus different Ca^{2+} spike frequency thresholds required for autophosphorylation. Combining these ideas with our data, it suggests that various CaMKII isoforms and their splice variants would have different response characteristics that are manifested into specific thresholds for changing substrate specificity. Thus, it's possible that this feature is part of the reason various isoforms/splice variants and developmentally regulated or cell-type specific is that they are precisely designed and tuned for specific functions; whether it be in neurons, astrocytes, pancreatic islet beta cells, cardiomyocytes, etc.

REFERENCES

Ashpole, N. M., A. W. Herren, K. S. Ginsburg, J. D. Brogan, D. E. Johnson, T. R. Cummins, D. M. Bers and A. Hudmon (2012). "Ca2+/calmodulin-dependent protein kinase II (CaMKII) regulates cardiac sodium channel NaV1.5 gating by multiple phosphorylation sites." J Biol Chem **287**(24): 19856-19869.

Bach, M. E., R. D. Hawkins, M. Osman, E. R. Kandel and M. Mayford (1995). "Impairment of spatial but not contextual memory in CaMKII mutant mice with a selective loss of hippocampal LTP in the range of the theta frequency." Cell **81**(6): 905-915.

Barcomb, K., I. Buard, S. J. Coultrap, J. R. Kulbe, H. O'Leary, T. A. Benke and K. U. Bayer (2014). "Autonomous CaMKII requires further stimulation by Ca2+/calmodulin for enhancing synaptic strength." FASEB J **28**(8): 3810-3819.

Bayer, K. U., P. De Koninck, A. S. Leonard, J. W. Hell and H. Schulman (2001). "Interaction with the NMDA receptor locks CaMKII in an active conformation." Nature **411**(6839): 801-805.

Bayer, K. U., P. De Koninck and H. Schulman (2002). "Alternative splicing modulates the frequency-dependent response of CaMKII to Ca(2+) oscillations." EMBO J **21**(14): 3590-3597.

Bayer, K. U., E. LeBel, G. L. McDonald, H. O'Leary, H. Schulman and P. De Koninck (2006). "Transition from reversible to persistent binding of CaMKII to postsynaptic sites and NR2B." J Neurosci **26**(4): 1164-1174.

Bayliss, R., T. Haq and S. Yeoh (2015). "The Ys and wherefores of protein kinase autoinhibition." Biochim Biophys Acta.

Benke, T. A., A. Luthi, J. T. Isaac and G. L. Collingridge (1998). "Modulation of AMPA receptor unitary conductance by synaptic activity." Nature **393**(6687): 793-797.

Bennett, M. K., N. E. Erondu and M. B. Kennedy (1983). "Purification and characterization of a calmodulin-dependent protein kinase that is highly concentrated in brain." J. Biol. Chem. **258**: 12735-12744.

Berridge, M. J. (2012). "Calcium signalling remodelling and disease." Biochem Soc Trans **40**(2): 297-309.

Berridge, M. J., P. Lipp and M. D. Bootman (2000). "The versatility and universality of calcium signalling." Nat Rev Mol Cell Biol **1**(1): 11-21.

Bhattacharyya, M., M. M. Stratton, C. C. Going, E. D. McSpadden, Y. Huang, A. C. Susa, A. Elleman, Y. M. Cao, N. Pappireddi, P. Burkhardt, C. L. Gee, T. Barros, H. Schulman, E. R. Williams and J. Kuriyan (2016). "Molecular mechanism of activation-triggered subunit exchange in Ca/calmodulin-dependent protein kinase II." Elife **5**.

Boulware, M. J. and J. S. Marchant (2008). "Timing in cellular Ca2+ signaling." Curr Biol **18**(17): R769-R776.

Bradshaw, J. M., A. Hudmon and H. Schulman (2002). "Chemical quenched flow kinetic studies indicate an intraholoenzyme autophosphorylation mechanism for Ca2+/calmodulin-dependent protein kinase II." J Biol Chem **277**(23): 20991-20998.

Brickey, D. A., R. J. Colbran, Y. L. Fong and T. R. Soderling (1990). "Expression and characterization of the alpha-subunit of Ca2+/calmodulin-dependent protein kinase

II using the baculovirus expression system." Biochem Biophys Res Commun **173**(2): 578-584.

Brocke, L., L. W. Chiang, P. D. Wagner and H. Schulman (1999). "Functional implications of the subunit composition of neuronal CaM kinase II." J Biol Chem **274**(32): 22713-22722.

Chao, L. H., P. Pellicena, S. Deindl, L. A. Barclay, H. Schulman and J. Kuriyan (2010). "Intersubunit capture of regulatory segments is a component of cooperative CaMKII activation." Nat Struct Mol Biol **17**(3): 264-272.

Chao, L. H., M. M. Stratton, I. H. Lee, O. S. Rosenberg, J. Levitz, D. J. Mandell, T. Kortemme, J. T. Groves, H. Schulman and J. Kuriyan (2011). "A mechanism for tunable autoinhibition in the structure of a human Ca2+/calmodulin- dependent kinase II holoenzyme." Cell **146**(5): 732-745.

Chen, C., B. H. Ha, A. F. Thevenin, H. J. Lou, R. Zhang, K. Y. Yip, J. R. Peterson, M. Gerstein, P. M. Kim, P. Filippakopoulos, S. Knapp, T. J. Boggon and B. E. Turk (2014). "Identification of a major determinant for serine-threonine kinase phosphoacceptor specificity." Mol Cell **53**(1): 140-147.

Cheng, K. Y., M. E. Noble, V. Skamnaki, N. R. Brown, E. D. Lowe, L. Kontogiannis, K. Shen, P. A. Cole, G. Siligardi and L. N. Johnson (2006). "The role of the phospho-CDK2/cyclin A recruitment site in substrate recognition." J Biol Chem **281**(32): 23167-23179.

Cho, Y. H., K. P. Giese, H. Tanila, A. J. Silva and H. Eichenbaum (1998). "Abnormal hippocampal spatial representations in alphaCaMKIIT286A and CREBalphaDelta-mice." Science **279**(5352): 867-869.

Cohen, P. (2001). "The role of protein phosphorylation in human health and disease. The Sir Hans Krebs Medal Lecture." Eur J Biochem **268**(19): 5001-5010.

Cohen, P. (2002). "The origins of protein phosphorylation." Nat Cell Biol **4**(5): E127-130.

Colbran, R. J. (1993). "Inactivation of Ca^{2+}/calmodulin-dependent protein kinase II by basal autophosphorylation." J Biol Chem **268**(10): 7163-7170.

Colbran, R. J. (2004). "Protein phosphatases and calcium/calmodulin-dependent protein kinase II-dependent synaptic plasticity." J Neurosci **24**(39): 8404-8409.

Colbran, R. J., Y. L. Fong, C. M. Schworer and T. R. Soderling (1988). "Regulatory interactions of the calmodulin-binding, inhibitory, and autophosphorylation domains of Ca2+/calmodulin-dependent protein kinase II." J Biol Chem **263**(34): 18145-18151.

Coultrap, S. J., K. Barcomb and K. U. Bayer (2012). "A significant but rather mild contribution of T286 autophosphorylation to Ca2+/CaM-stimulated CaMKII activity." PLoS One **7**(5): e37176.

Coultrap, S. J. and K. U. Bayer (2014). "Nitric oxide induces Ca2+-independent activity of the Ca2+/calmodulin-dependent protein kinase II (CaMKII)." J Biol Chem **289**(28): 19458-19465.

Coultrap, S. J., I. Buard, J. R. Kulbe, M. L. Dell'Acqua and K. U. Bayer (2010). "CaMKII autonomy is substrate-dependent and further stimulated by Ca2+/calmodulin." J Biol Chem **285**(23): 17930-17937.

Coultrap, S. J., R. K. Freund, H. O'Leary, J. L. Sanderson, K. W. Roche, M. L. Dell'Acqua and K. U. Bayer (2014). "Autonomous CaMKII mediates both LTP and LTD using a mechanism for differential substrate site selection." Cell Rep **6**(3): 431-437.

Crooks, G. E., G. Hon, J. M. Chandonia and S. E. Brenner (2004). "WebLogo: a sequence logo generator." Genome Res **14**(6): 1188-1190.

Cruzalegui, F. H., M. S. Kapiloff, J. P. Morfin, B. E. Kemp, M. G. Rosenfeld and A. R. Means (1992). "Regulation of intrasteric inhibition of the multifunctional calcium/calmodulin-dependent protein kinase." Proc Natl Acad Sci U S A **89**(24): 12127-12131.

Daile, P., P. R. Carnegie and J. D. Young (1975). "Synthetic substrate for cyclic AMP-dependent protein kinase." Nature **257**(5525): 416-418.

Dar, A. C. and K. M. Shokat (2011). "The evolution of protein kinase inhibitors from antagonists to agonists of cellular signaling." Annu Rev Biochem **80**: 769-795.

De Koninck, P. and H. Schulman (1998). "Sensitivity of CaM kinase II to the frequency of Ca2+ oscillations." Science **279**(5348): 227-230.

Dosemeci, A., J. H. Tao-Cheng, L. Vinade, C. A. Winters, L. Pozzo-Miller and T. S. Reese (2001). "Glutamate-induced transient modification of the postsynaptic density." Proc Natl Acad Sci U S A **98**(18): 10428-10432.

Ehlers, M. D. (2003). "Activity level controls postsynaptic composition and signaling via the ubiquitin-proteasome system." Nat Neurosci **6**(3): 231-242.

Erickson, J. R., B. J. He, I. M. Grumbach and M. E. Anderson (2011). "CaMKII in the cardiovascular system: sensing redox states." Physiol Rev **91**(3): 889-915.

Erickson, J. R., M. L. Joiner, X. Guan, W. Kutschke, J. Yang, C. V. Oddis, R. K. Bartlett, J. S. Lowe, S. E. O'Donnell, N. Aykin-Burns, M. C. Zimmerman, K. Zimmerman, A. J. Ham, R. M. Weiss, D. R. Spitz, M. A. Shea, R. J. Colbran, P. J. Mohler and M. E. Anderson (2008). "A dynamic pathway for calcium-independent activation of CaMKII by methionine oxidation." Cell **133**(3): 462-474.

Erickson, J. R., L. Pereira, L. Wang, G. Han, A. Ferguson, K. Dao, R. J. Copeland, F. Despa, G. W. Hart, C. M. Ripplinger and D. M. Bers (2013). "Diabetic hyperglycaemia activates CaMKII and arrhythmias by O-linked glycosylation." Nature **502**(7471): 372-376.

Eshete, F. and R. D. Fields (2001). "Spike frequency decoding and autonomous activation of Ca2+-calmodulin-dependent protein kinase II in dorsal root ganglion neurons." J Neurosci **21**(17): 6694-6705.

Espanel, X., S. Walchli, T. Ruckle, A. Harrenga, M. Huguenin-Reggiani and R. Hooft van Huijsduijnen (2003). "Mapping of synergistic components of weakly interacting protein-protein motifs using arrays of paired peptides." J Biol Chem **278**(17): 15162-15167.

Estep, R. P., K. A. Alexander and D. R. Storm (1989). "Regulation of free calmodulin levels in neurons by neuromodulin: relationship to neuronal growth and regeneration." Curr. Topics in Cellular Regulation **31**: 161-180.

Frank, R. (2002). "The SPOT-synthesis technique. Synthetic peptide arrays on membrane supports--principles and applications." J Immunol Methods **267**(1): 13-26.

Frank, R. and H. Overwin (1996). "SPOT synthesis. Epitope analysis with arrays of synthetic peptides prepared on cellulose membranes." Methods Mol Biol **66**: 149-169.

Gaertner, T. R., S. J. Kolodziej, D. Wang, R. Kobayashi, J. M. Koomen, J. K. Stoops and M. N. Waxham (2004). "Comparative analyses of the three-dimensional structures

and enzymatic properties of alpha, beta, gamma and delta isoforms of Ca2+-calmodulin-dependent protein kinase II." J Biol Chem **279**(13): 12484-12494.

Gaertner, T. R., J. A. Putkey and M. N. Waxham (2004). "RC3/Neurogranin and Ca2+/calmodulin-dependent protein kinase II produce opposing effects on the affinity of calmodulin for calcium." J Biol Chem **279**(38): 39374-39382.

Giese, K. P., N. B. Fedorov, R. K. Filipkowski and A. J. Silva (1998). "Autophosphorylation at Thr286 of the alpha calcium-calmodulin kinase II in LTP and learning." Science **279**(5352): 870-873.

Glazewski, S., K. P. Giese, A. Silva and K. Fox (2000). "The role of alpha-CaMKII autophosphorylation in neocortical experience-dependent plasticity." Nat Neurosci **3**(9): 911-918.

Gleason, M. R., S. Higashijima, J. Dallman, K. Liu, G. Mandel and J. R. Fetcho (2003). "Translocation of CaM kinase II to synaptic sites in vivo." Nat Neurosci **6**(3): 217-218.

Gorelick, F. S., J. K. Wang, Y. Lai, A. C. Nairn and P. Greengard (1988). "Autophosphorylation and activation of Ca2+/calmodulin-dependent protein kinase II in intact nerve terminals." J Biol Chem **263**(33): 17209-17212.

Grab, D. J., R. K. Carlin and P. Siekevitz (1981). "Function of a calmodulin in postsynaptic densities. II. Presence of a calmodulin-activatable protein kinase activity." J Cell Biol **89**(3): 440-448.

Gray, C. B. and J. Heller Brown (2014). "CaMKIIdelta subtypes: localization and function." Front Pharmacol **5**: 15.

Griffith, L. C., L. M. Verselis, K. M. Aitken, C. P. Kyriacou, W. Danho and R. J. Greenspan (1993). "Inhibition of calcium/calmodulin-dependent protein kinase in Drosophila disrupts behavioral plasticity." Neuron **10**(3): 501-509.

Gustin, R. M., B. C. Shonesy, S. L. Robinson, T. J. Rentz, A. J. Baucum, 2nd, N. Jalan-Sakrikar, D. G. Winder, G. D. Stanwood and R. J. Colbran (2011). "Loss of Thr286 phosphorylation disrupts synaptic CaMKIIalpha targeting, NMDAR activity and behavior in pre-adolescent mice." Mol Cell Neurosci **47**(4): 286-292.

Halt, A. R., R. F. Dallapiazza, Y. Zhou, I. S. Stein, H. Qian, S. Juntti, S. Wojcik, N. Brose, A. J. Silva and J. W. Hell (2012). "CaMKII binding to GluN2B is critical during memory consolidation." EMBO J **31**(5): 1203-1216.

Hanson, P. I., T. Meyer, L. Stryer and H. Schulman (1994). "Dual Role of Calmodulin in Autophosphorylation of Multifunctional Cam Kinase May Underlie Decoding of Calcium Signals." Neuron **12**(5): 943-956.

Hinds, H. L., I. Goussakov, K. Nakazawa, S. Tonegawa and V. Y. Bolshakov (2003). "Essential function of alpha-calcium/calmodulin-dependent protein kinase II in neurotransmitter release at a glutamatergic central synapse." Proc Natl Acad Sci U S A **100**(7): 4275-4280.

Hoffman, L., R. A. Stein, R. J. Colbran and H. S. McHaourab (2011). "Conformational changes underlying calcium/calmodulin-dependent protein kinase II activation." EMBO J **30**(7): 1251-1262.

Holmes, W. R. and L. M. Grover (2006). "Quantifying the magnitude of changes in synaptic level parameters with long-term potentiation." J Neurophysiol **96**(3): 1478-1491.

Hornbeck, P. V., J. M. Kornhauser, S. Tkachev, B. Zhang, E. Skrzypek, B. Murray, V. Latham and M. Sullivan (2012). "PhosphoSitePlus: a comprehensive resource for investigating the structure and function of experimentally determined post-translational modifications in man and mouse." Nucleic Acids Res **40**(Database issue): D261-270.

Hudmon, A., J. Aronowski, S. J. Kolb and M. N. Waxham (1996). "Inactivation and self-association of Ca2+/calmodulin-dependent protein kinase II during autophosphorylation." J Biol Chem **271**(15): 8800-8808.

Hudmon, A. and H. Schulman (2002). "Neuronal CA2+/calmodulin-dependent protein kinase II: the role of structure and autoregulation in cellular function." Annu Rev Biochem **71**: 473-510.

Hudmon, A. and H. Schulman (2002). "Structure-function of the multifunctional Ca2+/calmodulin-dependent protein kinase II." Biochem J **364**(Pt 3): 593-611.

Hund, T. J. and P. J. Mohler (2015). "Role of CaMKII in cardiac arrhythmias." Trends Cardiovasc Med **25**(5): 392-397.

Hutti, J. E., E. T. Jarrell, J. D. Chang, D. W. Abbott, P. Storz, A. Toker, L. C. Cantley and B. E. Turk (2004). "A rapid method for determining protein kinase phosphorylation specificity." Nat Methods **1**(1): 27-29.

Ikeda, A., S. Okuno and H. Fujisawa (1991). "Studies on the generation of Ca2+/calmodulin-independent activity of calmodulin-dependent protein kinase II by autophosphorylation. Autothiophosphorylation of the enzyme." J Biol Chem **266**(18): 11582-11588.

Jalan-Sakrikar, N., R. K. Bartlett, A. J. Baucum, 2nd and R. J. Colbran (2012). "Substrate-selective and calcium-independent activation of CaMKII by alpha-actinin." J Biol Chem **287**(19): 15275-15283.

Jiang, H. C., J. M. Hsu, C. P. Yen, C. C. Chao, R. H. Chen and C. L. Pan (2015). "Neural activity and CaMKII protect mitochondria from fragmentation in aging Caenorhabditis elegans neurons." Proc Natl Acad Sci U S A **112**(28): 8768-8773.

Johnson, L. N. (2009). "Protein kinase inhibitors: contributions from structure to clinical compounds." Q Rev Biophys **42**(1): 1-40.

Junger, M. A. and R. Aebersold (2014). "Mass spectrometry-driven phosphoproteomics: patterning the systems biology mosaic." Wiley Interdiscip Rev Dev Biol **3**(1): 83-112.

Kang, S. A., M. E. Pacold, C. L. Cervantes, D. Lim, H. J. Lou, K. Ottina, N. S. Gray, B. E. Turk, M. B. Yaffe and D. M. Sabatini (2013). "mTORC1 phosphorylation sites encode their sensitivity to starvation and rapamycin." Science **341**(6144): 1236566.

Katoh, T. and H. Fujisawa (1991). "Autoactivation of calmodulin-dependent protein kinase II by autophosphorylation." J Biol Chem **266**(5): 3039-3044.

Katoh, T. and H. Fujisawa (1991). "Calmodulin-dependent protein kinase II. Kinetic studies on the interaction with substrates and calmodulin." Biochim Biophys Acta **1091**(2): 205-212.

Kelly, P. T., T. L. McGuinness and P. Greengard (1984). "Evidence that the major postsynaptic density protein is a component of a Ca2+/calmodulin-dependent protein kinase." Proc Natl Acad Sci U S A **81**(3): 945-949.

Kelly, P. T. and P. R. Montgomery (1982). "Subcellular localization of the 52,000 molecular weight major postsynaptic density protein." Brain Res **233**(2): 265-286.

Kemp, B. E., D. B. Bylund, T. S. Huang and E. G. Krebs (1975). "Substrate specificity of the cyclic AMP-dependent protein kinase." Proc Natl Acad Sci U S A **72**(9): 3448-3452.

Kim, S. Y. and J. E. Ferrell, Jr. (2007). "Substrate competition as a source of ultrasensitivity in the inactivation of Wee1." Cell **128**(6): 1133-1145.

Kolb, S. J., A. Hudmon, T. R. Ginsberg and M. N. Waxham (1998). "Identification of domains essential for the assembly of calcium/calmodulin-dependent protein kinase II holoenzymes." J Biol Chem **273**(47): 31555-31564.

Kolodziej, S. J., A. Hudmon, M. N. Waxham and J. K. Stoops (2000). "Three-dimensional reconstructions of calcium/calmodulin-dependent (CaM) kinase IIalpha and truncated CaM kinase IIalpha reveal a unique organization for its structural core and functional domains." J Biol Chem **275**(19): 14354-14359.

Kreegipuu, A., N. Blom, S. Brunak and J. Jarv (1998). "Statistical analysis of protein kinase specificity determinants." FEBS Lett **430**(1-2): 45-50.

Kristensen, A. S., M. A. Jenkins, T. G. Banke, A. Schousboe, Y. Makino, R. C. Johnson, R. Huganir and S. F. Traynelis (2011). "Mechanism of Ca2+/calmodulin-dependent kinase II regulation of AMPA receptor gating." Nat Neurosci **14**(6): 727-735.

Kwiatkowski, A. P. and M. M. King (1989). "Autophosphorylation of the Type-Ii Calmodulin-Dependent Protein-Kinase Is Essential for Formation of a Proteolytic Fragment with Catalytic Activity - Implications for Long-Term Synaptic Potentiation." Biochemistry **28**(13): 5380-5385.

Lai, Y., A. C. Nairn, F. Gorelick and P. Greengard (1987). "Ca2+/calmodulin-dependent protein kinase II: identification of autophosphorylation sites responsible for generation of Ca2+/calmodulin-independence." Proc Natl Acad Sci U S A **84**(16): 5710-5714.

Lai, Y., A. C. Nairn and P. Greengard (1986). "Autophosphorylation reversibly regulates the Ca2+/calmodulin-dependence of Ca2+/calmodulin-dependent protein kinase II." Proc Natl Acad Sci U S A **83**(12): 4253-4257.

Langeberg, L. K. and J. D. Scott (2015). "Signalling scaffolds and local organization of cellular behaviour." Nat Rev Mol Cell Biol **16**(4): 232-244.

Lee, J. C. and A. M. Edelman (1995). "Activation of Ca(2+)-calmodulin-dependent protein kinase Ia is due to direct phosphorylation by its activator." Biochem Biophys Res Commun **210**(2): 631-637.

Lemeer, S. and A. J. Heck (2009). "The phosphoproteomics data explosion." Curr Opin Chem Biol **13**(4): 414-420.

Lengyel, I., M. Cammarota, V. A. Brent and J. A. Rostas (2001). "Autonomous activity and autophosphorylation of CAMPK-II in rat hippocampal slices: effects of tissue preparation." J Neurochem **76**(1): 149-154.

Leonard, A. S., K. U. Bayer, M. A. Merrill, I. A. Lim, M. A. Shea, H. Schulman and J. W. Hell (2002). "Regulation of calcium/calmodulin-dependent protein kinase II docking to N-methyl-D-aspartate receptors by calcium/calmodulin and alpha-actinin." J Biol Chem **277**(50): 48441-48448.

Levine, H., 3rd and N. E. Sahyoun (1987). "Characterization of a soluble Mr-30,000 catalytic fragment of the neuronal calmodulin-dependent protein kinase II." Eur J Biochem **168**(3): 481-486.

Liao, X., J. Su and M. Mrksich (2009). "An adaptor domain-mediated autocatalytic interfacial kinase reaction." Chemistry **15**(45): 12303-12309.
Lisman, J. (1994). "The CaM kinase II hypothesis for the storage of synaptic memory." Trends Neurosci **17**(10): 406-412.
Lisman, J., H. Schulman and H. Cline (2002). "The molecular basis of CaMKII function in synaptic and behavioural memory." Nat Rev Neurosci **3**(3): 175-190.
Lisman, J., R. Yasuda and S. Raghavachari (2012). "Mechanisms of CaMKII action in long-term potentiation." Nat Rev Neurosci **13**(3): 169-182.
Lisman, J. E. (1985). "A mechanism for memory storage insensitive to molecular turnover: a bistable autophosphorylating kinase." Proc Natl Acad Sci U S A **82**(9): 3055-3057.
Liu, Q., B. Chen, Q. Ge and Z. W. Wang (2007). "Presynaptic Ca2+/calmodulin-dependent protein kinase II modulates neurotransmitter release by activating BK channels at Caenorhabditis elegans neuromuscular junction." J Neurosci **27**(39): 10404-10413.
Lou, L. L., S. J. Lloyd and H. Schulman (1986). "Activation of the multifunctional Ca2+/calmodulin-dependent protein kinase by autophosphorylation: ATP modulates production of an autonomous enzyme." Proc Natl Acad Sci U S A **83**(24): 9497-9501.
Lou, L. L. and H. Schulman (1989). "Distinct autophosphorylation sites sequentially produce autonomy and inhibition of the multifunctional Ca2+/calmodulin-dependent protein kinase." J Neurosci **9**(6): 2020-2032.
Lu, H., H. T. Leung, N. Wang, W. L. Pak and B. H. Shieh (2009). "Role of Ca2+/calmodulin-dependent protein kinase II in Drosophila photoreceptors." J Biol Chem **284**(17): 11100-11109.
Lu, W., K. Isozaki, K. W. Roche and R. A. Nicoll (2010). "Synaptic targeting of AMPA receptors is regulated by a CaMKII site in the first intracellular loop of GluA1." Proc Natl Acad Sci U S A **107**(51): 22266-22271.
Lukas, S. M., R. R. Kroe, J. Wildeson, G. W. Peet, L. Frego, W. Davidson, R. H. Ingraham, C. A. Pargellis, M. E. Labadia and B. G. Werneburg (2004). "Catalysis and function of the p38 alpha.MK2a signaling complex." Biochemistry **43**(31): 9950-9960.
MacNicol, M., A. B. Jefferson and H. Schulman (1990). "Ca2+/calmodulin kinase is activated by the phosphatidylinositol signaling pathway and becomes Ca2(+)-independent in PC12 cells." J Biol Chem **265**(30): 18055-18058.
Malinow, R. and R. C. Malenka (2002). "AMPA receptor trafficking and synaptic plasticity." Annu Rev Neurosci **25**: 103-126.
Manning, G., D. B. Whyte, R. Martinez, T. Hunter and S. Sudarsanam (2002). "The protein kinase complement of the human genome." Science **298**(5600): 1912-1934.
Mattiazzi, A., R. A. Bassani, A. L. Escobar, J. Palomeque, C. A. Valverde, M. Vila Petroff and D. M. Bers (2015). "Chasing cardiac physiology and pathology down the CaMKII cascade." Am J Physiol Heart Circ Physiol **308**(10): H1177-1191.
Mayford, M., D. Baranes, K. Podsypanina and E. R. Kandel (1996). "The 3'-untranslated region of CaMKIIa is a cis-acting signal for the localization and translation of mRNA in dendrites." Proc Natl Acad Sci U S A **93**(23): 13250-13255.
Mayford, M., J. Wang, E. R. Kandel and T. J. Odell (1995). "Camkii Regulates the Frequency-Response Function of Hippocampal Synapses for the Production of Both Ltd and Ltp." Cell **81**(6): 891-904.

Meyer, T., P. I. Hanson, L. Stryer and H. Schulman (1992). "Calmodulin trapping by calcium-calmodulin-dependent protein kinase." Science **256**(5060): 1199-1202.
Miller, S. G. and M. B. Kennedy (1986). "Regulation of brain type II Ca2+/calmodulin-dependent protein kinase by autophosphorylation: a Ca2+-triggered molecular switch." Cell **44**(6): 861-870.
Miller, S. G., B. L. Patton and M. B. Kennedy (1988). "Sequences of autophosphorylation sites in neuronal type II CaM kinase that control Ca2(+)-independent activity." Neuron **1**(7): 593-604.
Molloy, S. S. and M. B. Kennedy (1991). "Autophosphorylation of type II Ca2+/calmodulin-dependent protein kinase in cultures of postnatal rat hippocampal slices." Proc Natl Acad Sci U S A **88**(11): 4756-4760.
Naffin, J. L., Y. Han, H. J. Olivos, M. M. Reddy, T. Sun and T. Kodadek (2003). "Immobilized peptides as high-affinity capture agents for self-associating proteins." Chem Biol **10**(3): 251-259.
Obenauer, J. C., L. C. Cantley and M. B. Yaffe (2003). "Scansite 2.0: Proteome-wide prediction of cell signaling interactions using short sequence motifs." Nucleic Acids Res **31**(13): 3635-3641.
Obradovic, Z., K. Peng, S. Vucetic, P. Radivojac and A. K. Dunker (2005). "Exploiting heterogeneous sequence properties improves prediction of protein disorder." Proteins **61 Suppl 7**: 176-182.
Omkumar, R. V., M. J. Kiely, A. J. Rosenstein, K. T. Min and M. B. Kennedy (1996). "Identification of a phosphorylation site for calcium/calmodulindependent protein kinase II in the NR2B subunit of the N-methyl-D-aspartate receptor." J Biol Chem **271**(49): 31670-31678.
Otmakhov, N., J. H. Tao-Cheng, S. Carpenter, B. Asrican, A. Dosemeci, T. S. Reese and J. Lisman (2004). "Persistent accumulation of calcium/calmodulin-dependent protein kinase II in dendritic spines after induction of NMDA receptor-dependent chemical long-term potentiation." J Neurosci **24**(42): 9324-9331.
Pearson, R. B. and B. E. Kemp (1991). "Protein kinase phosphorylation site sequences and consensus specificity motifs: tabulations." Methods Enzymol **200**: 62-81.
Peng, K., P. Radivojac, S. Vucetic, A. K. Dunker and Z. Obradovic (2006). "Length-dependent prediction of protein intrinsic disorder." BMC Bioinformatics **7**: 208.
Persechini, A. and P. M. Stemmer (2002). "Calmodulin is a limiting factor in the cell." Trends Cardiovasc Med **12**(1): 32-37.
Pinna, L. A. and M. Ruzzene (1996). "How do protein kinases recognize their substrates?" Biochimica Et Biophysica Acta-Molecular Cell Research **1314**(3): 191-225.
Putkey, J. A. and M. N. Waxham (1996). "A peptide model for calmodulin trapping by calcium/calmodulin-dependent protein kinase II." J Biol Chem **271**(47): 29619-29623.
Rellos, P., A. C. Pike, F. H. Niesen, E. Salah, W. H. Lee, F. von Delft and S. Knapp (2010). "Structure of the CaMKIIdelta/calmodulin complex reveals the molecular mechanism of CaMKII kinase activation." PLoS Biol **8**(7): e1000426.
Rich, R. C. and H. Schulman (1998). "Substrate-directed function of calmodulin in autophosphorylation of Ca^{2+}/calmodulin-dependent protein kinase II." J Biol Chem **273**(43): 28424-28429.
Roskoski, R., Jr. (1983). "Assays of protein kinase." Methods Enzymol **99**: 3-6.

Roskoski, R., Jr. (2015). "A historical overview of protein kinases and their targeted small molecule inhibitors." Pharmacol Res **100**: 1-23.

S., Y., F. K., Y. H., M. T. and M. E. (1988). "Activation of Ca^{2+}/calmodulin-dependent protein kinase II by autophosphorylation: specified substrates enhance the kinase activity." Biomed. Res. **9**: 497-502.

Sabatini, B. L., T. G. Oertner and K. Svoboda (2002). "The life cycle of Ca(2+) ions in dendritic spines." Neuron **33**(3): 439-452.

Saitoh, T. and J. H. Schwartz (1985). "Phosphorylation-dependent subcellular translocation of a Ca2+/calmodulin-dependent protein kinase produces an autonomous enzyme in Aplysia neurons." J Cell Biol **100**(3): 835-842.

Santalla, M., C. A. Valverde, E. Harnichar, E. Lacunza, J. Aguilar-Fuentes, A. Mattiazzi and P. Ferrero (2014). "Aging and CaMKII alter intracellular Ca2+ transients and heart rhythm in Drosophila melanogaster." PLoS One **9**(7): e101871.

Schulman, B. A., D. L. Lindstrom and E. Harlow (1998). "Substrate recruitment to cyclin-dependent kinase 2 by a multipurpose docking site on cyclin A." Proc Natl Acad Sci U S A **95**(18): 10453-10458.

Schworer, C. M., R. J. Colbran, J. R. Keefer and T. R. Soderling (1988). "Ca2+/calmodulin-dependent protein kinase II. Identification of a regulatory autophosphorylation site adjacent to the inhibitory and calmodulin-binding domains." J Biol Chem **263**(27): 13486-13489.

Shen, K. and T. Meyer (1999). "Dynamic control of CaMKII translocation and localization in hippocampal neurons by NMDA receptor stimulation." Science **284**(5411): 162-166.

Shen, K., M. N. Teruel, J. H. Connor, S. Shenolikar and T. Meyer (2000). "Molecular memory by reversible translocation of calcium/calmodulin-dependent protein kinase II." Nat Neurosci **3**(9): 881-886.

Sheng, M. and C. C. Hoogenraad (2007). "The postsynaptic architecture of excitatory synapses: a more quantitative view." Annu Rev Biochem **76**: 823-847.

Shepherd, J. D. and R. L. Huganir (2007). "The cell biology of synaptic plasticity: AMPA receptor trafficking." Annu Rev Cell Dev Biol **23**: 613-643.

Shonesy, B. C., N. Jalan-Sakrikar, V. S. Cavener and R. J. Colbran (2014). "CaMKII: a molecular substrate for synaptic plasticity and memory." Prog Mol Biol Transl Sci **122**: 61-87.

Silva, A. J., R. Paylor, J. M. Wehner and S. Tonegawa (1992). "Impaired spatial learning in alpha-calcium-calmodulin kinase II mutant mice." Science **257**(5067): 206-211.

Silva, A. J., C. F. Stevens, S. Tonegawa and Y. Wang (1992). "Deficient hippocampal long-term potentiation in alpha-calcium-calmodulin kinase II mutant mice." Science **257**(5067): 201-206.

Singla, S. I., A. Hudmon, J. M. Goldberg, J. L. Smith and H. Schulman (2001). "Molecular characterization of calmodulin trapping by calcium/calmodulin-dependent protein kinase II." J Biol Chem **276**(31): 29353-29360.

Smedler, E. and P. Uhlen (2014). "Frequency decoding of calcium oscillations." Biochim Biophys Acta **1840**(3): 964-969.

Songyang, Z., S. Blechner, N. Hoagland, M. F. Hoekstra, H. Piwnica-Worms and L. C. Cantley (1994). "Use of an oriented peptide library to determine the optimal substrates of protein kinases." Curr Biol **4**(11): 973-982.

Songyang, Z., K. P. Lu, Y. T. Kwon, L. H. Tsai, O. Filhol, C. Cochet, D. A. Brickey, T. R. Soderling, C. Bartleson, D. J. Graves, A. J. DeMaggio, M. F. Hoekstra, J. Blenis, T. Hunter and L. C. Cantley (1996). "A structural basis for substrate specificities of protein Ser/Thr kinases: primary sequence preference of casein kinases I and II, NIMA, phosphorylase kinase, calmodulin-dependent kinase II, CDK5, and Erk1." Mol Cell Biol **16**(11): 6486-6493.

Steiner, P., M. J. Higley, W. Xu, B. L. Czervionke, R. C. Malenka and B. L. Sabatini (2008). "Destabilization of the postsynaptic density by PSD-95 serine 73 phosphorylation inhibits spine growth and synaptic plasticity." Neuron **60**(5): 788-802.

Strack, S., S. Choi, D. M. Lovinger and R. J. Colbran (1997). "Translocation of autophosphorylated calcium/calmodulin-dependent protein kinase II to the postsynaptic density." J Biol Chem **272**(21): 13467-13470.

Strack, S. and R. J. Colbran (1998). "Autophosphorylation-dependent targeting of calcium/calmodulin-dependent protein kinase II by the NR2B subunit of the N-methyl- D-aspartate receptor." J Biol Chem **273**(33): 20689-20692.

Strack, S., R. B. McNeill and R. J. Colbran (2000). "Mechanism and regulation of calcium/calmodulin-dependent protein kinase II targeting to the NR2B subunit of the N-methyl-D-aspartate receptor." J Biol Chem **275**(31): 23798-23806.

Stratton, M., I. H. Lee, M. Bhattacharyya, S. M. Christensen, L. H. Chao, H. Schulman, J. T. Groves and J. Kuriyan (2014). "Activation-triggered subunit exchange between CaMKII holoenzymes facilitates the spread of kinase activity." Elife **3**: e01610.

Suzuki, T., K. Okumuranoji, R. Tanaka and T. Tada (1994). "Rapid Translocation of Cytosolic Ca2+/Calmodulin-Dependent Protein-Kinase-Ii into Postsynaptic Density after Decapitation." Journal of Neurochemistry **63**(4): 1529-1537.

Swulius, M. T., Y. Kubota, A. Forest and M. N. Waxham (2010). "Structure and composition of the postsynaptic density during development." J Comp Neurol **518**(20): 4243-4260.

Swulius, M. T. and M. N. Waxham (2008). "Ca(2+)/calmodulin-dependent protein kinases." Cell Mol Life Sci **65**(17): 2637-2657.

Takeuchi-Suzuki, E., T. Tanaka, W. F. Hink and M. M. King (1992). "High-level expression using baculovirus, purification, and characterization of a monomeric form of type II calmodulin-dependent protein kinase." Protein Expr Purif **3**(2): 160-164.

Tang, X., S. Orlicky, T. Mittag, V. Csizmok, T. Pawson, J. D. Forman-Kay, F. Sicheri and M. Tyers (2012). "Composite low affinity interactions dictate recognition of the cyclin-dependent kinase inhibitor Sic1 by the SCFCdc4 ubiquitin ligase." Proc Natl Acad Sci U S A **109**(9): 3287-3292.

Tao-Cheng, J. H., A. Dosemeci, C. A. Winters and T. S. Reese (2006). "Changes in the distribution of calcium calmodulin-dependent protein kinase II at the presynaptic bouton after depolarization." Brain Cell Biol **35**(2-3): 117-124.

Taylor, S. S., C. Kim, D. Vigil, N. M. Haste, J. Yang, J. Wu and G. S. Anand (2005). "Dynamics of signaling by PKA." Biochim Biophys Acta **1754**(1-2): 25-37.

Taylor, S. S., E. Radzio-Andzelm and T. Hunter (1995). "How do protein kinases discriminate between serine/threonine and tyrosine? Structural insights from the insulin receptor protein-tyrosine kinase." FASEB J **9**(13): 1255-1266.

Tokumitsu, H., H. Enslen and T. R. Soderling (1995). "Characterization of a Ca2+/calmodulin-dependent protein kinase cascade. Molecular cloning and expression of calcium/calmodulin-dependent protein kinase kinase." J Biol Chem **270**(33): 19320-19324.

Tokunaga, Y., K. Takeuchi, H. Takahashi and I. Shimada (2014). "Allosteric enhancement of MAP kinase p38alpha's activity and substrate selectivity by docking interactions." Nat Struct Mol Biol **21**(8): 704-711.

Tombes, R. M., M. O. Faison and J. M. Turbeville (2003). "Organization and evolution of multifunctional Ca(2+)/CaM-dependent protein kinase genes." Gene **322**: 17-31.

Tse, J. K., A. M. Giannetti and J. M. Bradshaw (2007). "Thermodynamics of calmodulin trapping by Ca2+/calmodulin-dependent protein kinase II: subpicomolar Kd determined using competition titration calorimetry." Biochemistry **46**(13): 4017-4027.

Ubersax, J. A. and J. E. Ferrell, Jr. (2007). "Mechanisms of specificity in protein phosphorylation." Nat Rev Mol Cell Biol **8**(7): 530-541.

Vallano, M. L., C. M. Beaman-Hall, A. Mathur and Q. Chen (2000). "Astrocytes express specific variants of CaM KII delta and gamma, but not alpha and beta, that determine their cellular localizations." Glia **30**(2): 154-164.

Wang, J., J. J. Renger, L. C. Griffith, R. J. Greenspan and C. F. Wu (1994). "Concomitant alterations of physiological and developmental plasticity in Drosophila CaM kinase II-inhibited synapses." Neuron **13**(6): 1373-1384.

Waxham, M. N., J. Aronowski, S. A. Westgate and P. T. Kelly (1990). "Mutagenesis of Thr-286 in monomeric Ca2+/calmodulin-dependent protein kinase II eliminates Ca2+/calmodulin-independent activity." Proc Natl Acad Sci U S A **87**(4): 1273-1277.

Waxham, M. N., A. L. Tsai and J. A. Putkey (1998). "A mechanism for calmodulin (CaM) trapping by CaM-kinase II defined by a family of CaM-binding peptides." J Biol Chem **273**(28): 17579-17584.

Yamagata, Y., A. J. Czernik and P. Greengard (1991). "Active catalytic fragment of Ca2+/calmodulin-dependent protein kinase II. Purification, characterization, and structural analysis." J Biol Chem **266**(23): 15391-15397.

Yamauchi, T., S. Ohsako and T. Deguchi (1989). "Expression and characterization of calmodulin-dependent protein kinase II from cloned cDNAs in Chinese hamster ovary cells." J Biol Chem **264**(32): 19108-19116.

Yasugawa, S., K. Fukunaga, H. Yamamoto, T. Miyakawa and E. Miyamoto (1991). "Autophosphorylation of Ca2+/calmodulin-dependent protein kinase II: effects on interaction between enzyme and substrate." Jpn J Pharmacol **55**(2): 263-274.

Yoshimura, Y., C. Aoi and T. Yamauchi (2000). "Investigation of protein substrates of Ca(2+)/calmodulin-dependent protein kinase II translocated to the postsynaptic density." Brain Res Mol Brain Res **81**(1-2): 118-128.

Yoshimura, Y., T. Nomura and T. Yamauchi (1996). "Purification and characterization of active fragment of Ca2+/calmodulin-dependent protein kinase II from the post-synaptic density in the rat forebrain." J Biochem **119**(2): 268-273.

Yoshimura, Y., T. Shinkawa, M. Taoka, K. Kobayashi, T. Isobe and T. Yamauchi (2002). "Identification of protein substrates of Ca(2+)/calmodulin-dependent protein kinase

II in the postsynaptic density by protein sequencing and mass spectrometry." Biochem Biophys Res Commun **290**(3): 948-954.
Zeng, Y. (2014). "Relative specificity: all substrates are not created equal." Genomics Proteomics Bioinformatics **12**(1): 1-7.
Zhang, J., P. L. Yang and N. S. Gray (2009). "Targeting cancer with small molecule kinase inhibitors." Nat Rev Cancer **9**(1): 28-39.

CURRICULUM VITAE

Derrick E. Johnson

Education

Indiana University, Indianapolis, IN
Doctor of Philosophy in Biochemistry and Molecular Biology 2016
Advisor: Dr. Andy Hudmon
Dissertation Title: *Autoregulatory and Structural Control of CaMKII Substrate Specificity.*

Purdue University, Indianapolis, IN
Bachelor of Science in Biology 2006

Research Experience

Indiana University School of Medicine 2009 – 2016
Department of Biochemistry and Molecular Biology
Graduate Research Assistant

- Studying structural and autoregulation of CaMKII as it relates to substrate specificity
- Exploration of the effect of oligomerization of the CaMKII holoenzyme on its enzymatic activity, targeting, and substrate specificity
- Studies on the phosphorylation of purified rodent post-synaptic densities by CaMKII exhibiting varying activation states associated with its physiological function
- Biochemical characterization of enzyme kinetics, substrate interactions, and substrate arrays

Indiana University School of Medicine 2005 – 2009
Department of Biochemistry and Molecular Biology
Center for Computational Biology and Bioinformatics
Research Technician

- Development of analytical methods for the rapid, high-throughput identification and characterization of intrinsically disordered regions within proteins
- Adapting these methodologies for the purpose of extending the characterization of proteins from the Protein Structure Initiative beyond simply the ordered regions of proteins
- Characterizing the structural and kinetic effects of aromatic amino acid content as it relates to enzyme function

Molecular Kinetics, Inc., Indianapolis, IN 46268 2005
Research Intern

- Researching computationally selected candidate proteins through literature review and data mining as well as extracting data from public and proprietary protein databases
- Assessing the experimental methods used to validate regions of intrinsic disorder within proteins
- Construction and maintenance of several internal research databases

Peer Reviewed Publications

Johnson D.E., Ramaswamy S.S., Hudmon A. (2016) Dynamic Substrate Gating in CaMKII. *Proc Natl Acad Sci U S A.* (In Submission)

Johnson D.E., Hudmon A. (2016) Controlling CaMKII Substrate Specificity via Multimeric Holoenzyme Activation. (In Preparation)

Johnson D.E., Xue B., Sickmeier M.D., Meng J., Cortese M.S., Oldfield C.J., Le Gall T., Dunker A.K., Uversky V.N. (2012) High-throughput characterization of intrinsic disorder in proteins from the Protein Structure Initiative. *J Struct Biol* 180(1):201-15. doi:10.1016/j.jsb.2012.05.013

Chawla A.R., Johnson D.E., Leeds B.P., Nelson R.M., Hudmon A. (2016) Homeostatic Regulation of the Glutamate/Aspartate Transporter EAAT1 by Calcium/Calmodulin-Dependent Protein Kinase II. In Submission

Zhou C., Ramaswamy S.S., Johnson D.E., Vitturi D.A., Schopfer F.J., Freeman B.A., Hudmon A., Levitan E.S. (2016) Novel Roles for Peroxynitrite in Angiotensin II and CaMKII Signaling. *Scientific Reports*. In Press

Gaji R.Y., Johnson D.E., Treeck M., Wang M., Hudmon A., Arrizabalaga G. (2015) Phosphorylation of a Myosin Motor by TgCDPK3 Facilitates Rapid Initiation of Motility during Toxoplasma gondii egress. *PLoS Pathogens* 11(11):e1005268. doi: 10.1371/journal.ppat.1005268.

Fieni F., Johnson D.E., Hudmon A., Kirichok Y. (2014) Mitochondrial Ca^{2+} uniporter and CaMKII in heart. *Nature: Brief Communication Arising* 513(7519):E1-2. doi:10.1038/nature13626

Adler J.J., Johnson D.E., Heller B.L., Bringman L.R., Ranahan W.P., Conwell M.D., Sun Y., Hudmon A., Wells C.D. (2013) Serum deprivation inhibits the transcriptional co-activator YAP and cell growth via phosphorylation of the 130-kDa isoform of Angiomotin by the LATS1/2 protein kinases. *Proc Natl Acad Sci U S A* 110(43):17368-73. doi:10.1073/pnas.1308236110

Ashpole N.M., Herren A.W., Ginsburg K.S., Brogan J.D., Johnson D.E., Cummins T.R., Bers D.M., Hudmon A. (2012) Ca^{2+}/calmodulin-dependent protein kinase II (CaMKII) regulates cardiac sodium channel $Na_V1.5$ gating by multiple phosphorylation sites. *J Biol* Chem 287(24):19856-69. doi: 10.1074/jbc.M111.322537

Wang W., Perovic I., Chittuluru J., Kaganovich A., Nguyen L.T., Liao J., Auclair J.R., Johnson D., Landeru A., Simorellis A.K., Ju S., Cookson M.R., Asturias F.J., Agar J.N., Webb B.N., Kang C., Ringe D., Petsko G.A., Pochapsky T.C., Hoang Q.Q. (2011) A soluble α-synuclein construct forms a dynamic tetramer. *Proc Natl Acad Sci U S A* 108(43):17797-802. doi: 10.1073/pnas.1113260108

Presentations/Conferences

Johnson D.E., Meng J., Hudmon A. (February 15-19, 2014) Mechanisms Underlying Cooperativity in CaMKII Autophosphorylation and Substrate Phosphorylation. Poster Session, 58th Biophysical Society Annual Meeting, San Francisco, California

Johnson D.E., Kaiser D.J., Ashpole, N.M., Hudmon, A. (February 2-6, 2013) The Multimeric Architecture of CaMKII Alters Substrate Regulation of Diffusion-Restricted Environments. Poster Session, 57th Biophysical Society Annual Meeting, Philadelphia, Pennsylvania

Johnson D.E., Kaiser D.J., Ashpole, N.M., Hudmon, A. (March 30, 2012) Structural Determinants Regulating CaMKII Substrate Selection. 2006 Biochemistry and Molecular Biology Research Day, Indiana University School of Medicine, Indianapolis, Indiana

Johnson D.E., Kaiser D.J., Ashpole, N.M., Hudmon, A. (February 25-29, 2012) Structural and Catalytic Mechanisms Underlying CaMKII Substrate Selection. Poster Session, 55th Biophysical Society Annual Meeting, San Diego, California

Johnson D.E., Sickmeier M.D., Meng J., Le Gall T., Uversky V.N., Dunker A.K. (March 2, 2009) High-throughput Characterization of Intrinsically Disordered Proteins from the Protein Structure Initiative. Platform X: Exploring the Unfolded State of Peptide & Proteins, 53nd Biophysical Society Annual Meeting, Boston, Massachusetts

Johnson D.E., Sickmeier M.D., Meng J., Le Gall T., Uversky V.N., Dunker A.K. (February 6, 2008) High-throughput Characterization of Intrinsically Disordered Proteins from the Protein Structure Initiative. Poster Session, 52nd Biophysical Society Annual Meeting and 16th IUPAB International Biophysics Congress, Long Beach, California

Johnson D.E., Cortese M.S., Uversky V.N., Dunker A.K. (March 6, 2007) Computationally Driven Experimentation: Predicting Protein-Protein Interaction Sites and Elucidating Partners from Cellular Extracts. Poster Session, 51st Biophysical Society Annual Meeting, Baltimore, Maryland

Teaching Experience

Indiana University Purdue University Indianapolis 2006
Teaching Assistant – Embryology Lab